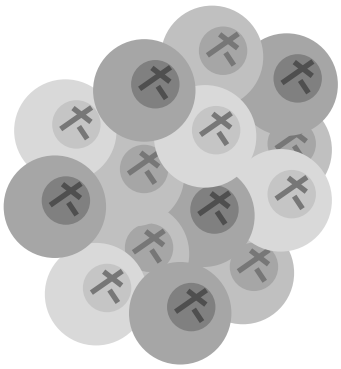
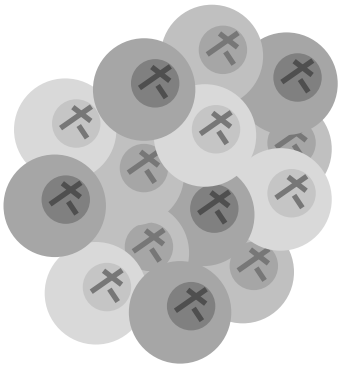
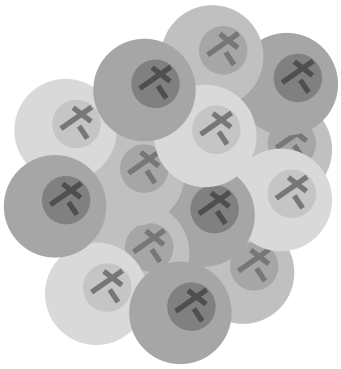

Optimal control of combined chemo-radiation therapy treatments for improving cancer care

C.G. van Furth

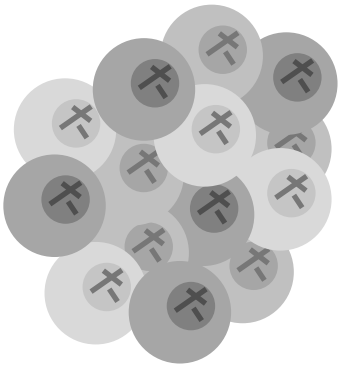
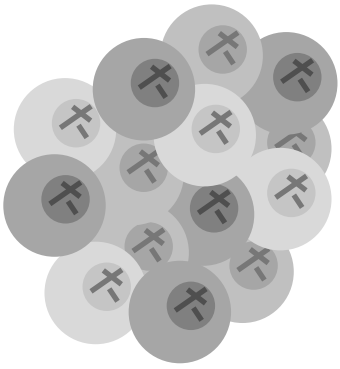
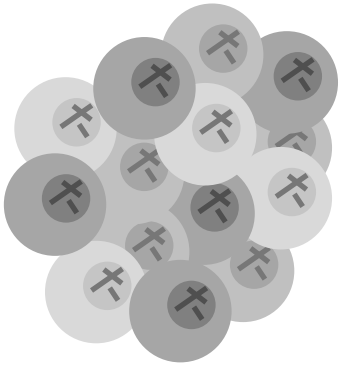

TU

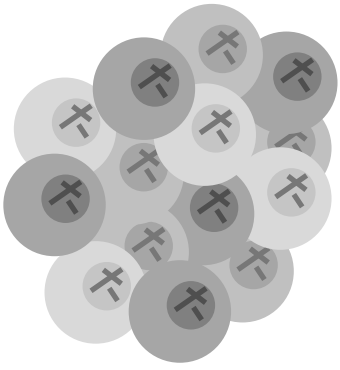
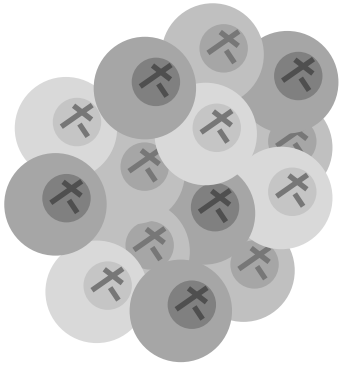

Optimal control of combined chemo-radiation therapy treatments for improving cancer care

Master of Science Thesis

For the degree of Master of Science in Systems and Control at Delft University of Technology

Ghiline van Furth

February 28, 2020

Faculty of Mechanical, Maritime and Materials Engineering (3mE) · Delft University of Technology

This work was in collaboration with the MP&T department from the TU Delft; their added knowledge is much appreciated. Furthermore, a clinical dataset was obtained from the Erasmus MC, and their contribution is gratefully acknowledged.

Delft University of Technology
Department of
Delft Center for Systems and Control (dcsc)

The undersigned hereby certify that they have read and recommend to the Faculty of Mechanical, Maritime and Materials Engineering (3mE) for acceptance a thesis entitled

Optimal control of combined chemo-radiation therapy treatments for improving cancer care

by

Ghiline van Furth

in partial fulfillment of the requirements for the degree of

Master of Science Systems and Control

Dated: February 28, 2020

Supervisor(s):

Dr. Ir. G. Giordano

Dr. Z. Perkó

Reader(s):

Dr. Ir. A.J.J. van den Boom

Dr. Ir. M. Keijzer

Abstract

Combined chemo-radiation treatments are often used to enhance tumor cell kill, with respect to their separate treatments. Currently, chemo-radiation therapy treatments are prescribed as a separately optimized radiotherapy treatment with the addition of a generic chemotherapy regimen. The dosing of the combined therapies is mostly based on clinical experience. Hence there is a clear need for the optimization of dosing for combined chemo-radiation therapy treatments. The goal of this thesis is to propose novel approaches to optimize cancer treatment efficiency when combining chemotherapy and radiotherapy by using control-theoretical methods as well as radiation therapy models.

A positive switched system is a dynamic system consisting of a set of Metzler state-space matrices and a specific switching law, which determines when and how to switch between the subsystems. Positive switched systems seem particularly appropriate to model cancer evolution under different treatments, and therefore to determine optimal treatment scheduling. They are used to model the effect of combined chemo-radiation treatments, thus enabling the systematic design of optimal therapy planning. The proposed model is especially appropriate for heterogeneous tumors, since it describes the impact of therapies on different tumor cell lines, and includes the possibility of mutations. Metastases are also included since the model considers separate tumor compartments, and the possibility of migrations between compartments are modeled as well. Undesired consequences due to toxicities are incorporated, and an upper bound can be set to limit the possible damage.

A clinical dataset was obtained from the Erasmus MC, which was used to validate chemotherapy-alone model outcomes. Combined chemo-radiation treatments were also developed for a set of initial tumors. The model shows promising applications for cancer treatment design. The use of positive switched systems for combined chemo-radiation treatments is a new approach to obtain optimal drug usage and radiation fractionation schemes for each body compartment. The achieved findings could have a significant impact on effective treatment planning by choosing optimal drug durations or by using radiotherapy in combination with chemotherapy, for instance, to target certain chemotherapy-resistant areas, to achieve tumor control with minimal side effects.

Table of Contents

List of Figures

List of Tables

Preface

This work was conducted as a graduation project for the master Systems and Control. When searching for a thesis, I hoped for a project where control-theoretical methods could be applied to a medical application. So when I found this project, I could not have been happier. I really enjoyed working on this thesis, but I am also excited that it has come to an end. I learned so much during the last year, not only in the expected fields but also in unexpected areas. I found myself digging into cell behavior, talking to medical experts about clinical decision making, and asking friends about pharmacological studies. I also learned a lot on a personal level by pushing and challenging myself.

The thesis was also tricky sometimes, especially when dealing with the unanswered questions in cancer care. A lot of information is uncertain or unknown, which causes some difficulties. Also, the topic of this thesis is multi-disciplinary, which is one of the things I enjoyed, but also what made it quite challenging.

I want to take the opportunity to thank some people. First, I would like to give a special thanks to my supervisors Giulia Giordano and Zoltán Perkó. Not only for their assistance throughout the project and giving helpful feedback but also for making me feel supported. I would like to thank Ton van den Boom, for helping me with the graduation administration and for being the committee chair, and Marleen Keijzer for being an enthusiastic and appreciated addition to the committee.

My gratitude also goes out to Stijn Koolen, Ron Mathijssen, and Sander Bins from the Erasmus MC, for helping me obtain clinical patient data. Furthermore, my appreciation goes out to medical oncologist Frank Speentjens from the LUMC for answering some clinical questions, Cees Haringa from DSM for helping me understand cell behavior, and my family and friends for encouraging me throughout this thesis.

Delft, University of Technology — Ghiline van Furth
February 28, 2020

Chapter 1

Introduction

1.1 Research motivation

Cancer is a huge problem worldwide. In over 50% of the tested countries, cancer is the first or second cause of death before the age of 70 years old, based on estimates of the World Health Organization (WHO) [1]. In 2018 there were 18.1 million new cases of cancer, and 9.6 million people died of cancer worldwide [2]. Due to the large scope, a lot of research has already been done in cancer treatment, and many cancers have already become curable [3]. Potential treatment options are, among others, radiation therapy, chemotherapy, surgery, targeted therapy, and combinations of these modalities. This thesis is focused on radiotherapy, chemotherapy, and combined chemo-radiation therapy.

Radiotherapy is one of the main cancer treatments. About 50% of all cancer patients receive radiation somewhere in their treatment [3]. The goal of radiotherapy is to maximize tumor cell death while minimizing the damage to surrounding healthy tissues [4]. This is done by refined computational models and computer algorithms that optimize the spatial delivery of radiation [4], [5], [6], [7]. Although the radiation is directed at the tumor, the surrounding healthy tissues inevitably suffer from the effect of radiation as well. However, healthy cells repair the damage done by radiation faster than the cancerous cells, which is the basis of the concept of repeated-dose delivery. The total dose is therefore delivered in multiple smaller doses, called the fractionated dose. The fractionation scheme, i.e., the combination of total dose and fractionated doses, is determined on clinical experience, and improvements can be made with optimization approaches.

For many cancers that are in a more advanced stage, treatments with only radiation are insufficient. Cancer has spread throughout the body, and the tumor cells cannot be exterminated without causing too much damage to the healthy surrounding tissues. Often a combination of chemotherapy and radiation is necessary to enhance tumor cell kill. Chemotherapy is a type of treatment that uses one or more anti-cancer drugs, referred to as chemotherapeutic agents. Even though chemotherapy is a widely used treatment for cancer, the modeling, and optimization of chemotherapy treatments are not much explored. The varying responses

of patients to the anti-cancer drugs and the rise of drug resistance makes them especially challenging to model. Moreover, the clinical application of algorithmic planning methods for individualized chemotherapy is practically non-existent [8]. The most significant limitations are the inadequacy of the current models in clinical realism [8]. As a result, are the current chemotherapy treatments mainly based on clinical experience and trials only.

Chemo-radiation treatments have shown lower incidence rates of distant metastases in patients compared to radiation-alone treatments [9]. Combined treatments also lead to better local tumor control for various sites, as has been clinically shown [9], [10]. On average more than a quarter of all cancer patients are treated with chemotherapy and radiation therapy in the United States during their course of illness [5]. However, currently, chemo-radiation therapy treatments are prescribed as a separately optimized radiotherapy treatment with the addition of a generic chemotherapy regimen. The dosing and scheduling of the combined therapies are mostly based on clinical experience, without the involvement of bio-mathematical modeling [5]. Only heuristic attempts have been made to optimize the combined application of chemo-radiation therapy [9], [10], hence there is a clear need for the optimization of dosing and scheduling for combined chemo-radiation therapy treatments as well.

A positive switched system is a dynamic system consisting of a set of Metzler state-space matrices and a certain switching law, which determines when and how to switch between the subsystems. Positive switched systems seem particularly appropriate to model cancer evolution under different treatments, and therefore to determine optimal treatment scheduling. This class of models has been successfully used to plan optimal treatment scheduling to minimize the viral load in HIV infection [11], [12], [13], [14], [15], and to minimize the tumor size in cancer targeted therapy [16], [17]. For a certain class of positive switched systems, the system dynamics are convex-monotone [18], [19], which is a useful property for optimization. Modeling the effect of combined chemo-radiation treatments as a positive switched system, thus enabling the systematic design of optimal therapy planning, is a new research effort. The achieved findings could have a significant impact on effective treatment planning by choosing optimal drug durations or by using radiotherapy in combination with chemotherapy, for instance, to target certain chemotherapy-resistant areas, to achieve tumor control with minimal side effects.

1.2 Research scope

The goal of this thesis is to propose novel approaches to optimize cancer treatment efficiency when combining chemotherapy and radiotherapy by using control-theoretical methods as well as radiation therapy models. The optimal drug durations for chemotherapy and fractionation schemes for radiotherapy should be calculated, as well as the optimal combined chemo-radiation therapy treatment plans. It is important that the model can be used for all tumor sites, and that it realistically models the treatment response of the patient. It is also essential to take the toxicity of the drugs and negative consequences of the radiation into account and make sure they are limited. Therefore, the sub-questions that are addressed in this thesis are:

- Can positive switched systems be used to optimize chemotherapy and radiotherapy, separately and combined?
- Is it possible to predict the probability that severe side effects, caused by chemotherapeutic drugs or radiation, will occur, and can it be incorporated into the model?
- It is desired that the model calculates optimal doses for radiation treatments. How can these be obtained?
- What is the predictive power of the model? Can it suitably replicate clinically measured tumor dynamics?

1.3 Report outline

This report is organized so that the reader can follow all results and, if needed, reproduce them. Since this is a multidisciplinary subject, the background information of the topics will be explained in detail.

In Chapter 2, the medical background related to this topic is given. Some general information about cancer, such as the biology properties and the staging of tumors is discussed. Then the treatments on which this thesis focuses are explained in more detail. First, chemotherapy is addressed, followed by radiotherapy. The currently available models that are used in this thesis are also explained.

Chapter 3 presents the theoretical background to determine optimal drug durations for chemotherapy. The multi-compartment model that is used to model the tumor dynamics is discussed here. The optimization formulation is also given, as well as an algorithm to schedule the drugs.

The theory will be applied to a tumor example, which is colorectal cancer (CRC). In Chapter 4, all tumor-related information will be given, such as the estimated parameters, the dataset for irinotecan from the Erasmus MC, and the parameters for the side effects for this type of cancer. The simulations on CRC with a chemotherapy treatment will be given in Chapter 5 and compared to the clinical data.

In Chapter 6, the focus will shift towards radiotherapy and especially combined chemo-radiation therapy. The theory to add radiation therapy to the model is handled. Then in Chapter 7, the model simulations are given for some initial conditions of CRC.

Last, the conclusions and recommendations are stated in Chapter 8. At the end of the thesis, a glossary can be found with a list of the used acronyms and mathematical symbols, to assist the reader.

Chapter 2

Medical background

This thesis is a multi-disciplinary project for which some fundamental medical knowledge is a crucial part. In this chapter, the required medical background is described. First, some background information on cancer is given in Section 2.1, where the biology of cancer, the staging of tumors, and what the treatment options are, is explained. Then the two treatment options that are considered in this project are described in more detail. Section 2.2 is focused on chemotherapy, how it works, and what the current mathematical models are. In Section 2.3 radiotherapy is explained in detail, then the biologically effective dose (BED) model is described, and finishing with the normal tissue complication probability (NTCP) model.

2.1 Cancer

2.1.1 The biological properties of cancer

The body consists of approximately $3.72 \cdot 10^{13}$ cells that form organs and tissues [20]. In these cells, some genes control the cells and tell them when to grow, divide, die, and how they should behave. Usually, this process goes well, and all organs function as they should. When a cell grows, it divides into two identical cells, which are copies from the cell of origin. So from one cell, two new cells are created, then four, and it continues in that way. Hence a constant growth rate means exponential cell growth. In Figure 2.1, the process of cell division is presented schematically.

In grown-ups, cells only grow and divide when the body needs it, for example, to replace damaged cells. However, sometimes a wrong mutation occurs in the genes, which causes the cell to turn into a cancerous cell. These wrong gene mutations can be inherited or caused by something damaging our genes, for example, ultraviolet (UV) sun radiation or cigarette smoke. However, the aging of cells can also cause wrong gene mutations. Different types of mutations can happen, from which different mutants can arise. Cancerous cells do not work as healthy cells; they divide and grow at an uncontrolled rate. They also develop differently from

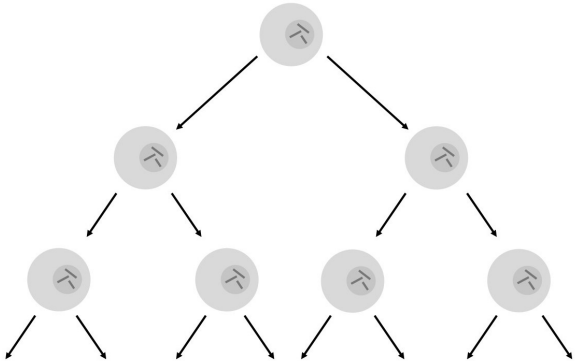

Figure 2.1: The process of cell division shows how each cell divides into two identical cells that are copies of the cell of origin. A constant cell growth rate means an exponential tissue growth.

healthy cells; they stay immature and undifferentiated, whereas normal cells mature with a specific job they should perform. Cancerous cells also dodge the immune system and ignore the signs telling them to die or stop dividing. What also makes these cells more dangerous is that they do not stick together, but they spread into other parts through the blood vessels or lymphatic system. In organs, cancerous cells damage and grow into the organs and tissues. All these properties make cancerous cells particularly dangerous [23].

A group of abnormal growing cells is called a tumor. A tumor can either be malignant, which means it is cancerous or benign (also called nonmalignant), which means that it does not spread to other parts of the body. Tumor cells have the same needs as healthy cells, involving a blood resource for oxygen and nutrients to keep growing. At the beginning of a tumor, so when it is still small, it can proliferate. However, when cancer becomes more prominent, it needs more blood to have enough oxygen and nutrient supply. Then the tumor can make new blood vessels and still keep growing. Therefore cancerous cells can smoothly go into the blood and spread to other parts of the body. When the cancerous cells spread from where the tumor first started, the primary site, to another part of the body, we speak of metastasis. Figure 2.2 shows how the cancerous cells spread to other parts of the body by going into blood and lymph vessels.

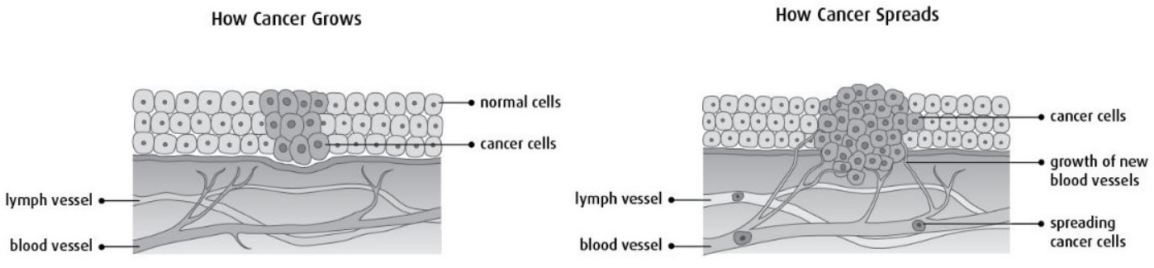

Figure 2.2: The process of cancerous cell growth and spread through the body. The cancerous cells go into the blood and lymph vessels, which results in metastasis [23].

There are many types of cancerous cells, each with their properties. Cell lines can be created from cancerous cells. A cell line is a cell culture that is developed from a single cell and hence has the same genome. Laboratories use these cell lines for research. A cell can mutate into another cell type when specific mutations happen. Tumors can also consist of different tumor cells, that are heterogeneous in their gene expression and metastatic potential, which is referred to as intratumor heterogeneity. Interpatient tumor heterogeneity also exists, where every tumor with the same subtype from a different patient behaves in a clinically different way, independent of treatment [24].

2.1.2 The staging of cancer

Cancer is often classified in stages, which refers to how much the disease is developed. Staging is useful, so there is a universal language in determining the size and the spread of cancer, and treatment outcomes and guidelines can be compared fairly. One of the generally used staging systems is the TNM system [25]. The TNM systems uses three subsystems [26]:

- The T refers to the primary tumor size, where it is classified as 1 (very small) up to 4 (large).
- The N stands for the regional lymph nodes involvement, ranging from 0 (no lymph nodes are cancerous) up to 3 (many lymph nodes are cancerous).
- The M refers to the metastases of cancer, where it can be either a 0 (no metastases) or 1 (cancer has spread through the body).

For example, severe cancer can be classified as T3 N3 M1, where cancer has spread through the body and to many lymph nodes. Some variations of the TNM system exist, for instance, where the subsystems are further classified using letters a,b,c, or more. These letters provide more information about cancer. For example, for lung cancer that has metastases M1a can refer to the metastasis being in the other lung, and M1b can refer to the metastasis being in another part of the body.

Another way that is used for describing the tumor stage is by the following five phrases:

- In situ: cancer that is in situ means that there are abnormal cells, but they have not spread to tissues in the area.
- Localized: a localized form of cancer is when the tumor is only in the primary tumor site.
- Regional: regional cancer is when the tumor has spread to surrounding lymph nodes, organs, or tissues.
- Distant: a distant cancer is when the tumor has spread to distant sites of the body.
- Unknown: when the cancer stage is unknown, there is not enough available information to determine the stage.

There are many other ways of defining cancer staging, and some tumors also have there own staging system, such as brain cancer.

2.1.3 Treatment options for cancer

There are many treatment options for cancer, and there are many more in development. The most suitable treatment option depends on many factors, such as the tumor site and stage, the overall health conditions, and the preferences of the patient. The main treatment options and their basic principle of operation are listed here:

- Surgery: a surgeon operates a patient, and the tumor is removed as much as possible with medical instruments. This treatment option is very efficient since a lot of the tumor is removed at once. However, it cannot always be used since not all sites are easy to access, or the health conditions of the patient do not allow the operation.

- Chemotherapy: a systematic drug is used to kill fast reproducing cells, including cancerous cells. Section 2.2 will elaborate further on how chemotherapy works.

- Radiation therapy (or radiotherapy): the tumor is locally treated with radiation, which eventually causes cell death. Section 2.3 will elaborate further on radiotherapy.

- Targeted therapy: this cancer treatment targets the specific properties that make cancerous cells different from healthy cells. An approach is, for example, to target proteins that exist in cancerous cells, but not in normal cells. The downside of this treatment is that, when it is given on its own, it is often not enough to kill the cancerous cells, and is therefore often combined with chemotherapy. Targeted therapy is also not available for all types of cancer.

- Immunotherapy: this is a biological therapy, which uses substances from organisms to treat cancer. It works by helping the immune system to identify and kill the cancer cells better.

- Hormone therapy: hormones nurture certain types of cancer; in these cases, hormone therapy can be used. By removing the hormones or by blocking their effect, this therapy forces cancerous cells to stop or reduce their growth.

There are more treatment options, such as bone marrow transplant, and many clinical trials are being done to find more treatments. The treatment options are very often combined. For example, the tumor is removed as much as possible with surgery, and the last remaining parts are treated with radiotherapy. The treatment options chemotherapy and radiotherapy will be described in more detail since they are the focus of this research project.

When deciding which treatment option is most suitable, it is important to consider the goal of the treatment, which is not always to cure the patient of cancer. These are the goals for which a treatment can be given:

- Curative: this is when a treatment option is given to completely remove or kill the cancerous cells and cure the patient. Any treatment can be used as a curative treatment, but the most common is surgery and radiotherapy.

- Palliative: these treatments are given to relieve the patient's suffering, caused, for example, by the symptoms of cancer or the side effects of some other treatment. It can be used at the same time as a curative treatment. Surgery, radiotherapy, chemotherapy, and hormone therapy can be used as palliative treatments.
- Adjuvant: an adjuvant treatment is given to treat the remaining cancerous cells after curative treatments, to make the chance of recurring cancer smaller.
- Neoadjuvant: a neoadjuvant therapy works based on the same principle as the adjuvant therapy, but the treatment is given before the curative treatment to make it more effective. Any treatment can be used as adjuvant or neoadjuvant treatment.

2.2 Chemotherapy

As mentioned in Section 2.1.3, chemotherapy is a commonly used cancer treatment, which can be given on its own or in combination with other treatments. This section discusses how chemotherapy works and the current state of the art regarding treatment scheduling.

Chemotherapy relies on drugs referred to as chemotherapeutic agents. They interfere with the cell cycle and the mitosis process [27], and therefore interrupt cell division. They effectively target the properties in cells that allow them to grow and divide, for example, such that they can replicate their DNA. Chemotherapy is a systematic treatment, which has the advantage that all metastases are treated at once. Chemotherapeutic agents are most effective on cancerous cells; however, healthy cells also need to replicate and are also affected by the toxic agents. The use of this treatment, therefore, gives many and often severe side effects, such as nausea, vomiting, and acute gastrointestinal effects. So there is a trade-off between the reduction of cancer cells and the cytotoxicity effects. The chemotherapeutic agents have the most harmful side effect on the healthy cells that have a high cell turnover, such as bone marrow and hair follicles [32]. The toxicity can vary per patient and is different for specific drugs, doses, and schedules.

When determining a chemotherapy schedule, certain factors are taken into account. The cancer type and stage, results of tests, and the patient's age and overall health conditions are all included in the decisionmaking. This information is combined with information from studies and similar patients, and a drug or drug combination is determined. Currently, the chemotherapeutic agents are given at their highest tolerable dose to obtain the optimal reaction [28]. The dose is either dependent on the patient's body weight or their body surface area (BSA), calculated from the height and weight. Chemotherapy is normally given in cycles, which are regular intervals of drug administration. A cycle is a day or multiple days on which a dose is given, followed by a period without treatment, in which the healthy cells get the time to recover. The final treatment schedule is most useful for the specific cancer it is developed for, and if possible, the patient needs to receive the full course of chemotherapy. However, sometimes side effects can become severe, and it is necessary to alter the planned dose and schedule, making it very important to monitor the patient during treatment.

Next to the side effects that can occur, patients can also become resistant to the chemotherapeutic agents due to random mutations [8]. To lower the chance of resistance, often, several drugs are given together. Different anti-cancer drugs work in different ways and can be used

together to work more effectively. When a single drug is used, and resistance occurs, it is possible to switch to another drug. However, there is only a limited amount of chemo drugs available for each type of cancer, which can result in running out of options of chemotherapy treatments.

During the process of determining a chemotherapy treatment schedule, no optimization is done: the choice is based on clinical experience and the outcomes of research and trials. The modeling and optimization of chemotherapy schedules are still a relatively uninvestigated field. This is partly due to the unknown when a treatment will be successful or unsuccessful. Much research is done to determine this and investigate what the precise influences are. Within the field of chemotherapy modeling, the "log kill" hypothesis was the general standard for a long time, stating that, independent of the tumor size, the amount of tumor cells killed by the chemotherapeutic agents is solely dependent on the given dose of chemotherapy [29], [30]. Currently, the focus has shifted to the Goldie-Coldman hypothesis, which states [5]:

- The probability that the patient will be fully cured of cancer by the treatment of chemotherapy is inversely related to the volume of the tumor. Therefore the treatment should be initiated as early as possible.
- To obtain the optimal effect against heterogeneous cell groups, different chemotherapeutic agents should be used at the same time. When that is not possible, it is beneficial to switch among different chemotherapeutic agents.

Another central theory within chemotherapy effect modeling is the Norton-Simons hypothesis, saying that the tumor regression rate as a consequence of the chemotherapeutic agents is proportional to the growth rate of the undisturbed tumor of similar size [31].

2.3 Radiotherapy

In this section, it will be discussed how radiotherapy works and how a treatment plan is obtained. Then two models will be discussed that are used in the thesis, the BED model, and the NTCP model.

2.3.1 Radiotherapy treatments

As mentioned in Section 2.1.3, radiotherapy works by irradiating the tumor, which causes cell death. It aims to inhibit the reproduction of tumor cells, while normal cells get spared as much as possible [4]. There are two types of radiation therapy, internal and external beam radiotherapy, of which the latter is the most common option. With the internal type, also called brachytherapy, a radioactive source is placed inside or near the tumor and irradiates the tumor locally. In external radiation, a machine, a linear accelerator (LINAC), emits highly energized particles, such as X-rays, and deposits this energy in the tissues it passes through. The beams are directed from different angles, overlapping at the targeted region, such that the tumor volume receives the highest radiation dose, and the surrounding healthy tissue gets spared as much as possible. This energy is disruptive for cells; it can cause cell death or genetic changes. The genetic changes that occur prevent the cells from reproducing and

eventually also cause cell death since the radiation has a direct effect on the DNA of a cell and can cause damage. Radiation also has an indirect effect on the DNA, which is caused by free radicals produced by ionization or excitation of the water in cells [3]. Since DNA molecules consist of two strands, either a double-strand break (DSB) or a single-strand break (SSB) can occur. Repairing a DSB is more complex than a SSB and causes more cancerous cells to die. The DNA breaks are visualized in Figure 2.3.

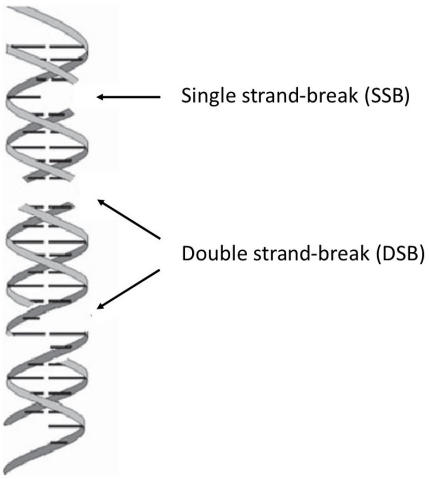

Figure 2.3: Radiation targets to damage the DNA of cancerous cells, which can lead to cell death. This can occur from a double-strand break and a single-strand break, where a double-stand break creates more damage and causes more cells to die.

The radiation does not kill the cells immediately; this process takes days or weeks of treatment. Although the radiation is directed at the tumor, the surrounding healthy tissues inevitably suffer from the effect of radiation as well. The side effects caused by radiation are therefore dependent on the tumor site, and they can be severe and long term. Many patients also experience fatigue during treatment. Repeated dose delivery is applied to minimize the damaging effect in the normal cell since healthy cells repair the damage done by radiation faster than cancerous cells. The effect of radiation on cancerous cells can differ per tumor type [3].

Before the treatment can start, a radiation plan has to be made. The physical dose of radiation is described in units of Gray (Gy), which is defined as the absorption of one joule (J) radiation energy per kilogram (kg) of matter; hence 1 $Gy = 1\ \frac{J}{kg}$ [6]. A standard radiotherapy treatment, referred to as fractionation scheme, can be a total dose of 60 Gy delivered in fractions of 2 Gy, referred to as the fractionated dose. The treatment doses are based on clinical experience and standard protocols, there is no individual optimization done. The delivery schedule of the radiation is, in contrary to the treatment doses, patient-specific, and optimized with computational algorithms. A computed tomography (CT) scan is made, and in the CT slices are the organs and the targeted region defined, generally with a margin around the tumor to account for microscopic spread [32]. Much research exists on how to optimally make a radiation delivery plan [33], [34], [35], hence a plan that specifies how the beams should be directed to obtain a maximal dose delivery in the tumor and a minimal dose delivery in the surrounding tissues.

2.3.2 Biologically effective dose (BED) model

Within radiotherapy modelling, the linear-quadratic (LQ) model is widely accepted to model the biological effects of radiotherapy [4], [5], [6]. It can be derived in multiple ways, one of which expresses the surviving fraction $\frac{N_d}{N_0}$ for a clonogenic cell population N_d after receiving a dose d as:

$$\ln\left(\frac{N_d}{N_0}\right) = -\alpha_T d - \beta_T d^2 \tag{2.1}$$

Equation (2.1) describes the radiation dose d in Gy, and the amount of tumor cells before and after dose d are N_0 and N_d respectively. The parameters α_T and β_T depend on the type of tissue of the tumor volume [7]. Parameter α_T in Gy^{-1} represents the coefficient of DSBs caused by the radiation, and β_T in Gy^{-2} the coefficient of the combination of two SSBs caused by radiation [4]. After rewriting Equation (2.1) the surviving fraction of tumor cells, S, after dose d can be described as:

$$S(\alpha_T, \beta_T, d) = \frac{N_d}{N_0} \tag{2.2}$$

$$= \exp(-\alpha_T d - \beta_T d^2) \tag{2.3}$$

Since S is the surviving fraction of tumor cells, $1-S$ can be taken as the fraction of cell death. The total dose P_{tot} is administered in a number of fractions n_f to limit the toxic effects to the healthy tissues. The fractionated dose is described as $d_1, d_2, ..., d_{n_f}$. Then the survival fractions from all individual fractionated doses can be multiplied with each other, assuming independent dose effects, and their resulting survival fraction is [21]:

$$S(\alpha_T, \beta_T, d_f) = \exp(-\sum_{f=1}^{n_f}(\alpha_T d_f + \beta_T d_f^2)) \tag{2.4}$$

To further analyze the structure of this formula, a comparison is made between two cases. When the dose is delivered at once, according to Equation (2.3), and in multiple fractions, according to Equation (2.4). The result can be seen in Figure 2.4: the effect of the quadratic factor becomes less prominent when the dose is delivered in multiple fractions. Hence there is a larger survival fraction than when the dose is delivered at once. However, the toxic effects become larger when a higher dose is given. So there is a trade-off between maximizing the cell death with large single doses and sparing the healthy tissues with fractionated doses [21].

The BED is commonly used to model nonstandard fractionation schemes [21]. The BED can be defined as:

$$\mathrm{BED}(\alpha_T, \beta_T, d_f) = -\ln(S)/\alpha_T \tag{2.5}$$

$$= \sum_{f=1}^{n_f}\left(d_f + \frac{d_f^2}{[\alpha/\beta]_T}\right) \tag{2.6}$$

where the ratio $[\alpha/\beta]_T$ is normally approximated as a constant, and differs per type of tumor [7]. The $[\alpha/\beta]_T$ ratio corresponds to the tissue sensitivity to fractionation.

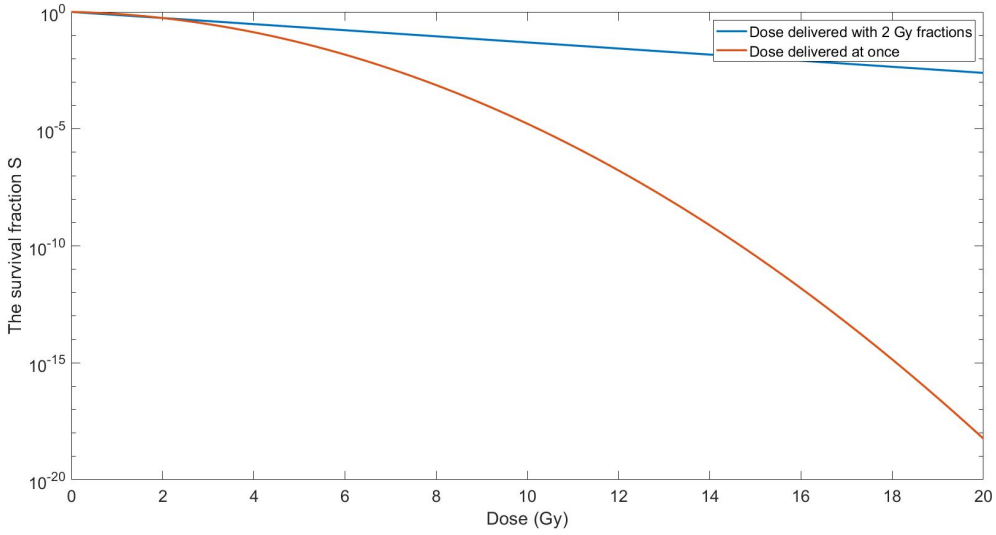

Figure 2.4: A comparison between the survival fraction of cells when the dose is delivered at once or in 2 Gy fractions. The survival fraction S is calculated with the LQ model with $\alpha_T = 0.1$ and $\beta_T = 0.3$.

2.3.3 Normal tissue complication probability (NTCP) model

Within the modeling of radiotherapy, the NTCP models are used to quantify the probability of complications in healthy organs and tissues. For the organs at risk (OARs), this probability can be calculated for a plan, and it can be checked if it meets clinical constraints. OARs are normally organs near the tumor site. It is inevitable that they also receive some radiation, which puts their functioning at risk.

One of the NTCP models is the logit model. This model depends on the X Gray equivalent dose (EQDX), with X the reference dose. The OAR does not receive as much radiation as the tumor, so the fractionated dose d_f is multiplied with the organ sparing factor s, with $0 \leq s \leq 1$. When $s = 1$, the OAR is radiated just as much as the tumor, and when $s = 0$, the organ is not radiated at all. The formula for the EQDX is [36]:

$$EQDX_{OAR} = \frac{BED_{OAR}}{1 + \frac{X}{[\alpha/\beta]_N}} \tag{2.7}$$

$$= \frac{\sum_{f=1}^{n_f} sd_f \left(1 + \frac{sd_f}{[\alpha/\beta]_N}\right)}{1 + \frac{X}{[\alpha/\beta]_N}} \tag{2.8}$$

with d_f the fractionated dose and $[\alpha/\beta]_N$ the tissue dependent parameters. It is important to take the $[\alpha/\beta]$ ratio from the normal tissues, noted as $[\alpha/\beta]_N$. Healthy tissues respond different to radiation then tumor tissues so different parameters are required.

An example of the EQDX is when a treatment plan of 60 Gy is given in fractionated doses of 4 Gy; then, the EQD2 is the equivalent dose when given in fractions of 2 Gy. For $[\alpha/\beta]_N = 3$ and $s = 1$ this will be 84 Gy, calculated as $EQD2 = \frac{60(1+4/3)}{1+2/3}$. Often the EQD2 is used since

2 Gy is a typical fractionated dose in clinical practice. However, other fractionated doses can be used, as well.

There are many different forms of NTCP models, but all models represent the response curve typically with a sigmoid shaped function that depends on the dose. For this thesis the logit model is used, for which the formula is [37]:

$$NTCP_{logit} = \left(1 + \left(\frac{D_{50}}{EQDX_{OAR}}\right)^{4\gamma_{50}}\right)^{-1} \tag{2.9}$$

where NTCP refers to the probability of a severe side effect occurring. D_{50} is the radiation dose that gives a response probability of 50% and γ_{50} is the slope of the response curve at the D_{50} point [38]. These parameters depend on the type of side effect. The $EQDX_{OAR}$ is defined by Equation (2.8).

Chapter 3

Theoretical background for the chemotherapy model

This chapter discusses the theoretical background behind the model to optimize and schedule chemotherapy. The approach used in [16] to determine optimal targeted therapy treatments will be adapted for chemotherapy applications. In Section 3.1 positive switched systems will be presented, discussing how they can be used for this treatment. Then the multi-compartment model will be addressed in Section 3.2. The optimization problem will be formulated in Section 3.3 and last an algorithm to schedule the drugs will be introduced in Section 3.4.

3.1 Positive switched systems

A positive switched system is a dynamic system consisting of a set of Metzler state-space matrices and a certain switching law σ. This switching law determines when and how to switch between the subsystems [39]. Positive switched systems are suitable for many applications, including health and biological systems. In [13], [14], [19] a positive switched linear system is used to describe HIV infection treatments and in [16], [17] for treatments with targeted therapy. In current treatments for HIV infection and cancer treatment with targeted drugs, resistant mutations are normally observed after some time, and the treatment no longer works as desired [40]. When this happens, a new treatment therapy is initiated. However, switching therapies well in advance of the failure may be more efficient. The mentioned literature proposes methods to treat this scheduling problem as a switching control problem. In cancer treatment with chemotherapeutic drugs, similar resistant mutations are observed, and switching therapies in advance of resistance could also provide more efficient treatments. This section describes how positive switched systems can be used to model cancer evolution under chemotherapy treatments.

The optimal control will be derived for a switched autonomous positive linear system of the class:

$$\begin{aligned} \dot{x}(t) &= M_{\sigma(x(t))}x(t) \\ x(0) &= x_0 \end{aligned} \tag{3.1}$$

In case of cancer treatment with chemotherapy, the states $x(t) \in \mathbb{R}^n_+$ describe the concentration of mutant cell lines in a patient. In this model $\sigma(x(t))$ is the switching signal, in this case the drug selection, with $\sigma : \mathbb{R}^n_+ \to \{1, \dots, d\}$. The matrices $M_\sigma \in \mathbb{R}^{nxn}$ corresponds to different choices of σ. The system, Equation (3.1), is positive when the system matrices M_σ are Metzler for all σ. The definition for Metzler is as follows:

Definition 3.1.1. A square matrix M is *Metzler* if its off-diagonal entries are non-negative, hence when $[M]_{ij} \geq 0$ for all $i \neq j$ [19].

The switched system, Equation (3.1), will be modified so that the sliding trajectories are also included. Sliding trajectories occur when an infinite frequency switching of $\sigma(t)$ happens. Although this is clinically impossible, it often leads to the optimal solution and is hence important to consider. The overarching system is:

$$\dot{x}(t) = \sum_{s=1}^{d} M_s(l(t))x(t) \tag{3.2}$$

with control vector $l(t) \in \mathbb{U}^d_+$, the unit simplex, and where $[l(t)]_s$ (the s-th component of $l(t)$) represents the normalized concentration of drug s. Equation (3.2) contains Equation (3.1) since $l(t)$ is the unit simplex, hence $[l(t)]_s = 1$ implies $[l(t)]_z = 0$ for $z \neq s$, and this corresponds to $\sigma(x(t)) = s$. If $l(t)$ does not correspond to a vertex of the unit simplex, for any $t \geq 0$, then no direct equivalent exists for σ. The set of all possible trajectories generated by Equation (3.1) is dense in the set of possible trajectories of Equation (3.2). The optimal control of Equation (3.2) is therefore considered, which extends the original switching laws to infinite frequency switching with suitable differential inclusions.

An optimal control $[l]_s$ will be derived for this class of systems, which minimizes the cost function:

$$J = h^T x(T_F) \tag{3.3}$$

with the vector $h \in \mathbb{R}^n_+$, typically $h = \mathbf{1}_n$, and the final time $T_F > 0$ fixed. In the case of cancer treatment, it is in general not required for the treatment to completely make the tumor disappear, hence to make $\mathbf{1}^T x(T_F) = 0$, for a patient to heal. When the tumor cell population is small enough, the immune system can naturally destroy them, and a shorter therapy duration (when possible) is beneficial to contain the side effects harming the patient. The immune system is not modeled in the positive switched system described by Equation (3.1), but can take care of a small enough number of cancer cells [17].

Based on [16], [18], [19], [22] some remarks regarding the convexity can be made. Given the system described by Equation (3.2) with cost function Equation (3.3), and assuming the

off-diagonal entries of matrix M_s for $s = 1, ..., d$ are not depending on s, then matrices M_s can be written as:

$$M_s(l(t)) = A - D_s[l(t)]_s \tag{3.4}$$

where A is a Metzler matrix describing the mutation dynamics without drugs and D_s, for $s = 1, ..., d$, are positive diagonal matrices describing the effects of the drugs. For $[l(t)]_s = 1$, drug s is at the maximum dose that is tolerated at time t and its efficacy is given by $D_s(t)$. When $[l(t)]_s = 0$, drug s is not used at all at time t. Then the system can be rewritten as:

$$\dot{x}(t) = \left[A - \sum_{s=1}^{d} D_s[l(t)]_s\right] x(t) \tag{3.5}$$

The system described by Equation (3.5) is of the same form as the system in [22] where it is proved that this system is a convex-monotone system, see Definition 3.1.4. This means that the system is monotone and the state trajectory is a convex function of the initial state as well as the input trajectory [16]. This also implies that when convex constraints are used and the objective function is also convex, optimal drug doses $[l(t)]_s$ for $s = 1, ..., d$ can be found via convex optimization [22].

Definition 3.1.2. Consider a system of the form

$$\begin{aligned} \dot{x}(t) &= f(x(t), u(t)) \\ x(0) &= a \end{aligned} \tag{3.6}$$

with $x(t) \in X \subset \mathbb{R}^n$, $u(t) \in U \subset \mathbb{R}^d$, and X and U convex sets. Denote the unique solution of Equation (3.6) as $x(t) = \phi_t(a, u)$. Then the system in Equation (3.6) is said to be *monotone* if the solution is a monotone function of the initial state a and the input trajectory u, i.e. if

$$(a_0, u_0) \leq (a_1, u_1) \Longrightarrow \phi_t(a_0, u_0) \leq \phi_t(a_1, u_1) \tag{3.7}$$

for all $t \geq 0$, where the inequalities are element-wise [22].

Definition 3.1.3. A scalar function $g(x, u)$ is said to be *convex* if for any two points (x_1, u_1) and (x_2, u_2)

$$g(\lambda x_1 + (1-\lambda)x_2, \lambda u_1 + (1-\lambda)u_2) \leq \lambda g(x_1, u_1) + (1-\lambda) g(x_2, u_2) \tag{3.8}$$

for all $\lambda \in [0, 1]$.

Definition 3.1.4. A system of the form in Equation (3.6) that is monotone and where every row of $f(x(t), u(t))$ is also convex, is said to be *convex-monotone* [22].

3.2 Multi-compartment evolutionary model

A multi-compartment evolutionary model is proposed to describe the dynamics of the tumor and the influence of anti-cancer drugs [16], [17]. This model makes use of compartments to describe the growth of a tumor, the metastasis, the possibility for mutation, and the influence of drugs on the different components of a heterogeneous tumor. For a tumor with m different mutant species that has spread to p compartments and where there are d different chemotherapeutic drugs (or specified appropriate drug combinations) available the following variables and parameters are defined:

- $x_i^k \in \mathbb{R}_+$ represents the amount of cells of cell line i in compartment k
- r_i^k describes the growth rate of mutant cell line i in compartment k
- $q_{ij,k}$ describes the probability that mutant cell line j mutates to mutant cell line i in compartment k
- $\mu_{ck,i}$ represents the migration rate of mutant cell line i from compartment k to compartment c
- $l \in \mathbb{R}_+^d$ represents the vector of drug concentrations, where each component $[l]_s$ belongs to a drug s
- $\psi_i^k(l)$ is the overall drug dose response in compartment k for mutant cell line i

Then the dynamics of the concentration of tumor cells are described as:

$$\dot{x}_i^k = r_i^k q_{ii,k} x_i^k + \sum_{j=1,j\neq i}^{m} r_i^k q_{ij,k} x_j^k + \sum_{c=1}^{p} \mu_{kc,i} x_i^c - \sum_{c=1,c\neq k}^{p} \mu_{ck,i} x_i^k - \psi_i^k(l) x_i^k \tag{3.9}$$

These dynamics are unstable when no therapy is administered, hence when $[l]_s = 0$ for all $s \in \{1, ..., d\}$. The first positive term of these dynamics represent the growth of cell line i in compartment k, $r_i^k q_{ii,k}$. The growth rate is multiplied with the probability that cell line i will not mutate, $q_{ii,k}$. The second positive term represents the possibility that other cell lines mutate into cell line i, $\sum_{j=1,j\neq i}^{m} r_i^k q_{ij,k}$, and the third of cells that are migrated to compartment k, $\sum_{c=1}^{p} \mu_{kc,i}$. The negative terms represent the possibility of migrating to another compartment, $\sum_{c=1,c\neq k}^{p} \mu_{ck,i}$, and the effect of the drugs, $\psi_i^k(l)$. The dynamics of cell line i in compartment k are mostly determined by the growth rate of that cell line and the influence of drugs on that cell line. The possibility of migration and mutation of cells is several orders of magnitude smaller than the growth of cells.

The possibility of migration and mutation is visualized in Figure 3.1. Panel (A) shows that a tumor cell line i in compartment c can either migrate to another compartment, described by μ_{kc}, or stay in place, described by μ_{cc}. The right panel, (B), shows a zoomed-in version of compartment c, where the tumor cell lines i and j are shown. There is a chance of mutating into the other mutant described by q_{ij} and q_{ji}, and a chance that no mutation occurs described by q_{ii} and q_{jj}.

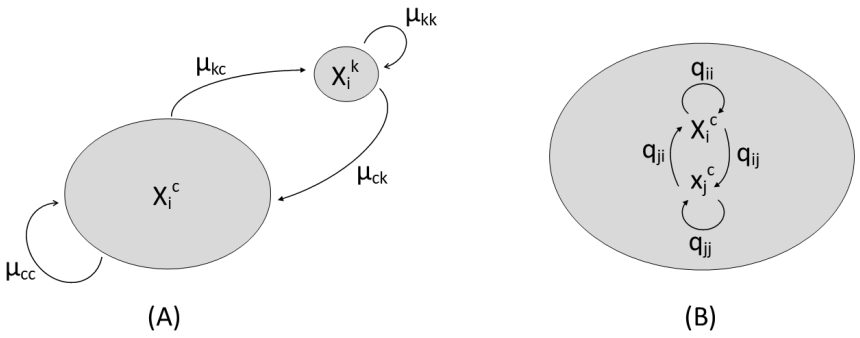

Figure 3.1: Visualization of the multi-compartment model which shows the possibility of migration between compartments c and k (A) and the possibility of mutation within compartment c (B).

The model described by Equation (3.9) can be rewritten as:

$$\dot{x}(t) = [A - \Psi(l(t))]\, x(t) \tag{3.10}$$

which emphasizes the model structure more specifically, since the matrix $A \in \mathbb{R}^{nxn}$, with $n = mp$, describes the dynamics without the influence of drugs, and the matrix $\Psi(l) \in \mathbb{R}^{nxn}$ describes the drug effects. Both matrices A and Ψ are chosen to be consistent with the dynamics in Equation (3.9). Furthermore, matrix A is an unstable Metzler matrix and matrix $\Psi(l)$ is a diagonal matrix, where each diagonal entry is an increasing function of l. The vector $x \in \mathbb{R}^n$ is the stacked vector of the tumor cell line populations. Due to the biological properties involved are the diagonal elements of matrix A several orders of magnitude bigger than the off-diagonal elements. As mentioned, the growth has a significant bigger impact on the dynamics than the migration and mutation possibility. The matrix A is therefore close to diagonal.

The matrix function $\Psi(l)$ can be approximated using linear functions of l. Because the doses of the drugs are not taken greater than the Maximum Tolerated Dose (MTD), and for drug amounts that are taken far from saturation, the drug effects can be well approximated to be linear. The drug concentration vector $l(t)$ that is considered is the unit simplex for each t, so $[l(t)]_s \in \{0, 1\}\ \forall s, t$ and $\sum_{s=1}^{d} [l(t)]_s = 1\ \forall t$, since a drug should either be used at its MTD or not at all. So the effect of all drugs can be taken as the sum of each drug separately, for each mutant species, in each compartment. Hence Equation (3.10) can then be rewritten into:

$$\dot{x}(t) = \left[A - \sum_{s=1}^{d} D_s [l(t)]_s\right] x(t) \tag{3.11}$$

with the positive diagonal matrix $D_s \in \mathbb{R}^{nxn}$ representing the effect of drug s. The system in Equation (3.11) is precisely in the form of Equation (3.5), and hence is a convex-monotone system.

3.3 Optimization problem formulation

It is desired to design an optimal drug scheduling that minimizes the tumor size. The problem is split up into two separate problems. First, the optimal drug doses are calculated that minimize the total number of tumor cells at the end of the treatment horizon. Then the scheduling of the drugs is addressed with an algorithm that specifies in which order the drugs need to be used. In this section, the optimization formulation for the first problem is given.

The tumor size of each metastasis is represented by the number of tumor cells in each compartment. The total tumor size at the end of treatment is minimized, hence $\mathbf{1}_n^T x(T_F)$ is minimized over finite treatment horizon T_F. The control vector is the drug concentrations $l(t)$, which is the unit simplex per time t. When the drug is used, the MTD is given, so $[l(t)]_s$ is normalized to $[l(t)]_s = 1$ for all s. Furthermore, the switching therapy should specify a single drug per time instance, which should stay constant for a minimum amount of time. As a consequence is the drug dose $l(t)$ described as piecewise-constant in time. For an implemented dwell time, is the total treatment time $[0, T_F]$ divided into N_T intervals $T_1, T_2, ..., T_{N_T}$ with a desired amount of time between them, and the drug choice becomes:

$$l(t) = \begin{cases} l^{(1)}, & t \in [0, T_1) \\ l^{(2)}, & t \in [T_1, T_1 + T_2) \\ \vdots & \vdots \\ l^{(N_T)}, & t \in \left[\sum_{i=1}^{N_T - 1} T_i, T_F\right) \end{cases} \tag{3.12}$$

The optimization to obtain the optimal drug concentrations per time interval, $l(t)^*$, is described by:

$$\min_{l^{(1)},...,l^{(N_T)}} \quad \mathbf{1}_n^T \prod_{i=1}^{N_T} \exp\left[\left(A - \sum_{s=1}^{d} D_s [l^{(i)}]_s\right) T_i\right] x(0) \tag{3.13}$$

$$\text{s.t.} \quad [l^{(i)}]_s \in \{0, 1\}, \quad \forall s \in \{1, ..., d\}, \forall i \in \{1, ..., N_T\} \tag{3.14}$$

$$\sum_{s=1}^{d} [l^{(i)}]_s \leq 1, \quad \forall i \in \{1, ..., N_T\} \tag{3.15}$$

The cost function Equation (3.13) minimizes the total tumor size at the end of the treatment, i.e. $\mathbf{1}_n^T x(T_F)$. Equation (3.14) specifies that when a drug is used it is used at its MTD and Equation (3.15) specifies that the total MTD used per time interval cannot exceed 1. Due to the first constraint, convex mixed integer nonlinear programming is necessary to solve this problem. When the constraint is relaxed to $[l^{(i)}]_s \geq 0$ the problem can be solved with convex optimization. This optimization problem is convex as shown in [19], since the system Equation (3.11) is convex-monotone and the objective function and the constraints are also convex. However, the resulting outcome corresponds to applying multiple drugs at the same time interval at lower doses than their MTD. This is not always appropriate to all chemotherapeutic drug combinations. Only specified combinations are allowed, or else undesired consequences could arise.

Note that when matrix A is a diagonal matrix, the optimization problem Equation (3.13) up to Equation (3.15) can, in fact, be solved with convex optimization, while also making sure that only one drug is used in each time interval [16]. When matrix A is diagonal, the matrices $\left(A - \sum_{s=1}^{d} D_s[l^{(i)}]_s\right)$ commute and the formulation can be rewritten.

Another approach can also be adapted. Instead of defining the control vector as the drug concentrations, it will be defined as the fraction of time each drug should be used at its MTD. Define $\tilde{l}$ as the vector of time fractions, where each component $[\tilde{l}]_s$ refers to the fraction of the total treatment horizon T_F drug s should be used at its MTD. To be precise, define $[\tilde{l}]_s$, the s-th component of $\tilde{l}$, as:

$$[\tilde{l}]_s = \frac{\sum_{i=1}^{N_T} [l^{(i)}]_s T_i}{T_F}, \quad \forall s \in \{1, ..., d\} \tag{3.16}$$

The following example can be used to clarify. A time horizon of 60 days is considered, which is divided into 3 intervals of 20 days. When 2 drugs are considered the optimal model outcome is to use drug 1 in the first 2 intervals at its MTD, and drug 2 in the last interval at its MTD. This treatment schedule corresponds to $l^{(1)} = [1\ 0]^T$, $l^{(2)} = [1\ 0]^T$, and $l^{(3)} = [0\ 1]^T$ with the previous formulation. In the new formulation this corresponds to $[\tilde{l}]_1 = 2/3$ and $[\tilde{l}]_2 = 1/3$ since drug 1 should be used 2/3 of the time and drug 2 for 1/3 of the time. The total amount of days drug s is used, is $\sum_{i=1}^{N_T} [l^{(i)}]_s T_i$ in the previous formulation and $T_F[\tilde{l}]_s$ in the new formulation.

The optimization formulation is rewritten for the adjusted control vector. The optimization problem, to minimize the total number of tumor cells at the end of the finite treatment horizon T_F, becomes:

$$\min_{\tilde{l}} \quad \mathbf{1}_n^T \exp\left[\left(A - \sum_{s=1}^{d} D_s[\tilde{l}]_s\right) T_F\right] x(0) \tag{3.17}$$

$$\text{s.t.} \quad [\tilde{l}]_s \geq 0, \quad \forall s \in \{1, ..., d\} \tag{3.18}$$

$$\sum_{s=1}^{d} [\tilde{l}]_s \leq 1 \tag{3.19}$$

The cost function, Equation (3.17), minimizes the total final number of tumor cells, $\mathbf{1}_n^T x(T_F)$, with respect to the new control vector $\tilde{l}$. The outcome is the optimal duration each drug should be used, denoted by $\tilde{l}^*$. The first constraint, Equation (3.18), specifies that the fraction of drug usage cannot be smaller than zero, i.e., no negative times are allowed. The second constraint, Equation (3.19), specifies that the total days of drug usage is not greater than the final treatment horizon T_F. These constraints do not imply directly that only one drug at a time is used, but that criteria can be easily implemented in the scheduling by applying the drugs after each other. This optimization formulation can now be solved with convex optimization, while still making sure that drugs are used at their MTD.

Note that, with this formulation of the optimization problem, the term $\sum_{s=1}^{d} [\tilde{l}]_s$ will always be pushed to 1, since no negative consequences are included due to the given drugs. Chemotherapy, however, is a toxic drug and does provoke side effects. The chemotherapy-induced side effects should preferably be based on the total dose. The total dose given is most likely the biggest determining factor regarding side effects. However, due to a lack of clinical data, the

required information to calculate this is unavailable. Therefore, assume a roughly constant dosage of chemotherapy, then the total treatment time is a good indicator of the total dose. So for simplicity, it is assumed that the probability of having severe side effects increases over the chemotherapy treatment time. A constraint can be added to the optimization problem to incorporate these side effects. The probability of having severe side effects is defined as a function dependent on the treatment time, $g(t)$. Unfortunately, there is a lack of models in the literature to describe this, so the NTCP model from radiotherapy is implemented. The NTCP logit model, Equation (2.9), is adjusted for the chemotherapy application in the following way:

$$g(t_{chem}) = \left(1 + \left(\frac{D_{50,chem}}{t_{chem}}\right)^{4\gamma_{50,chem}}\right)^{-1} \tag{3.20}$$

with $0 \leq t_{chem} \leq T_F$, $D_{50,chem}$ the treatment time with a 50% response probability, and $\gamma_{50,chem}$ the slope at that point. Then the constraint that should be added to the optimization problem defined by Equation (3.17) up to Equation (3.19) is:

$$g(t_{chem}) \leq g_{max} \tag{3.21}$$

with g_{max} the set maximum probability of severe side effects and t_{chem} the treatment days of chemotherapy. Now the final treatment time T_F can be limited by the side effects, when T_F is chosen long enough. This constraint can be recast into a linear constraint by taking Equation (3.20) out of the optimization. For the fixed maximum probability of severe chemotherapy-induced side effects, g_{max}, the associated maximum treatment duration T_{max} can be calculated by solving $g(T_{max}) = g_{max}$. This is equivalent to solving $T_{max} = \frac{D^*_{50,chemo}}{\tilde{\gamma}^*\sqrt{1/g_{max}-1}}$ with $\tilde{\gamma}^* = 4\gamma^*_{50,chemo}$. The linear constraint then becomes:

$$T_F \sum_{s=1}^{d} [\tilde{l}]_s \leq T_{max} \tag{3.22}$$

The total treatment days of all chemotherapeutic drugs are calculated by $T_F \sum_{s=1}^{d} [\tilde{l}]_s$, which should not exceed the maximum allowed treatment duration T_{max}. When $T_{max} \leq T_F$, instead of using the constraint, also $T = T_{max}$ can be used in the optimization problem. When $T_{max} > T_F$, i.e. when the finite horizon is smaller than then the maximum allowed treatment duration regarding side effects, the constraint will not be active. This can, for example, be the case when chemotherapy is used as neoadjuvant treatment, and there is only a short time interval for the therapy. The complete optimization problem becomes:

$$\min_{\tilde{l}} \quad \mathbf{1}_n^T \exp\left[\left(A - \sum_{s=1}^{d} D_s [\tilde{l}]_s\right) T_F\right] x(0) \tag{3.23}$$

$$\text{s.t.} \quad [\tilde{l}]_s \geq 0, \quad \forall s \in \{1, ..., d\} \tag{3.24}$$

$$\sum_{s=1}^{d} [\tilde{l}]_s \leq 1 \tag{3.25}$$

$$T_F \sum_{s=1}^{d} [\tilde{l}]_s \leq T_{max} \tag{3.26}$$

where T_{max} is the solution of $g(T_{max}) = g_{max}$ with function $g(t_{chem})$ defined by Equation (3.20). Also, $\sum_{s=1}^{d}[\tilde{l}]_s$ in Equation (3.25) will not necessarily become 1 anymore, since the toxicity can become too large. The treatment time that is used can be defined as $T^* = T_F \sum_{s=1}^{d}[\tilde{l}]_s^*$.

3.4 Drug scheduling problem

With the optimization formulation described in Section 3.3 the optimal days of each treatment are calculated, described by $T_F[\tilde{l}]_s^*$. However, the problem when and in which order to schedule the drugs arises, which is addressed in this section. An important criterion is that the drugs are scheduled after each other, and not at the same time, due to the unknown consequences that could arise.

The idea is that the tumor should be minimized as soon as possible, in line with the first statement of the Goldie-Coldman hypothesis. The optimization will decide the second statement of the Goldie-Coldman hypothesis. So if there is a choice of multiple drugs to schedule, the "strongest" drug should be used first in order to reduce the tumor as soon as possible. The strongest drug will be defined as the drug that has the most significant effect on the specific tumor when given on its own.

The procedure that will be used to calculate this is as follows. For a certain initial tumor, described by $x(0)$, the optimization described by Equation (3.23) up to Equation (3.26) calculates the optimal fraction of time each drug should be used, described by $[\tilde{l}]_s^*$ for $s = \{1, ..., d\}$. To decide in which order the drugs should be used, calculate the effect they have, when administered on their own, on the specific tumor. So for a time horizon T_F apply each possible drug for the entire time interval and calculate the effect of the drugs as the sum over the final tumor states: $N_s = \mathbf{1}_n^T \exp\left[(A - D_s)\, T_F\right] x(0)$. Another time interval than T_F can also be used, as long as the same time is used for all drugs for an equal comparison. Order the outcome effect from low to high with the corresponding drugs. This will be the order in which the drugs are used, with the drug that caused the smallest final tumor given first. Of course, the drugs will not be used for T_F days, but for their corresponding optimal amount of days $T_F[\tilde{l}]_s^*$. The entire procedure can be summarized in the following algorithm:

Algorithm 1: Drug scheduling

input : Matrices A and D_s, $s = 1, ..., d$, final time T_F, initial condition $x(0)$, optimal drug durations $\tilde{l}^*$.

output: A treatment plan to schedule the chemotherapeutic drugs with their optimal duration

1 **for** *s=1:d* **do**
2 | Calculate the effect of drug s for time interval T_F on the tumor with initial condition $x(0)$:
3 | $N_s = \mathbf{1}_n^T \exp\left[(A - D_s)\, T_F\right] x(0)$
4 **end**
5 Arrange all N_1 up to N_d from small to large.
6 Give the drugs in that order, with drug s first, that has the smallest N_s, for $T_F[\tilde{l}]_s^*$ days.

It is possible that when $[\tilde{l}]_s^*$ is too small, the drug will not have any effect. However, it is not precisely known after how much time this is. For simplicity, this aspect will not be taken into account. Also, a schedule where drugs are alternated may provide a better outcome. However, then the problem arises for how long the drugs need to be administered after each other to be useful and for how long a pause can be held before the drugs do not become effective anymore. This aspect is not explored much since the focus of this thesis was not on the scheduling. Also, due to the almost diagonal property of matrix A, the overall drug duration is significantly more important than when each drug is used.

Chapter 4

Case study: colorectal cancer

The model will be tested on a clinical example. The tumor site that is chosen is colorectal cancer (CRC). In this chapter, all CRC related parts will be discussed. First, the properties of this tumor are mentioned in Section 4.1, then the dataset that was obtained from the Erasmus MC is discussed in Section 4.2. The model parameters are estimated in Section 4.3, and the chemotherapy-induced side effects are estimated in Section 4.4.

4.1 Some information about colorectal cancer

CRC is cancer that originates in the colon or rectum. It is sometimes also referred to as rectal, bowel, or colon cancer. CRC is the third most diagnosed type of cancer, and the fourth cause of death [41], [42], [43]. This type of cancer was chosen as a case study since many types of chemotherapy are available as treatment, and combined chemo-radiation treatments are commonly used. Also, since this type of cancer is of frequent occurrence, much research has been done concerning the properties and effects of treatments.

Many treatment options exist for CRC. When it is caught at an early stage, then polyps or cancerous cell groups can be removed with a colonoscopy. When it is caught in a more advanced stage, surgery can be used to eliminate parts or, in exceptional cases, even the whole colon. Chemotherapy and radiotherapy are often used as an adjuvant or neoadjuvant treatment to surgery. In some cases, immunotherapy or targeted therapy can also be used as treatments. For the model, three chemotherapeutic drugs are chosen: capecitabine, irinotecan, and 5-fluorouracil (5-FU). For a list of all approved drugs, the reader is referred to [44]. These drugs are often used in combination with other drugs, enhancers, or radiotherapy. However, for this example, the effects are studied when they are administered on their own.

A property of CRC is high intra-tumor heterogeneity, which can result in reduced treatment effects [45]. Sub-populations of the tumor can have different sensitivity to certain drugs, and even be resistant, which can cause recurrence after treatment. The intra-tumor heterogeneity causes different therapeutic outcomes, even when the tumors have equivalent TNM stages [46]. These properties emphasize the need for optimal treatment calculations. For treatment

determination, extensive tests should be done to classify the sub-populations as accurately as possible. These tests include TNM staging and the mutation analysis that specifies the specific mutation status, from which certain cell properties can be derived.

There are many different CRC cell lines, of which six will be chosen for the model: HT29, HCT116, SW620, DLD1, HCT15, and SW48. Each of these cell lines has its own properties and sensitivity to drugs and radiation. Each CRC cell line has a cell line origin, which can be found in [47]. The cell line types, mutation status, and properties are shown in [48]. The diameter of one CRC tumor cell is, on average, approximately 11 μm [49], which is equal to $11 \cdot 10^{-3}$ mm.

4.2 Erasmus MC dataset irinotecan

The CPCT01 dataset was obtained from the Erasmus MC, thanks to Dr. S. Bins. The data file contains information about 43 patients who were treated with irinotecan (CPT-11), and it was used to validate the model. The most useful data given in the dataset will be explained.

The dataset contains all 43 patients' information about the primary tumor site. The available primary tumor sites are CRC, esophagus, pancreas, stomach, major duodenal papilla, cholangio, duodenum, appendix, and adenocarcinoma of unknown primary (ACUP). These are all sites in the human digestive system. For each patient, a measure is made of the tumor size at baseline and after each even number of cycles, so after 2 cycles, 4 cycles, and so on up to 12 cycles. The doses and dates of treatment are given per cycle, with an average time of 22 days between two consecutive cycles. When the dose is changed or when the treatment is stopped, the reason for this is given. The date of death is also given when a patient is deceased.

The tumor size is measured according to RECIST 1.1 [50]. RECIST is used in clinical applications in the Erasmus MC. It is an assessment for the change in tumor burden, which measures the tumor shrinkage as well as disease progression. The RECIST measure contains tumor lesions and malignant lymph nodes. The sum of the diameters is taken for the target lesions. For the non-nodal lesions, the longest diameter is taken, and the diameters are incorporated for a minimum size of 10 mm when measured on a CT scan. For the nodal lesions, the short axis diameter is taken when the size is at least 15 mm established on a CT scan. All other lesions are classified as non-target lesions, for example, that have smaller sizes or that are non-measurable.

Before this dataset was used to validate the model, it was examined closely. In Table 4.1 information of the data set is summarized. The number of patients per group can be found. Information is given on the sex of the patient, their primary tumor, prior treatments, the amount of cycles administered, their RECIST size at baseline, and how much the tumor has grown or decreased after treatment. Especially this last category stresses the different reactions patients have to treatment. On some patients, the treatment is effective, with a reduction of up to 60%. However, for most patients, 21 in total, the treatment was insufficient to make the tumor decrease.

Table 4.1: Patient information of the Erasmus MC dataset. Number of patients are given per sex, primary tumor, prior treatment options, treatment duration, RECIST size at baseline, and how much the tumor has grown/decreased after treatment.

Category	Sub categories	Number of patients
Sex patient	Male	29
	Female	14
Primary tumor	CRC	19
	Esophagus	9
	Stomach	4
	ACUP	3
	Cholangio	3
	Pancreas	2
	Appendix	1
	Duodenum	1
	Major duodenal papilla	1
Prior treatment	Radiotherapy	14
	Surgery	26
Treatment duration (cycles)	1	5
	2	18
	3	1
	4	5
	5	3
	6	6
	7	0
	8	2
	9	1
	10	1
	11	0
	12	1
RECIST size at baseline (mm)	0 - 50	8
	51 - 100	19
	101 - 150	7
	151 - 200	8
	201 - 250	1
Percentage of tumor growth after treatment	1 - 20%	11
	21 - 40%	7
	41 - 60%	3
Percentage of tumor reduction after treatment	1 - 20%	6
	21 - 40%	6
	41 - 60%	2

4.3 Model parameter estimations

The parameters that are needed for the model are estimated for this tumor example. The estimated parameters for the growth rates and drug effects are obtained from mouse tumor xenograft models. These in vivo studies can be used for the analysis of human cell and gene therapies as pre-clinical oncology research. Typically a human cell line is cultured to a certain amount and injected into a number of mice. Nude mice are commonly used since they have a reduced immune system. Depending on the research goal of the study, the mice receive different drug quantities or drug combinations, and the tumor volume over time is studied and compared to each other.

Another type of study that can be used is the in vitro study to obtain the half-maximal inhibitory concentration (IC50). The IC50 quantifies how much of a drug, or other inhibitory substance, is needed to cause a 50% inhibition of a particular biological process. The IC50 is typically measured in the molar concentration. The murine tumor models are preferred for the model parameter estimations, since they examine the drug effects over time and because they are in vivo experiments.

4.3.1 Growth rates of the cell lines

The growth rate of the CRC cell lines without the influence of drugs has to be calculated. In Equation (3.9) the growth rate of cell line i in compartment k is represented by r_i^k. Without considering migration, mutation, and drug effects the dynamics can be reduced to $\dot{x}_i^k = r_i^k x_i^k$, for which $x_i^k(t) = e^{r_i^k t} x_i^k(0)$ describes the solution. It is assumed that the growth rate of each mutant is independent of the compartment, hence $r_i^k = r_i$. An exponential curve is fitted through the line in the xenograft graph that represents the tumor growth without the influence of drugs, typically referred to as vehicle or control, to obtain the growth rate of r_i. An example of how the growth rate is fitted is shown in Appendix A.1. The growth rates for the six human CRC cell lines can be found in Table 4.2.

Table 4.2: The growth rate parameters for the six human CRC cell lines derived from existing mouse tumor xenograft studies as listed. Where there are multiple references, an average is taken.

CRC cell line	Growth (rate/day)	Ref.
HT29	0.0976	[52], [53], [54]
HCT116	0.133	[55]
SW620	0.0813	[56]
DLD1	0.269	[57]
HCT15	0.186	[58], [59]
SW48	0.193	[58]

Table 4.2 shows that the fastest-growing cell line is DLD1, with a rate of 0.269, and the slowest growing cell line is SW620, with a rate of 0.0813.

4.3.2 Migration rates

There is a chance of migration for mutant i from compartment k to c, described by the migration probability $\mu_{ck,i}$. It is assumed that the chance of migration is the same for all mutant cell lines, hence $\mu_{ck,i} = \mu_{ck}$. Furthermore, it is assumed that the cells only migrate away from the primary site and not back again. So there is a chance p_m of migrating from the primary site to another site, and a chance $1 - p_m$ of staying in the primary site. The probability of staying in the primary site is taken from the SEER dataset [51]. In this dataset, the amount of examined lymph nodes that are found positive for CRC is, amongst other things, described. Of the data 49% of all CRC cases are found to have no positive lymph nodes, so $1 - p_m = 0.49$ and $p_m = 0.51$. The parameter μ_{ck} is the probability per cell and per time instance. On average, those tumors have a diameter of 40 mm, so approximately $5 \cdot 10^{10}$ cells when estimated as a sphere. The time it takes for a tumor to grow to that size is taken as 50 days, which is approximately in line with the growth parameters. The probability of migration per cell per day is approximately $0.51/(5 \cdot 10^{10})/50 \approx 2 \cdot 10^{-13}$.

To conclude, for CRC where compartment c is the primary site and compartment k a lymph node, then the migration rate per day per cell line is $\mu_{ck} = 0$ and $\mu_{kc} = 2 \cdot 10^{-13}$. The migration rate between lymph nodes is also taken as 0, so for compartment k_1 a lymph node, and compartment k_2 also a lymph node, then $\mu_{k_1 k_2} = \mu_{k_2 k_1} = 0$.

4.3.3 Mutation rates

There is also a chance of mutation from mutant j to mutant i in compartment k, which is described by $q_{ij,k}$. It is assumed that the mutation rate is independent of the compartment, hence $q_{ij,k} = q_{ij}$. It is not well known what the actual chance of mutation into another cell line is, so an estimate is made. For a cell line to mutate into another cell line, a series of independent mutations need to happen. In [70], it is stated that a common estimate of order for the possibility that a mutation will happen in stem cells is at least 10^{-8}. CRC cells have a lower mutation rate than stem cells, so the lower bound of 10^{-8} is taken. These CRC cell lines have five different mutation statuses (BRAF, KRAS, TP53, PTEN, and PIK3CA), so if five independent mutations need to happen, then $(10^{-8})^5 = 10^{-40}$ is q_{ij}. The reader is referred to [48], [71] for the specific mutation status of the CRC cell lines. Some cell lines may be more likely to arise than others. Also, assuming equal mutation rates for all cell lines signifies that all cell lines are just as likely to mutate into one another. So when the same amount of cells are considered, the mutation rate has no influence. A variation in mutation rate is therefore used per cell line. Since the mutation rates are not exactly known, the following assumption is made: cell line j can mutate into i, but not the other way around, for $j < i$. With $j < i$ is meant the order in which they are listed in Table 4.2. For example, cell line HT29 can mutate into cell line SW48 with a probability of $q_{ij} = 10^{-40}$, but SW48 cannot mutate into HT29.

Hence the probability for a cell line j to mutate into cell line i in any compartment is $q_{ij} = 10^{-40}$ for $j < i$ and $q_{ij} = 0$ for $j > i$. And the probability of staying the same cell line is $q_{jj} = 1 - \sum_w q_{wj}$. This can be summarized by:

$$q_{ij} = \begin{cases} 10^{-40}, & j < i \\ 1 - \sum_w q_{wj}, & j = i \\ 0, & j > i \end{cases} \tag{4.1}$$

4.3.4 Chemotherapeutic drug effects

The effect of the three anti-cancer drugs is calculated on the six CRC cell lines. In Equation (3.11) the effect of the drugs is described by $-\sum_{s=1}^{d} D_s l_s(t)$, and each entry $[D_s]_{ii}$ represents the effect of drug s on cell line i. It is assumed that the drug effects are the same for each compartment; hence they only depend on the cell line and the drugs. Note that for some compartments, like the brain, certain boundaries exist through which the drugs do not penetrate well. So for those compartments, a conversion ratio should be used between the drug effects in different compartments.

For the chemotherapeutic drugs capecitabine, irinotecan, and 5-FU, the effects on the six CRC cell lines are calculated for the MTD schedule of each drug. An exponential curve is fitted through the line in the xenograft that represents the MTD schedule of the drug. This growth rate of cell line i with the influence of drug s is represented by $\tilde{r}_i^s$. When $\tilde{r}_i^s < 0$, the drugs have a reducing effect on the cells, and when $\tilde{r}_i^s = r_i$, the drugs do not affect the cells. The drug effect parameters $[D_s]_{ii}$ can then be calculated in the following way:

$$[D_s]_{ii} = r_i - \tilde{r}_i^s \tag{4.2}$$

First, the tumor growth rates with the influence of drugs, hence $\tilde{r}_i^s$, are given in Table 4.3. The only drug that has a reducing effect is irinotecan on cell line SW620. The other drugs have either no effect (resistance) or an inhibitory effect on the growth of the tumor. For the drugs that are assumed to be resistant, when no information was found, the tumor growth rate with the influence of drugs is taken the same as the growth rate without the influence of drugs in Table 4.2, i.e., $\tilde{r}_i^s = r_i$.

Table 4.3: Tumor growth rates of six CRC cell lines with the influence of the chemotherapy treatment capecitabine, irinotecan, or 5-FU, derived from existing mouse tumor xenograft studies as listed, $*$ adjusted for the MTD treatment plan based on reference, $\diamond$ estimated based on IC50, $\circ$ no information found so resistance is assumed.

CRC cell line	Capecitabine (rate/day)	Ref.	Irinotecan (rate/day)	Ref.	5-Fluorouracil (rate/day)	Ref.
HT29	0.0106	[60]	0.0638	[54]	0.0705	[61]
HCT116	0.0764	[62]	0.0318*	[55]	0.0659	[63]
SW620	0.0752	[64]	-0.0283*	[56]	0.0653	[65]
DLD1	0.269°		0.0156	[66]	0.0606	[65], [67]
HCT15	0.186°		0.129*	[59]	0.0322*	[68]
SW48	0.193°		0.0210$^\diamond$	[69]	0.193°	

The actual drug effect parameters that are used in the model are given in Table 4.4. These parameters represent the entries of the diagonal matrix D_s for each drug. These drug effects correspond to the effect when the treatment is given on its own. An example of how the drug effect parameters are obtained is in Appendix A.2.

Table 4.4: Drug effect model parameters for the chemotherapeutic drugs capecitabine, irinotecan and 5-FU. Calculated by subtracting the growth rate with the influence of drugs, in Table 4.3, from the growth rate without the influence of drugs, in Table 4.2.

CRC cell line	Capecitabine (rate/day)	Irinotecan (rate/day)	5-Fluorouracil (rate/day)
HT29	0.0870	0.0338	0.0271
HCT116	0.0566	0.101	0.0671
SW620	0.00610	0.110	0.00160
DLD1	0	0.253	0.208
HCT15	0	0.0570	0.154
SW48	0	0.172	0

A higher drug effect parameter in Table 4.4 corresponds to a more significant difference between the tumor volume with and without the influence of drugs, hence the more significant the effect of the drugs. Even though irinotecan is the only drug is that made one of the cell lines decrease, namely SW620, the effect of the drug on that cell line is not the largest. Some cell lines are assumed to be resistant to some drugs, which is represented by a 0 drug effect parameter.

4.4 Chemotherapy side effects estimation

The parameters for the side effects caused by the chemotherapeutic drugs are also estimated. The Erasmus MC dataset was used to do this. Even though this dataset is for irinotecan, it will be used to describe the side effects of all three chemo drugs due to a lack of other data.

In the dataset, all patients are taken, not just the patients that have CRC as primary tumor site. All patients are taken since the side effects of the drugs are considered, regardless of the tumor site, and else data points would be insufficient. Hence it is assumed that the drug has the same side effects on all patients independent of their primary tumor site. This assumption is reasonable since chemotherapy is a systematic drug that works on all cells in the body and not just on the cancerous cells. The data that are used are the number of cycles given and the reason for dose adjustment. The number of patients that had a dose adjustment because of severe side effects is counted. Examples of these side effects are fever, vomiting, diarrhea, ascites (stomach fluid), dyspnea (shortness of breath), cholangitis (biliary tract infection), and a general worsening of conditioning. Other factors could be necessary for the reaction of a patient to a drug that is not taken into account. Such factors are the overall health conditions of the patient, the reaction of the patient to other drugs, whether the patient received another chemotherapeutic treatment before, or the patient's age. The data points that are obtained from the Erasmus MC dataset are given in Table 4.5. The number of cycles is coupled per two cycles, to obtain slightly bigger and more reliable patient groups. So for patients that either receive 1 or 2 cycles of irinotecan, the probability of dose adjustment, hence severe side effects, is 13%. This is done for the other cycles as well.

Table 4.5: Information obtained from the Erasmus MC dataset about the number of patients that had their irinotecan treatment dose adjusted per total number of cycles. The percentage per two treatment cycles is given.

Total cycles	Total patients	Patients with dose adjustment	Percentage
1,2	23	3	13 %
3,4	6	1	17 %
5,6	9	2	22 %
7,8	2	1	50 %
9,10	2	0	0 %
11,12	1	1	100 %

The information from Table 4.5 is transformed into data points. The y-axis of the data points come from the number of cycles, that is transformed into treatment time, by multiplying it with 22 days. The data points that are used for the side effects are: $(0, 0)$, $(33, 0.13)$, $(77, 0.17)$, $(121, 0.22)$, $(165, 0.50)$, $(253, 1)$. The point for 9 or 10 cycles is not taken into account, since it seems unrealistic, and is probably caused by the few patients in that group.

The side effects caused by chemotherapy are represented with a converted NTCP model, for which the formula is:

$$g(t_{chem}) = \left(1 + \left(\frac{D_{50,chem}}{t_{chem}}\right)^{4\gamma_{50,chem}}\right)^{-1} \tag{4.3}$$

which is the same as Equation (3.20). The parameters $D_{50,chem}$ and $\gamma_{50,chem}$ should be estimated such that the function fits the data points best. With the Matlab function `lsqcurvefit` the function $g(t_{chem})$ is fitted to the data points with the parameters $D_{50,chem}$ and $\gamma_{50,chem}$ using the Trust-region-reflective algorithm to do a non-linear least square fitting. The result of the algorithm gives the optimal parameter values $D^*_{50,chem} = 158$ and $\gamma^*_{50,chem} = 1.20$. The curve with the used data points can be seen in Figure 4.1.

The curve cannot fit the data points exactly, due to the s-shape of the function. However, the sum of the squared 2-norm of the residual is 0.0478, which is low enough for this rough estimate. When a maximum probability of side effects has been chosen, the maximum allowed treatment time can be read from this graph. This corresponds to:

$$T_{max} = \frac{D^*_{50,chemo}}{\sqrt[\tilde{\gamma}^*]{1/g_{max} - 1}} \tag{4.4}$$

with $\tilde{\gamma}^* = 4\gamma^*_{50,chemo}$. Since the side effects from each chemotherapeutic drug are assumed to be equal, and the side effects are assumed to have an additive effect, T_{max} is the total treatment time that is allowed for all drugs. So T_{max} should be distributed over the optimal drugs to use.

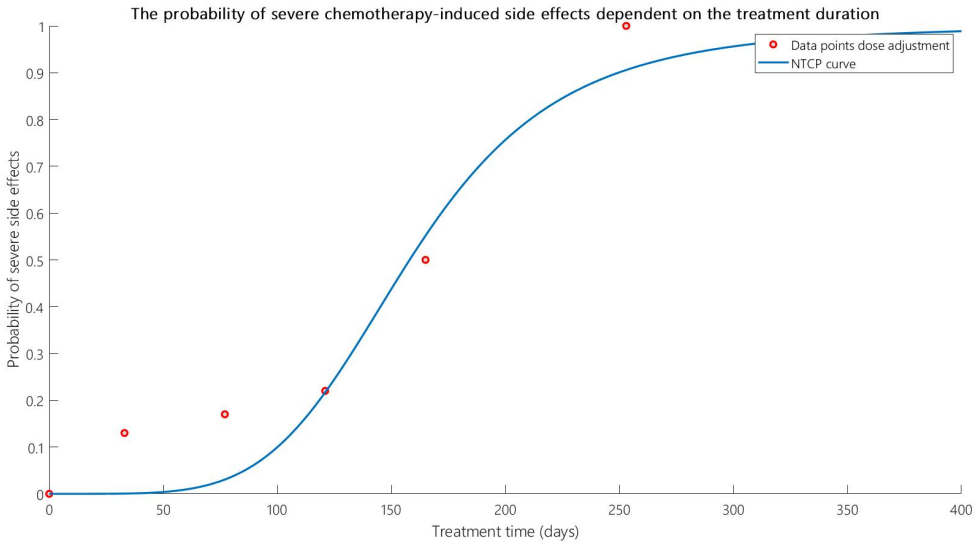

Figure 4.1: Fitting of $g(t_{chem})$ to the data points obtained from the Erasmus MC irinotecan dataset, given in Table 4.5, based on patients that had a dose adjustment due to severe side effects.

It is important to note that this is not a standard prediction of the probability of chemotherapy-induced side effects; it is only a very rough estimate based on a novel approach to model side effects. As this has not been done in the literature before, and it is not precisely known what causes the different reactions to chemotherapy, this approach is adopted. Also, ideally, different functions would be used for each of the drugs, but due to a lack of data, this function will be implemented for all drugs.

Chapter 5

Chemotherapy model simulations

To validate the model, its outcomes will be compared to real clinical data from the Erasmus MC. The data shows patients that received an irinotecan treatment. In this section, the model outcomes are compared with the clinical data in Section 5.1. Then, the initial tumors of the clinical data are used as input for the model optimization in Section 5.2. Last, the chapter is summarized in Section 5.3.

5.1 Model validation with clinical data

The model results will be compared to the Erasmus MC dataset. The dataset contains data of patients that received an irinotecan treatment. The model will be used to model the effect of this treatment. However, since only one treatment option is available, there is no need to do the optimization. Thus, the dataset is used to validate the model formulation described by Equation (3.11), which is simplified to:

$$\dot{x}(t) = [A - D_2]\, x(t) \tag{5.1}$$

where D_2 refers to the drug effect matrix from irinotecan. The drug concentration $[\tilde{l}]_2 = 1$ is used, since irinotecan is given during the whole treatment horizon. The side effects will be ignored for the comparison, since the final model time is taken as the clinical treatment duration.

It will be assumed that the doses given to the patients correspond to the MTD. Even though the doses are sometimes lowered, this will not be taken into account. All these assumptions can influence the outcomes. However, the most crucial goal is to show that, when the right information is known, the model can simulate all types of responses, which is a wide variety, as shown in Section 4.2.

We select the patients in the Erasmus MC dataset with a treatment time of at least two cycles, since the tumor sizes are measured after every two cycles. This gives a total of 38 patients. All these patients will be used, not only the ones that have CRC as the primary site,

to have a bigger comparison set. Even though the model is used with CRC cell lines, due to the different responses the patients have, the other sites are comparable to them as well. The essential characteristics of each patient will be described in Table 5.1. The primary tumor site is given for each patient, where the underlined patients correspond to the ones that have CRC as the primary tumor. The RECIST size at baseline, the total number of cycles, and the reason why the treatment has stopped are also listed.

The tumor size of the patients is measured in RECIST, as explained in Section 4.2. Unfortunately, it is not known if there are metastases, how many, where they are, and what their size is. Therefore some general assumptions are made so that the clinical data can be compared to the model outcomes. It is assumed that for each patient, 80% of their RECIST size corresponds to their primary tumor diameter. If the full RECIST size was used as the primary tumor diameter, the model would predict a faster-growing tumor than the clinical case. Since the model assumes an exponential growth, a bigger primary tumor corresponds to a faster-growing tumor. However, in the clinical case, that volume is probably distributed over different locations, and therefore grows slower. The fraction of the RECIST size is taken as primary tumor diameter, to compensate for this effect roughly. The lesions will be left out, so only the primary tumor site will be compared. The lesions are not considered since their location and size are unknown, which can have large influences on the growth. Also, since their separate growth is unknown, the additional value in comparison is little. The initial condition of the model will be taken as the clinical situation. However, the initial condition uses the number of tumor cells and not the diameter. So the diameter will be transformed into the number of tumor cells in the following way. The tumor volume is approximated as sphere [73], as well as the cell volume, for which the following formula is used [74]:

$$V_{\text{sphere}} = \frac{4}{3}\pi\frac{\varnothing^3}{8} \tag{5.2}$$

where $\varnothing$ corresponds to the diameter of the tumor or a cell, both in mm. Once the volume is known, the number of tumor cells can be calculated. The diameter of one CRC tumor cell is approximately $11 \cdot 10^{-3}$ mm [49]. The number of tumor cells per compartment can be calculated by dividing the tumor volume with the CRC cell volume.

The initial condition for the model will be taken as the total amount of tumor cells corresponding to a tumor of 80% of the RECIST size. However, it is not known how these tumor cells are distributed over the different cell lines. The difference in tumor composition is one of the possible explanations for the different reactions of each patient to the same drug. Unfortunately, this information is not given in the dataset. The following approach will, therefore, be carried out. Optimization with respect to the tumor composition (given the total amount of cells) is done to give the best fit to the clinical data. This will be done in three steps. First, in Section 5.1.1, the clinical data is compared to the model data at every two cycles, to see whether all possible final tumor sizes can be replicated. Then, in Section 5.1.2, the whole treatment time is considered, to see if the model can replicate the tumor volume evolution over time. Finally, in Section 5.1.3, the drug effects are varied slightly to see if a better fit can be obtained.

The following rule of thumb can be used to check if realistic states are obtained. A rough estimate for the number of tumor cells per cm^3 of tissue volume is around 10^8 - 10^9. The number of tumor cells can be divided by the volume in cm^3, to check whether this is the case for the states.

Table 5.1: The clinical patient set used for the validation and optimization of the model. The underlined patients have CRC as primary tumor site. ACUP refers to adenocarcinoma of unknown primary, PD stands for progressive disease, AE are adverse events and $\#N/B$ means no data available.

Patient	Primary tumor	RECIST(0)	Cycles	Reason stop
1	esophagus	175	12	PD
2	CRC	29	10	#N/B
3	duodenum	75	8	Other
4	stomach	166	9	#N/B
5	CRC	129	6	PD
6	CRC	72	6	Other (maximum number of cycles according to protocol)
7	CRC	93	6	PD
8	stomach	11	6	PD
9	CRC	46	6	PD
10	esophagus	71	6	PD
11	ACUP	147	5	Clinically determined (vomiting, ascites, malaise, diarrhea)
12	cholangio	157	5	AE
13	CRC	49	5	#N/B
14	CRC	90	4	PD
15	esophagus	84	4	PD
16	appendix	62	4	PD
17	CRC	66	4	AE
18	CRC	194	4	#N/B
19	esophagus	103	4	PD
20	CRC	83	2	AE
21	ACUP	99	2	AE (patient's refusal because of AE's during cycle 1+2)
22	CRC	70	2	PD
23	CRC	81	2	PD
24	esophagus	78	2	PD
25	stomach	87	2	PD
26	esophagus	53	2	PD
27	CRC	71	2	PD
28	papil Vater	117	2	PD
29	CRC	196	2	PD
30	ACUP	166	2	PD
31	esophagus	215	2	PD
32	esophagus	101	2	PD
33	CRC	153	3	Clinically determined (fever, renal insufficiency, increasing belly, swollen legs)
34	CRC	157	2	PD
35	pancreas	38	2	PD
36	esophagus	22	2	PD
37	CRC	92	2	Clinically determined (progression of primary tumor requiring radiotherapy.)
38	CRC	94	2	PD

5.1.1 Comparison at each clinically measured point

As mentioned in Section 4.2, the Erasmus MC dataset consists of RECIST tumor measures per patient per two treatment cycles. Each cycle is, on average, 22 days long, and the total amount of cycles is different per patient. The approach that will be carried out in this subsection is to neglect the time horizon and look at each tumor measurement separately. The tumor measurements are done per two treatment cycles, so at 44 days, 88 days, and so on. The initial tumor composition will be optimized such that the difference between the true clinical tumor and the modeled tumor is minimized at those time points separately, so at 44 days, 88 days, and so on.

To be more precise, at a certain time T_c, which corresponds to the duration of an even number of treatment cycles, the true clinical amount of tumor cells N_{true} is calculated, which is defined as:

$$N_{true}(T_c) = \frac{V_{true}(T_c)}{V_{cell}} \tag{5.3}$$

$$= \frac{\frac{4}{3}\pi \frac{\varnothing_{true}(T_c)^3}{8}}{\frac{4}{3}\pi \frac{\varnothing_{cell}^3}{8}} \tag{5.4}$$

$$= \frac{\varnothing_{true}(T_c)^3}{\varnothing_{cell}^3} \tag{5.5}$$

with $\varnothing_{true}(T_c)$ the fraction of the RECIST size at time T_c and $\varnothing_{cell}$ the diameter of a CRC cell. It should be noted that N_{true}, V_{true} and $\varnothing_{true}$ are not the actual true values, but approximations of the clinically measured data and are used as the true data to compare with the model.

The model predicts the total amount of tumor cells at time T_c, which is represented by $N_{pred}(T_c)$ and calculated in the following way:

$$N_{pred}(T_c, x(0)) = \mathbf{1}_n^T x(T_c) \tag{5.6}$$

$$= \mathbf{1}_n^T \exp\left[(A - D_2)\, T_c\right] x(0) \tag{5.7}$$

with D_2 the drug effect matrix for irinotecan, and $x(0)$ the initial condition. The optimization problem is now formulated. Optimize with respect to the initial composition, for a set time T_c, such that the difference between the true and predicted total amount of cells is minimized. For a fixed T_c the mathematical formulation is:

$$\min_{x(0)} \quad \left(N_{pred}(x(0)) - N_{true}\right)^2 \tag{5.8}$$

$$s.t. \quad [x(0)]_i \geq 0, \quad \forall i \in \{1, ..., n\} \tag{5.9}$$

$$\sum_{i=1}^{n} [x(0)]_i = N_{true}(0) \tag{5.10}$$

with $N_{true}(0)$ the initial amount of tumor cells, N_{true} the clinical amount of tumor cells at point T_c, and $N_{pred}(x(0))$ the models prediction of the amount of tumor cells at point T_c. The squared difference is taken as the cost function in Equation (5.8). The first constraint,

Equation (5.9), specifies that the amount of each cell line at the start cannot be negative. The second constraint, Equation (5.10), specifies that the total amount of tumor cells at the start is equal to the clinical problem, meaning that $N_{pred}(0) = N_{true}(0)$. The optimization is solved with constrained optimization. Constrained optimization minimized an objective function with respect to variables, which have restrictions on them. In this case they are hard constraints, i.e., they have to be satisfied. To solve this optimization, the `Matlab` function *fmincon* is used with a "for" loop over 40 different starting points to reduce the chance of getting stuck in a local optimum.

This optimization problem is solved for all patients, and the difference in the amount of tumor cells and in tumor diameter is calculated. For each patient the mean difference, μ, the standard deviation, σ, and the maximum difference, max, are presented in Table 5.2. The parameters are as specified in Section 4.3.

Table 5.2: The mean difference, standard deviation and maximum difference of the true and predicted number of tumor cells and diameter with optimization formulation Equation (5.8) to Equation (5.10) and parameters as in Section 4.3.

	Difference in tumor cells			**Difference in diameter (mm)**		
Days	$\boldsymbol{\mu_N}$	$\boldsymbol{\sigma_N}$	$\boldsymbol{max_N}$	$\boldsymbol{\mu_\varnothing}$	$\boldsymbol{\sigma_\varnothing}$	$\boldsymbol{max_\varnothing}$
44	$1.76 \cdot 10^7$	$1.08 \cdot 10^8$	$6.67 \cdot 10^8$	0.0742	0.458	2.82
88	58.7	138	489	$2.49 \cdot 10^{-9}$	$5.40 \cdot 10^{-9}$	$1.95 \cdot 10^{-8}$
132	151	299	925	$1.92 \cdot 10^{-8}$	$2.64 \cdot 10^{-8}$	$7.55 \cdot 10^{-8}$
176	459	531	1084	$2.02 \cdot 10^{-8}$	$9.36 \cdot 10^{-9}$	$2.76 \cdot 10^{-8}$

The maximum difference in tumor cells in Table 5.2 is $6.67 \cdot 10^8$ cells, which corresponds to a diameter of 2.82 mm. Consider this patient, hence the patient with the maximum difference in tumor diameter. This patient had a smaller tumor size than the model could replicate on the 44-day horizon. In the clinical case, the tumor size decreases from 22 mm to 8.8 mm. However, the smallest the model could obtain is a diameter of 11.6 mm, which is 32% bigger than the actual tumor. An explanation for this is that not all existing CRC cell lines are included in the model. So the true tumor may consist of cell lines that are more sensitive to irinotecan than the ones included in the model. The mean difference between the true and predicted tumor diameter is 0.0742 mm for the first time interval. So even with this patient, where the difference is 2.82 mm, the mean difference is little. These results get better when a longer treatment horizon is considered, and the difference in diameter is practically negligible. When a longer treatment horizon is considered, the model has more time to obtain the true tumor size, and can, therefore, obtain a better prediction. Thus Table 5.2 shows that each point of treatment can be replicated well when the entire time evolution is not considered.

The true tumor diameter and the predicted tumor diameter after 44 days and 88 days are plotted against each other in Figure 5.1. The model predicts the clinical data very precisely since the points are on or near the linear line. The plots of the other time intervals can be found in Figure B.1.

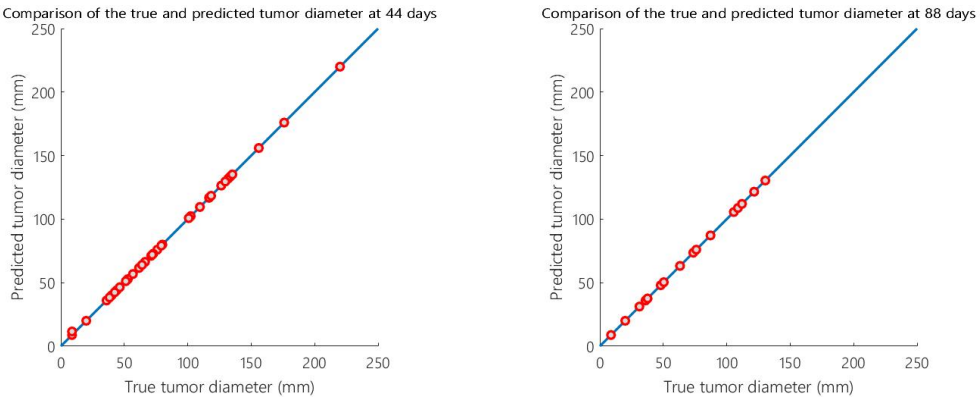

Figure 5.1: The true and predicted tumor diameter plotted against each other at 44 days (left) and 88 days (right). Optimization is performed as in Equation (5.8) to Equation (5.10) and parameters are taken as in Section 4.3.

5.1.2 Comparison over the whole treatment duration

Section 5.1.1 shows that given the same initial point, the model can predict the clinical data well at each point separately. It will be explored if the tumor dynamics over the whole treatment time can also be replicated. Optimization with respect to the initial composition is again performed, but the cost function will be altered such that the whole treatment horizon is considered. By taking the sum over the differences between the predicted and true tumor size at each time point for each patient, the whole time evolution will be examined. The new optimization formulation is:

$$\min_{x(0)} \quad \sum_{T_c=T_s}^{T_m} (N_{pred}(x(0), T_c) - N_{true}(T_c))^2 \tag{5.11}$$

$$s.t. \quad [x(0)]_i \geq 0, \quad \forall i \in \{1, ..., n\} \tag{5.12}$$

$$\sum_{i=1}^{n} [x(0)]_i = N_{true}(0) \tag{5.13}$$

with T_s the starting time and T_m the total amount of treatment cycles the patient received. The functions $N_{true}(T_c)$ and $N_{pred}(x(0), T_c)$ are defined as in Equation (5.5) and Equation (5.7) respectively. This problem is solved with constrained optimization with the `Matlab` function *fmincon*, with a "for" loop over 40 different initial points to reduce the chance of getting stuck in a local minimum.

This optimization is performed for all patients when considering all time points. Per patient the difference between $N_{pred}(T_c)$ and $N_{true}(T_c)$ and between $\varnothing_{pred}(T_c)$ and $\varnothing_{true}(T_c)$ is taken, over all time points without $T_c = 0$ since at that time they are always equal. The mean, standard deviation, and maximum difference are calculated per patient. The complete outcomes of the results can be found in Table B.1. The average mean difference between the true and predicted amount of tumor cells over all patients is $1.36 \cdot 10^{11}$ with an average standard deviation of $5.62 \cdot 10^{10}$. The average mean difference between the true and predicted tumor diameter over all patients and all time points (except the first) is 4.04 mm with an average standard deviation of 1.99 mm. The average mean difference between the true and predicted

tumor diameter over all CRC patients is 2.50 mm, so in general, the model can predict these patients better. In Table B.1, the CRC patients are underlined, and the differences that are higher than the mean of that column are printed in red. It can be seen that patients that received more treatment cycles are more difficult to replicate, which is logical since more points need to be considered. All patient-specific plots with the true tumor diameter and the obtained prediction are presented in Appendix B.4.

Figure 5.2 shows the percentage difference of the tumor diameter for each time point (without the first) for each patient. So at each time point, the difference is calculated between the true and predicted tumor diameter, and this is divided by the true tumor diameter at that time point. For each patient is the percentage difference given for each time point. The patients differ in treatment length, so the number of points per patient are also different. The last 19 patients, for example, only have two data points, which corresponds to only one percent difference in Figure 5.2 since the first point is not shown. The mean percentage difference is also given for each patient. Patients with fewer treatment cycles are overall easier to predict, except for patient 36, which has a significant percentage difference. The percentage difference in 8 out of 38 patients is more significant than 10%; of these 8, only patient 13 is a CRC patients. The average mean percentage difference is 5.17% over all patients, and 3.34% over the CRC patients. The model can replicate the CRC patients, therefore, better in comparison to the other patients in the data set.

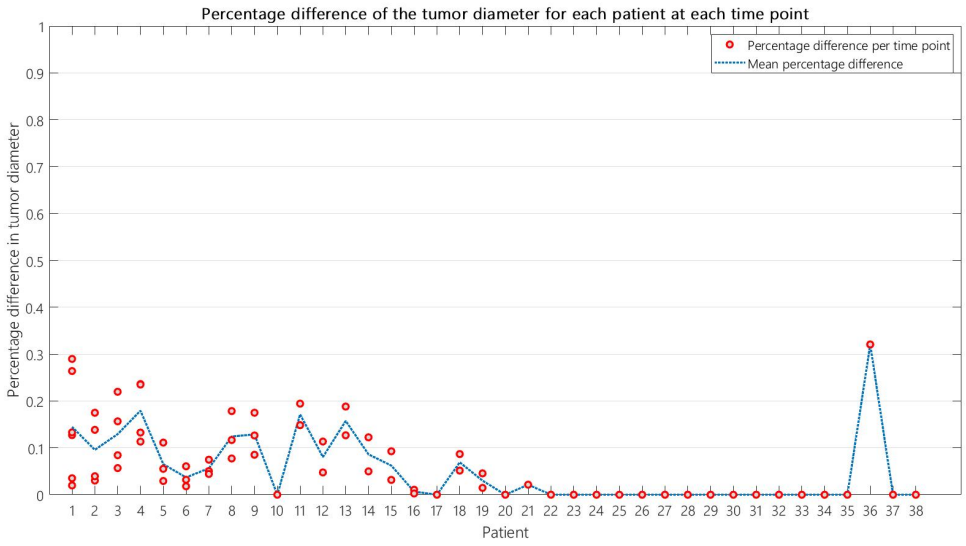

Figure 5.2: A plot of the percentage difference between the true and predicted tumor diameter for each time point for each patient. Optimization is performed as in Equation (5.11) to Equation (5.13) and parameters are taken as in Section 4.3.

Some patient-specific cases will be highlighted, as well. Figure 5.2 shows that the tumor dynamics of 30 patients can be represented well with a mean percentage difference of less than 10%. Examples of such patients are patient 6 and patient 10, for which the tumor dynamics over time are visualized in Figure 5.3. The clinical treatment stops after 132 days, but the model is simulated to show the effect of the treatment if it would continue. For patient 6 not all clinical points are precisely represented. However, the difference is small,

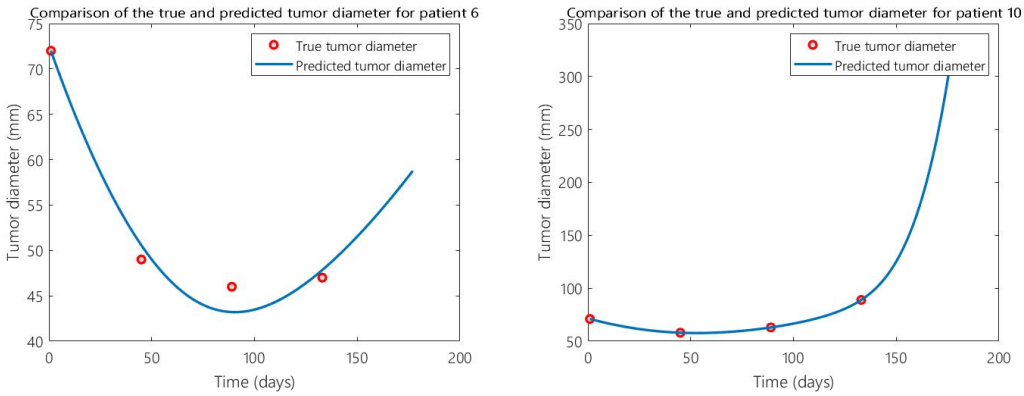

Figure 5.3: The true and predicted tumor diameter over time for patient 6 (left) and patient 10 (rigth), when the optimization is performed as in Equation (5.11) to Equation (5.13).

which results in a mean percentage difference of 3.69%. For patient 10, all clinical points are almost exactly represented, which explains the zero percentage difference in Figure 5.2. It can be seen that the tumor diameter first decreases slightly and then keeps increasing. This is because the best fitting initial condition for patient 10 consists of mostly cell line 3 (SW620) but also of the other cell lines. Irinotecan has a decreasing effect on SW620, but only restricting effects on the other cell lines. So even though SW620 is reduced, the other cell lines keep growing, and hence the tumor diameter keeps growing.

Even though most patients have a mean percentage difference below 10%, some patients are challenging to replicate, and have large percentage differences. The patient that has the most significant percentage difference is patient 36 with 32.1%. After the first treatment cycle, the tumor diameter of this patient was half of the initial diameter. The drug effect of irinotecan on the cell lines that are incorporated in the model are not strong enough to obtain such an effect, which caused a large percentage difference. Another shape that is difficult to replicate is one of the patients that have a more or less constant tumor diameter, such as patients 1, 2, 4, 8, 9, and 12. The dynamics of patient 1 are shown in Figure 5.4. The model can replicate the last two points, but all the points in between are poorly represented. This can be the result of lacking cell lines, and hence missing drug effect parameters. This especially is a plausible explanation for patients 1, 4, 8, and 12 since these patients do not have CRC as primary tumor type, but the cell lines are for CRC. For patients 2 and 9, the primary tumor type is CRC, but only 6 cell lines are implemented in the model while many more exist. Flexible drug effects of the patients will also be considered in Section 5.1.3 to account for the additional cell lines and the patient to patient variation, to see if the dynamics can be better approximated.

Another dynamic in patients that are difficult to simulate is the patients that first have an increase in tumor diameter and then a decrease, such as patient 13 in Figure 5.4. This shape of tumor diameter is difficult to explain with different effects of cell lines and only one treatment. It can be explained, however, with a delay before the treatment becomes efficient. This time delay is not directly incorporated in the model; however, it is implicitly incorporated in the parameters. The drug effect parameters represent the effect of the treatment after a certain duration, without considering how it responds in the time in between. For these patients, it would be interesting to see if the model can replicate the dynamics when more clinical samples

are available. Since it is not known for patient 13 how the patient reacts, it is difficult to see if the model can replicate the rest of the treatment time and only miss the first point, explained by the drug time delay.

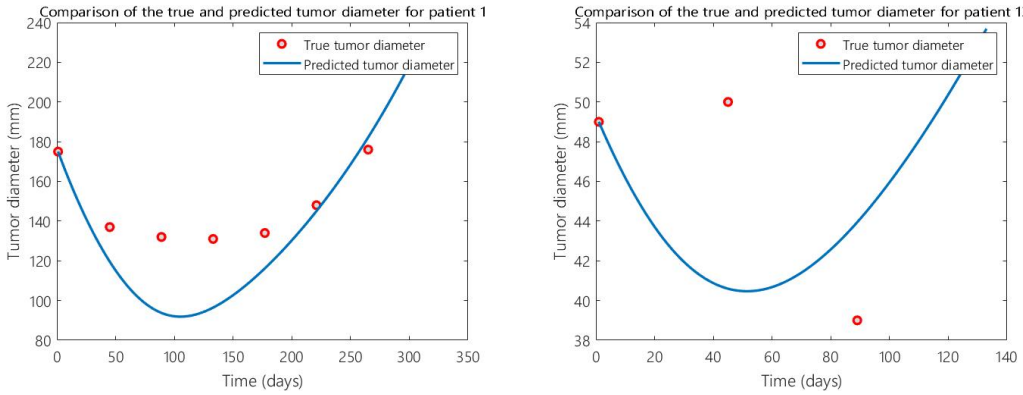

Figure 5.4: The true and predicted tumor diameter over time for patient 1 (left) and 13 (right), when the optimization is performed as in Equation (5.11) to Equation (5.13).

To conclude, the model can represent the tumor dynamics of most patients sufficiently well, even with the variation in responses to the irinotecan treatment. This shows that assuming the right information is known, the model can predict the tumor dynamics over time with a mean percentage difference over all patients of 5.17%. Some of the more difficult patients to replicate are the patients with a tumor size that is increasing at first and then decreasing (for example, patients 11, 12, and 13). The clinical explanation for this effect could be a delay in the effect of treatment, which is not incorporated in the model. Other shapes that are difficult to replicate are tumor diameters that stay relatively constant in time, such as patient 1. This can be caused by cell lines that are not considered in the model and that simulate such a response.

5.1.3 Comparison over the whole treatment duration with variable drug effects

As explained in Section 5.1.2, since only 6 cell lines are incorporated in the model, while many more exist, the drug effects are varied to obtain realistic new drug effects. This could also account for the missing cell lines for other cancer types, that are not CRC since other patients are also considered. The optimization problem will become slightly different. The original matrix D_2 consisted of fixed values representing the effect of irinotecan on each cell line. They will be varied to see if better predictions can be obtained. The existing cell lines are taken and varied to obtain new made up cell lines that are close to the known ones, which also accounts for the patient to patient variability since the drug effect is different on each patient. The matrix D_2 will be changed to $\tilde{D}_2$ in the following way:

$$\tilde{D}_2(w) = w^T D_2 \tag{5.14}$$

$$\tag{5.15}$$

with each entry of the vector w bound between w_{min} and w_{max}, hence $w_{min} \leq [w]_i \leq w_{max}$ for all $i \in \{1, ..., n\}$. Now each entry of D_2 can be scaled up or down with a margin, depending

on w_{min} and w_{max}. The estimated amount of tumor cells becomes:

$$N_{pred}(T_c, \tilde{D}_2(w)) = \mathbf{1}_n^T \exp\left[\left(A - \tilde{D}_2(w)\right) T_c\right] x(0) \tag{5.16}$$

The optimization will be performed with respect to w with the same cost function. It is possible to also optimize over $x(0)$, however, to compare the results fairly $x(0)^*$ is taken that is the outcome of the optimization problem in Equation (5.11), hence the initial condition that fitted the predicted data best to the clinical data with the original fixed drug effects. The mathematical formulation for each patient is:

$$\min_{w} \quad \sum_{T_c=T_s}^{T_m} \left(N_{pred}(T_c, \tilde{D}_2(w)) - N_{true}(T_c)\right)^2 \tag{5.17}$$

$$s.t. \quad w_{min} \leq [w]_i \leq w_{max}, \quad \forall i \in \{1, ..., n\} \tag{5.18}$$

with w_{min} and w_{max} the minimum and maximum value of each $[w]_i$ respectively, for all $i \in \{1, ..., n\}$. The optimization problem defined by Equation (5.17) and Equation (5.18) is solved with the `Matlab` function *fmincon*, with multiple initial values for w to reduce the chance of obtaining a local minimum.

The optimization problem in Equation (5.17) will be solved with the constraint in Equation (5.18) with $w_{min} = 0.80$ and $w_{max} = 1.20$, so with a 20% margin around the fixed original drug effect. The optimization problem will also be performed without a constraint to see what the best possible prediction is, even though the drug effects might not be realistic. The only bound that is set is $w_{min} = 0$ since negative drug effects correspond to a deteriorated effect of the drug on the tumor. The results for the mean difference over all time points can be seen in Table B.2. The underlined patients are for CRC, and the red numbers are higher than the average of that column. The average difference in tumor diameter over all patients is 4.04 mm with the original drug effects. With the constrained optimization problem, this can be reduced to 1.41 mm, and with the unconstrained problem, this can be further reduced to 0.89 mm. By varying the drug effects with a margin of 20%, the diameter prediction error can be significantly improved. When the problem has no constraints, the prediction error can be improved further.

A plot of the percentage difference is made for the constrained problem with a 20% margin, which is shown in Figure 5.5. When comparing this plot to Figure 5.2, the results have improved significantly. The mean percentage difference of the patients is all below or near 10%, where most are below 5%. The patient specific tumor dynamics are presented in Appendix B.4, where the prediction with and without flexible drug effects is compared.

When comparing the mean difference in tumor diameter between the constrained problem and the unconstrained problem in Table B.2, some patient dynamics cannot be replicated precisely. The dynamics that the model is unable to replicate are those that show a delayed response to the drug, which applies to patients 11, 12, 13, and 14. Other dynamics that the model is unable to replicate are those that show a more or less constant response to the drug (during the whole treatment period or a part), which applies to patients 1, 4, and 6.

To conclude, the results could be improved significantly with flexible, realistic drug effects (with the 20% margin), compared to the results with the original drug effects. The mean difference in tumor diameter over all patients over all time points could be reduced from 4.04

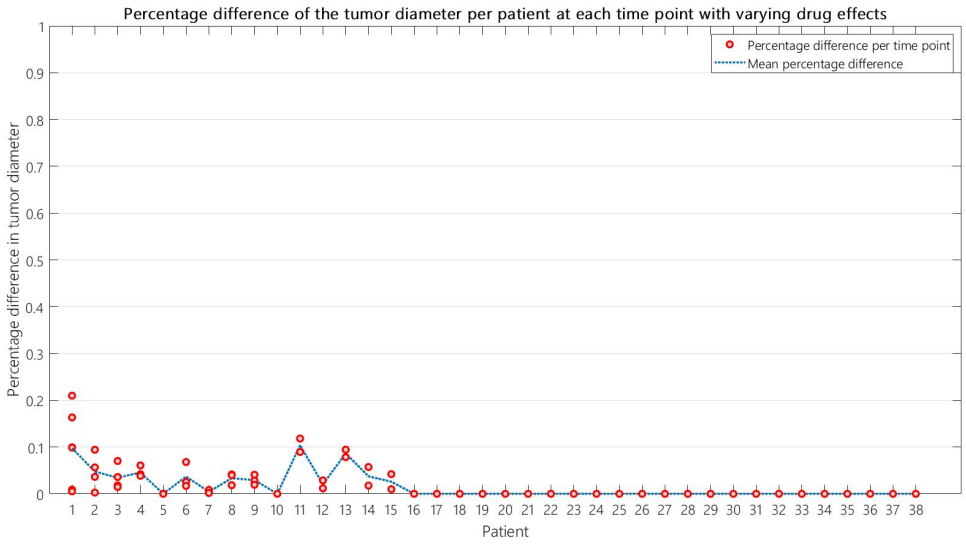

Figure 5.5: A plot of the percentage difference between the true and predicted tumor diameter per patient. Optimization is performed as in Equation (5.17) with Equation (5.18) with a 20% margin and parameters are taken as in Section 4.3.

mm to 1.41 mm. This corresponds to a reduction of the mean percentage difference from 5.17% to 1.59%. From these results, it can be concluded that, when the right information is known, the model can replicate most clinical data well with an average difference over all patients and all time points of 1.41 mm. The dynamics that the model is incapable of replicating, even with varying drug effects, are tumors that first increase and then decrease due to the therapy. These effects can be explained by a delayed drug effect, which is not incorporated in the model. The model is also unable to replicate an almost constant tumor size for a period of time, such as for patient 1. The prediction got significantly better when the drug effects were flexible, however, there is still room for further improvement.

5.2 Model optimization on clinical data

The goal of the previous section was to replicate the clinical data as precisely as possible. In this section, the goal is to show how the current clinical treatments can be improved when the model optimization is performed. It is important to ensure the best possible treatment for each patient to optimize the output response. However, in clinical application, no optimizations are done, and treatment decisions rely on clinical experience. In this section, it is shown what improvements can be achieved thanks to optimization, assuming the right information is known.

The optimization problem defined by Equation (3.17) up to Equation (3.19) is used to calculate the optimal drugs and their duration for each patient. This will be done with the optimal initial condition, $x(0)^*$, as results from Equation (5.11), hence the initial condition that fits the clinical data at best. The optimization is performed on each patient, and the results are compared with the clinical data. In Table 5.3, the true and optimal final amount of tumor

cells and tumor diameter are shown. Only patients are shown where significant improvement can be made, which is for patients 22 and 25. Patient 6 is also shown to substantiate the decision of the model. The final tumor diameter could not be decreased in most patients since irinotecan is already the best drug for almost all included cell lines. When looking at Table 4.3, it can be seen that only for cell line HT29 and HCT15, better drug response can be obtained with capecitabine and 5-FU respectively. It should be noted that when other, stronger drugs are used in the optimization problem, the improvements with respect to clinical treatments could have a bigger impact.

Table 5.3: The true and optimized final amount of tumor cells and final tumor diameter. Only patients are shown that have improved. Optimization is performed with Equation (3.17) up to Equation (3.19), with parameters as in Section 4.3. The underlined patients have CRC as primary tumor.

	Difference in number of cells			**Difference in diameter(mm)**		
Patient	N_{true}	N_{opt}	$N_{true} - N_{opt}$	$\varnothing_{true}$	$\varnothing_{opt}$	$\varnothing_{true}$-$\varnothing_{opt}$
6	$7.80{\cdot}10^{10}$	$8.23{\cdot}10^{10}$	$-4.28{\cdot}10^{9}$	47	47.9	-0.845
22	$3.43{\cdot}10^{11}$	$2.99{\cdot}10^{11}$	$4.37{\cdot}10^{10}$	77	73.6	3.42
25	$1.50{\cdot}10^{12}$	$1.03{\cdot}10^{12}$	$4.73{\cdot}10^{11}$	126	111	14.9

For patient 6 the final tumor diameter could not be reduced. The optimal drug duration for this patient is to give irinotecan for the whole treatment duration. The tumor diameter and the cell line dynamics are shown in Figure 5.6. The initial composition consists mostly of cell line 3, on which irinotecan has a reducing effect. Cell line 4 still increases over time since irinotecan inhibits the growth but is not strong enough to decrease these cells. However, no other drug, of the considered drugs, is more effective against this cell line, and the optimal treatment plan is, therefore, to administer irinotecan during the whole treatment horizon.

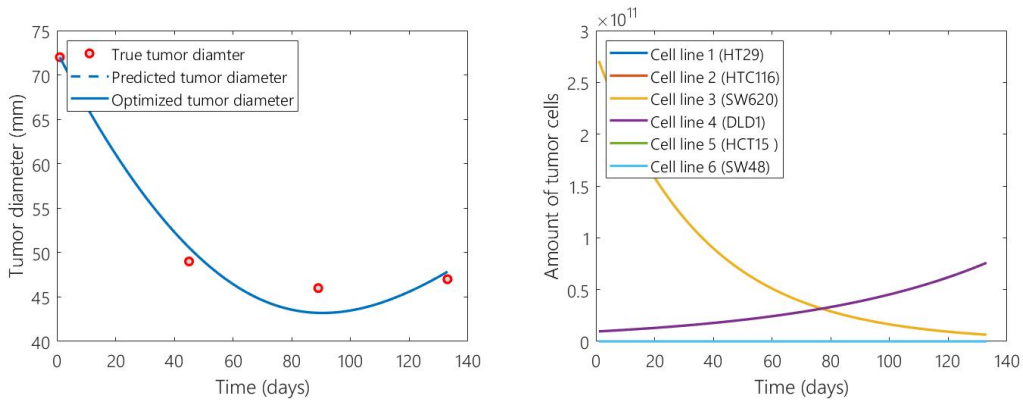

Figure 5.6: The true, predicted and optimized tumor diameter (left), and the optimized states (right) for patient 6. Optimization is performed as in Equation (3.17) up to Equation (3.19) and parameters are taken as in Section 4.3.

The final tumor diameter of patient 25 can be reduced by 14.9 mm, by merely switching from drug 2 to drug 3. The treatment schedule for this patient is to administer drug 2 first, followed by drug 3, which is obtained by Algorithm 1. The predicted and optimized tumor diameter of patient 25 and their cell line dynamics are given in Figure 5.7. Irinotecan has a reducing effect

on cell line 3; however cell line 5 increases rapidly. The entire tumor, therefore, also increases. During the last treatment days, there is a switch to 5-FU, which inhibits the growth of cell line 5 more. The additional reduction in tumor diameter caused by the switching of the drug is almost 15 mm. A similar situation applies to patient 22, where cell line 5 also becomes more substantial during the treatment, and a switch to 5-FU can reduce the tumor diameter. The tumor diameter and cell line dynamics over time for patient 22 are given in Figure B.21.

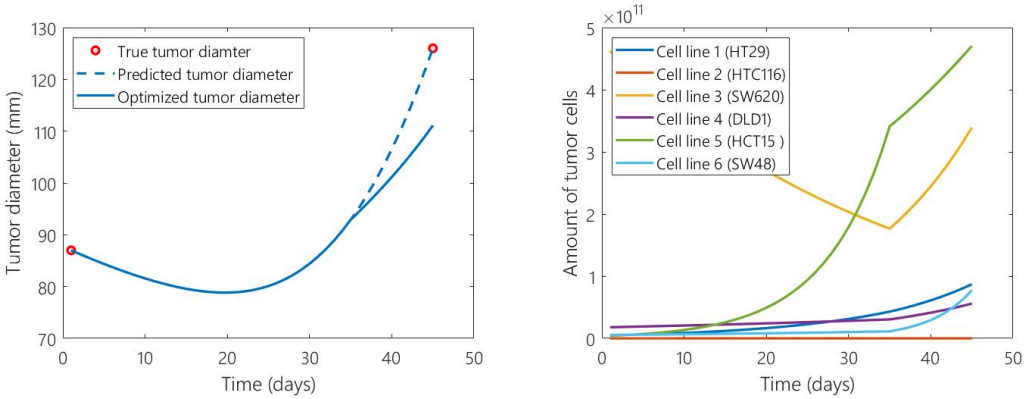

Figure 5.7: The true, predicted and optimized tumor diameter (left), and the optimized states (right) for patient 25. Optimization is performed as in Equation (3.17) up to Equation (3.19) and parameters are taken as in Section 4.3.

5.3 Summary

This chapter used the clinical patient data from the Erasmus MC dataset to validate the model outcomes. This dataset contains information about patients that received an irinotecan treatment. First, the predicted tumor diameters were compared to the clinical tumor diameters at each measured clinical data point without considering the whole treatment duration. The prediction on the 44-day horizon had a mean difference of 0.0742 mm between the predicted and true tumor diameter. When a more extended treatment horizon was considered, got these predictions significantly more accurate, with a mean difference in diameter of $2.49 \cdot 10^{-9}$ mm for the 88-day horizon.

Next, a comparison over the whole treatment duration was considered, to see if the model can replicate the whole time evolution of the patient tumor dynamics. The mean difference in the predicted and true tumor diameter over all data points and all patients is 4.04 mm, which corresponds to a mean percentage difference in tumor diameter of 5.17%. Tumor dynamics that are difficult to replicate showed a delayed response to the treatment, which effect is not incorporated in the model. Other dynamics that are difficult to replicate have a fast decreasing tumor size or a more or less constant tumor diameter for some time. The lack of prediction of these dynamics can be explained by the fact that only 6 CRC cell lines were incorporated in the model, and many more exist. To account for these missing cell lines, and for the patient to patient variation in drug sensitivity, were the original drug effects also taken as a variable. With a 20% margin around the original drug effects, the mean difference in tumor diameter could be reduced to 1.41 mm, which corresponds to a mean percentage difference in tumor diameter of 1.59%.

Optimal drug durations for capecitabine, irinotecan, and 5-FU were also obtained for the initial tumor compositions of the patients in the Erasmus MC dataset with the model optimization. The final tumor sizes that are obtained with the clinical treatment plan of irinotecan were compared to the final tumor sizes that are obtained with the optimal drug scheduling. The final tumor sizes could not be improved for most patients since irinotecan already has the strongest effect on most of the cell lines that are considered. For patient 25, however, could a reduction of 14.9 mm be obtained, by switching from irinotecan to 5-FU.

Chapter 6

Theoretical background for the chemo-radiation model

In clinical applications, chemotherapy and radiotherapy are often combined as treatment modalities. However, they are never optimized together, and dosing and scheduling are mainly based on clinical experiences. In previous literature, some attempts have been made to combine the two modalities, for example, by minimizing the combined BED (biologically effective dose) [9]. However, calculating the combined effect on the tumor cell lines in each compartment and using control theoretical methods to optimize the treatments is an entirely new approach. In this section, the theoretical background of this approach is discussed. First, the general combined chemo-radiation optimization is described in Section 6.1. Then it is explained how the optimal total doses for radiotherapy and optimal treatment times can be obtained in Section 6.2. Last, it is explained how the modalities can be scheduled together in Section 6.3.

6.1 Adding radiotherapy to the model

It is desired to add radiotherapy to the model as well so that the optimal combined treatment plan is calculated. Chemotherapy and radiotherapy are different treatment modalities since chemotherapy is a systematic drug, and radiation therapy is a local externally administered treatment (only EBRT (external beam radiation therapy) is considered). It is desired that the two modalities are combined so that the convexity properties still hold. For radiotherapy, it is assumed that, once the optimal total dose and fractionated doses are obtained, the optimal spatial delivery can be calculated as well.

Radiotherapy and chemotherapy work in different ways and need to be optimized in different ways. Chemotherapy has different effects on the cell lines per drug, and there is a freedom in scheduling the drugs to obtain the best treatment response. The chemotherapy treatment dose is, however, taken as fixed, namely as the MTD (maximum tolerated dose) of each drug.

Radiotherapy only has one possible treatment approach ("equivalent drug"), but the change cannot be so sharp as it is when the chemotherapeutic drug is changed. However, even when more radiation is administered, the effect will be enhanced, but it cannot change in such a way as by changing the chemo drug. We wish to calculate the optimal number of days each chemotherapeutic drug is used and the optimal fractionation scheme per compartment for radiotherapy so that the treatments take each other's response into account. Furthermore, the side effects caused by both separate treatments need to stay below a maximum probability value.

First, it is assumed that each compartment has the same parameters, and therefore the same optimal fractionation scheme. This is referred to as the simplified radiation fractionation scheme. Then the model will be extended so that the compartments can have different parameters, and therefore an optimal radiation fractionation scheme for each compartment. This is referred to as the advanced radiation fractionation scheme.

6.1.1 Simplified radiation fractionation scheme

The model describing the dynamics of the tumor and the drug effects used for chemotherapy was described by Equation (3.10) as:

$$\dot{x}(t) = [A - \psi(\tilde{l})]x(t) \tag{6.1}$$

with $A \in \mathbb{R}^{nxn}$ describing the tumor dynamics without the influence of drugs, and $\psi(\tilde{l}) \in \mathbb{R}^{nxn}$ describing the drug effects. Now it is desired that ψ also describes the effects of radiation, and if possible in such a way that the convexity properties are preserved.

For chemotherapy $\tilde{l} \in \mathbb{R}^d_+$ was defined as the vector of drug durations for d choices of chemotherapeutic drugs. Radiation therapy can be added as another "drug" option, where each entry of the vector belongs to a different fractionated dose (with 0 Gy also included as an option). So let there be r choices of the fractionated dose for radiotherapy, then define the vector of radiation treatment durations as $u \in \mathbb{R}^r_+$. Also let $\rho \in \mathbb{R}^r_+$ be the vector with the fractionated doses, with $[\rho]_1 = 0$. The w'th entry of u, $[u]_w$, corresponds to the amount of time that dose $[\rho]_w$ should be used. Hence:

$$\tilde{l} = \begin{bmatrix} \text{"Treatment duration of drug 1"} \\ \text{"Treatment duration of drug 2"} \\ \vdots \\ \text{"Treatment duration of drug d"} \end{bmatrix}, \tag{6.2}$$

$$u = \begin{bmatrix} \text{"Treatment duration of fractionated dose 1"} \\ \text{"Treatment duration of fractionated dose 2"} \\ \vdots \\ \text{"Treatment duration of fractionated dose r"} \end{bmatrix} \quad \text{and} \quad \rho = \begin{bmatrix} \text{"Dose 1"} \\ \text{"Dose 2"} \\ \vdots \\ \text{"Dose r"} \end{bmatrix} \tag{6.3}$$

with the treatment duration given as the fraction of the total treatment time. It is important that "dose 1" corresponds to 0 Gy. The function $\psi(\tilde{l}, u)$ is defined as follows:

$$\psi(\tilde{l}, u) = \sum_{s=1}^{d} D_s[\tilde{l}]_s + \sum_{w=1}^{r} R_w[u]_w \tag{6.4}$$

with positive diagonal matrices $D_s \in \mathbb{R}^{nxn}$ and $R_w \in \mathbb{R}^{nxn}$ expressing the effect of drug s and fractionated dose $[\rho]_w$ respectively. The system becomes:

$$\dot{x}(t) = \left[A - \sum_{s=1}^{d} D_s[\tilde{l}]_s - \sum_{w=1}^{r} R_w[u]_w \right] x(t) \tag{6.5}$$

This system is a convex-monotone system, since matrix A is still a Metzler matrix, and matrices D_s and R_w are positive diagonal matrices [16], [22].

The side effects of chemotherapy had already been added as linear constraint, ensuring that the probability of having severe chemotherapy-induced side effects stays below a maximum value. The side effects of radiotherapy should also be added, and should also remain below a maximum probability. Having a low side effect probability is very important since radiation therapy can cause severe and long term complications. The side effects of chemotherapy and radiotherapy are entirely different in nature, so it does not make sense to combine them, and they are therefore added as separate constraints. The radiation therapy side effects will also be included by the NTCP (normal tissue complication probability) model, described by Equation (2.9), which was:

$$NTCP_{logit} = \left(1 + \left(\frac{D_{50}}{EQDX_{OAR}} \right)^{4\gamma_{50}} \right)^{-1} \tag{6.6}$$

$$EQDX_{OAR} = \frac{\sum_{f=1}^{n_f} sd_f \left(1 + \frac{sd_f}{[\alpha/\beta]_N} \right)}{1 + \frac{X}{[\alpha/\beta]_N}} \tag{6.7}$$

So the NTCP depends on the site-depending parameters, D_{50}, γ_{50}, $[\alpha/\beta]_N$, on the organ sparing factor s, and on the fractionated dose d_f and the amount of fractions n_f. For now it is assumed that the site-dependent parameters are the same for all the radiated sites, meaning that the same fractionation scheme will be optimal for each site. In Section 6.1.2 it will be explained how this can be changed.

For fixed parameters D_{50}, γ_{50}, $[\alpha/\beta]_N$, s, and a fixed total dose $P_{tot} = \sum_{f=1}^{n_f} d_f$, define the function of radiation-induced side effects as:

$$h(d_f) = \left(1 + \left(\frac{D_{50}}{EQDX_{OAR}(d_f)} \right)^{4\gamma_{50}} \right)^{-1} \tag{6.8}$$

with $EQDX_{OAR}$ defined as in Equation (6.7). These side effects need to stay below a maximum probability h_{max}, hence $h(d_f) \leq h_{max}$. This constraint can be recast into a linear constraint, with a similar approach as for the chemotherapy-induced side effects. Let d_{max} be the fractionated dose that gives side effects h_{max} for a certain total dose P_{tot}, hence $h(d_{max}) = h_{max}$. Now define the last entry of ρ as d_{max}, hence $[\rho]_r = d_{max}$, which means

that $[u]_r$ is fraction of the total time that dose d_{max} should be used. So instead of adding a constraint that assures a low enough NTCP value, now the available choices for the fractionated dose all satisfy the NTCP constraint for a certain P_{tot}. The constraint that should be satisfied now is a linear constraint, namely:

$$\sum_{w=1}^{r} T_F[u]_w[\rho]_w \leq P_{tot} \tag{6.9}$$

In Equation (6.9) the number of days for which each fractionated dose should be used is described by $T_F[u]_w$ and is multiplied by the corresponding doses $[\rho]_w$, for each w. Taking the sum over these values gives the total dose that is used, which should stay below the fixed total dose P_{tot}.

The complete optimization formulation, for a combined chemo-radiation treatment with fixed total dose P_{tot}, fixed total treatment horizon T_F, and identical fractionation scheme for each compartment, becomes:

$$\min_{\tilde{l},u} \quad \mathbf{1}_n^T \exp\left[\left(A - \sum_{s=1}^{d} D_s[\tilde{l}]_s - \sum_{w=1}^{r} R_w[u]_w\right) T_F\right] x(0) \tag{6.10}$$

$$\text{s.t.} \quad [\tilde{l}]_s \geq 0, \quad \forall s \in \{1, ..., d\} \tag{6.11}$$

$$[u]_w \geq 0, \quad \forall w \in \{1, ..., r\} \tag{6.12}$$

$$\sum_{s=1}^{d} [\tilde{l}]_s \leq 1 \tag{6.13}$$

$$\sum_{w=1}^{r} [u]_w = 1 \tag{6.14}$$

$$\sum_{s=1}^{d} T_F[\tilde{l}]_s \leq T_{max} \tag{6.15}$$

$$\sum_{w=1}^{r} T_F[u]_w[\rho]_w \leq P_{tot} \tag{6.16}$$

The cost function in Equation (6.10) minimizes the final amount of tumor cells, $\mathbf{1}_n^T x(T_F)$, over the finite total treatment horizon T_F. The first constraint, Equation (6.11), assures that the chemotherapeutic drugs are used for a non-negative amount of days, and Equation (6.12) specifies that the radiation doses are used for a non-negative amount of days. The third constraint, Equation (6.13), makes sure that the total chemotherapy treatment days do not exceed the final treatment time T_F, and the fourth constraint, Equation (6.14), ensures the same for the total amount of radiotherapy treatment days. In this formulation, a day when 0 Gy is given is also described as treatment day, an equality is therefore used in Equation (6.14). Constraint Equation (6.15) makes sure that the chemotherapy treatment days stay below T_{max}, to limit the chemotherapy-induced side effects. T_{max} refers to the maximum treatment days of chemotherapy that are allowed regarding the chemotherapy-induced side effects, whereas T_F refers to the fixed total treatment horizon. The last constraint, Equation (6.16), describes that the total dose, that is given in smaller fractionated doses, cannot exceed the fixed total dose P_{tot}. The doses corresponding to each entry of $[u]_w$, for $w \in \{1, ..., r\}$, are described by $[\rho]_w$, and all available doses are sufficient in terms of NCTP. This constraint will be pushed to

P_{tot} since the higher the total dose, the more effective the radiation will be. The optimization problem can be solved with convex optimization, since the objective function is convex and the constraints are linear and hence convex.

Even though this optimization problem has two variables, they can easily be combined into one variable. Define the vector of drug durations and radiation durations as $z = \begin{bmatrix} \tilde{l}^T & u^T \end{bmatrix}^T$, then the optimization can be performed over one variable. The solution of this optimization problem is denoted as z^*, of which the first d entries correspond to the optimal treatment durations that each drug should be used, $\tilde{l}^*$, and the last r entries to the optimal treatment durations that each fractionated dose should be used, u^*. The optimal treatment durations are given as fractions of the fixed total treatment duration, T_F. For radiotherapy, an equal radiation fractionation scheme is obtained for all compartments. The optimal total amount of tumor cells at the end of the treatment horizon is denoted as $x(T_F)^*$.

6.1.2 Advanced radiation fractionation scheme

In Section 6.1.1, the same fractionation scheme for each compartment was obtained by taking the same tissue-dependent parameters, and the same total dose. In reality, these parameters most likely vary for each compartment. For example, if compartment 1 is the lung and compartment 2 the brain, the side effects caused by radiation in each compartment are entirely different. Therefore an optimal fractionation scheme needs to be obtained for each compartment to assure the best possible treatments.

In principle the same optimization will be performed as in Section 6.1.1, however, the vector u will now be determined for each compartment. Define $u^k \in \mathbb{R}_+^{r^k}$ as the vector of radiation treatment durations for compartment k. Each entry $[u^k]_w$ corresponds to the fractionated dose $[\rho^k]_w$, with $\rho^k \in \mathbb{R}_+^{r^k}$. The function $\psi(\tilde{l}, u)$ is extended to $\psi(\tilde{l}, u^1, u^2, ..., u^p)$, which is defined as follows:

$$\psi(\tilde{l}, u^1, u^2, ..., u^p) = \sum_{s=1}^{d} D_s[\tilde{l}]_s + \sum_{w=1}^{r^1} R_w^1[u^1]_w + \sum_{w=1}^{r^2} R_w^2[u^2]_w + ... + \sum_{w=1}^{r^p} R_w^p[u^p]_w \qquad (6.17)$$

where the positive diagonal matrices $D_s \in \mathbb{R}^{n\text{x}n}$ and $R_w^k \in \mathbb{R}^{n\text{x}n}$ represent the effect of drug s and fractionated dose $[\rho]_w^k$, respectively. Matrices R_w^k specify the effect of radiation on each cell line in compartment k. These matrices have still size nxn, but only have non-zero entries for compartment k. For example, in the presence of 2 compartments and 3 cell lines, we can define the matrices R_w^1 and R_w^2 as:

$$R_w^1 = \left[\begin{array}{ccc|ccc} a_w & 0 & 0 & 0 & 0 & 0 \\ 0 & b_w & 0 & 0 & 0 & 0 \\ 0 & 0 & c_w & 0 & 0 & 0 \\ \hline 0 & 0 & 0 & 0 & 0 & 0 \\ 0 & 0 & 0 & 0 & 0 & 0 \\ 0 & 0 & 0 & 0 & 0 & 0 \end{array}\right] \quad \text{and} \quad R_w^2 = \left[\begin{array}{ccc|ccc} 0 & 0 & 0 & 0 & 0 & 0 \\ 0 & 0 & 0 & 0 & 0 & 0 \\ 0 & 0 & 0 & 0 & 0 & 0 \\ \hline 0 & 0 & 0 & a_w & 0 & 0 \\ 0 & 0 & 0 & 0 & b_w & 0 \\ 0 & 0 & 0 & 0 & 0 & c_w \end{array}\right] \qquad (6.18)$$

where a_w, b_w, c_w represent the effect of radiation dose $[\rho]_w$ in the cell lines a, b, c. When one compartment is considered, the formulation is equal to the formulation in Section 6.1.1.

The radiation-induced side effects can now be defined for each compartment. The probability of having severe side effects caused by radiation will be defined for compartment k as:

$$h^k(d_f) = \left(1 + \left(\frac{D_{50}^k}{EQDX_{OAR}^k(d_f)}\right)^{4\gamma_{50}^k}\right)^{-1} \tag{6.19}$$

$$EQDX_{OAR}^k = \frac{\sum_{f=1}^{y} s^k d_f \left(1 + \frac{s^k d_f}{[\alpha/\beta]_N^k}\right)}{1 + \frac{X}{[\alpha/\beta]_N^k}} \tag{6.20}$$

where D_{50}^k, γ_{50}^k, $[\alpha/\beta]_N^k$ and s^k depend on compartment k. In each compartment the probability should stay below a corresponding maximum, hence $h^k(d_f) \leq h_{max}^k$. Define d_{max}^k as the maximum fractionated dose that is allowed ($h^k(d_{max}^k) = h_{max}^k$ for a certain total dose P_{tot}^k). Define the last entry of ρ^k as d_{max}^k, hence $[\rho^k]_{r^k} = d_{max}^k$. This means that each u^k can have a different size, and different maximum fractionated dose. The linear constraint that should be satisfied now is:

$$\sum_{w=1}^{r^k} T_F [u^k]_w [\rho]_w \leq P_{max}^k, \quad \forall k \in \{1, ..., p\} \tag{6.21}$$

The overall total optimization problem, for a combined chemo-radiation treatment with fixed final treatment horizon T_F, and fixed total dose P_{tot}^k for compartment k, becomes:

$$\min_{\tilde{l}, u^1, ..., u^p} \quad \mathbf{1}_n^T \exp\left[\left(A - \sum_{s=1}^{d} D_s [\tilde{l}]_s - \sum_{k=1}^{p} \sum_{w=1}^{r^k} R_w^k [u^k]_w\right) T_F\right] x(0) \tag{6.22}$$

$$\text{s.t.} \quad [\tilde{l}]_s \geq 0, \quad \forall s \in \{1, ..., d\} \tag{6.23}$$

$$[u^k]_w \geq 0, \quad \forall w \in \{1, ..., r^k\}, \forall k \in \{1, ..., p\} \tag{6.24}$$

$$\sum_{s=1}^{d} [\tilde{l}]_s \leq 1 \tag{6.25}$$

$$\sum_{w=1}^{r^k} [u^k]_w = 1, \quad \forall k \in \{1, ..., p\} \tag{6.26}$$

$$\sum_{s=1}^{d} T_F [\tilde{l}]_s \leq T_{max} \tag{6.27}$$

$$\sum_{w=1}^{r^k} T_F [u^k]_w [\rho]_w \leq P_{tot}^k, \quad \forall k \in \{1, ..., p\} \tag{6.28}$$

The constraints are the same as Equation (6.11) up to Equation (6.16), but now extended per compartment. This optimization problem is still a convex optimization problem. The multiple variables can be combined by the same trick as used before. Define $\tilde{z} = \begin{bmatrix} \tilde{l}^T & u^{1^T} & ... & u^{p^T} \end{bmatrix}^T$, then the solution of the optimization problem can be denoted as $\tilde{z}^*$, which is again the stacked vector of the separate optimal treatments $\tilde{l}^*$, u^{1^*} up to u^{p^*}. The optimal total amount of tumor cells at the end of the treatment horizon is $x(T_F)^*$.

6.2 Optimizing over the treatment duration and total radiation dose

Up to now, the final treatment horizon and total radiation dose in this chapter were fixed. These values influence the final tumor size and optimal treatment plan, and optimizing over them can result in better outcomes.

Consider a free-horizon problem. It is expected that an optimal treatment duration of T_F^* exists. A longer treatment duration is not necessarily better since prolonging the treatment duration also means that the body is harmed more, causing more severe side effects. In the chemo-alone treatments, the optimal treatment duration T_F^* is equal to the maximum treatment duration allowed by the side effects, T_{max}. In the combined chemo-radiation treatments, the optimal treatment duration is less clear, and there will, therefore, be determined what the best value is.

The total radiation dose P_{tot}^k influences the fractionated dose that can be used when taking the side effects into account. Changing the total radiation dose can result in a different optimal fractionation scheme. An optimization will, therefore, be computed with respect to the total radiation dose to obtain the best combination of total dose and fractionated dose.

So an optimization with respect to the final treatment duration and the total radiation dose is computed. To find T_F^* and $P_{tot}^{k^*}$, the cost function Equation (6.22) can be changed into:

$$\min_{T_F} \quad \min_{P_{tot}^k} \quad \min_{\tilde{l},u^1,\ldots,u^p} \quad \mathbf{1}_n^T \exp\left[\left(A - \sum_{s=1}^{d} D_s[\tilde{l}]_s - \sum_{k=1}^{p}\sum_{w=1}^{r} R_w^k[u^k]_w\right) T_F\right] x(0) \tag{6.29}$$

with the same constraints in Equation (6.23) up to Equation (6.28). This optimization can be solved by taking T_i values between $0 \leq T_F \leq T_L$, with T_L the upper limit of the treatment time, and P_i^k values between $0 \leq P_{tot}^k \leq P_L^k$ for each $k = 1, ..., p$, with P_L^k the upper limit of total dose for compartment k. Then the inner convex optimization, i.e. the minimization over $\tilde{l}, u^1, ..., u^p$, can be solved $T_i P_i$ times and the smallest can be chosen. Note that this way of solving does not give the actual T_F^* and $P_{tot}^{k^*}$, but when enough samples T_i and P_i^k are taken, the outcome will be close enough.

6.3 Scheduling drug administration and radiation

After the combined treatment plans are determined with the optimization, the optimal radiation fractionation scheme and optimal duration of each drug intake is determined. However, the next step is to determine the best way to schedule drug administration and radiation. This problem is considered as two separate problems, for each treatment alone, since they are also applied as different treatments. It is essential to model the modalities together so that the treatments will consider the effect of each other.

When considering the treatment schedule, the tumor should be reduced as much as possible as soon as possible, in line with the first statement of the Goldie-Coldman hypothesis. The treatments are, therefore, started at the same time. The duration of each treatment can be different, so one modality may continue while the other has finished already. It is also possible

that the optimal radiation fractionation scheme is different per compartment, and therefore also has different durations. The scheduling of the chemotherapeutic drugs has already been handled in Section 3.4 and the same algorithm will be used for the combined treatment. For radiotherapy, there is less freedom in the scheduling problem, whose solution is, therefore, more straightforward. As a result of the optimization problem in Equation (6.29), the optimal radiation fractionation scheme is determined, and the optimal fractionated doses need to be scheduled. This problem is different from chemotherapy, in the sense that there is only one "drug". This "drug" can have different doses that should be used in the case when the optimal fractionation scheme is to use different fractionated doses. It is desired to shrink the tumor as soon as possible, and therefore, when different fractionated doses should be administered, the highest doses are given first.

The optimal treatment plan is to radiate the patient each day. However, out of practical and clinical considerations, the patient usually is only radiated on weekdays. Some rest days also allow the patient to recover from the radiation and the healthy cells to get healed. So for the scheduling of radiation, there will be two algorithms. The first, described by Algorithm 2, calculates the effect of radiation when it is given each day until the maximum dose is reached. The second, represented by Algorithm 3, calculates the impact of radiation when it is administered each weekday until the maximum dose is reached. In this case, the tumor grows on the weekends, so these effects are incorporated. The loss in the treatment effect can be measured by calculating the difference in the final number of tumor cells as a consequence of the two algorithms: $\Delta_N = N_{subopt}(T_F) - N_{opt}(T_F)$. The loss in final tumor diameter can also be measured: $\Delta_{\varnothing} = \varnothing_{subopt} - \varnothing_{obt}$.

Algorithm 2: Optimal scheduling of radiotherapy on all treatment days

input : Matrices A and R_w^k, for $w = 1, ..., r^k$ and $k = 1, ..., p$, optimal final time T_F^*, initial condition $x(0)$, optimal radiation fractionation schemes u^{k^*}, for $k = 1, ..., p$, and the corresponding doses $[\rho]_w$, for for $w = 1, ..., r^k$.

output: A treatment plan and its outcome when radiation is scheduled on each day until the maximum dose is achieved, for each compartment.

Define the radiation days per fractionated dose for compartment k as rad_d^k, with $rad_d^k = round(u^{k^*} T_F^*)$, and set $\zeta^k = r^k$.
Define the length of $x(0)$ as n.
for $t = 1 : T_F^*$ **do**
    Set $M = A$.
    for $k = 1 : p$ **do**
        if $rad_d^k(\zeta^k) > 0$ **then**
            Subtract a day of the days left for that fractionated dose:
            $rad_d^k(\zeta^k) = rad_d^k(\zeta^k) - 1$
            Subtract the effect of radiation in compartment k:
            $M = M - R_{\zeta^k}^k$
        end
        Check if there are still radiation days left for that fractionated dose in each compartment:
        if $rad_d^k(\zeta^k) \leq 0$ **then**
            $\zeta^k = \zeta^k - 1$
        end
    end
    Calculate the states on day t:
    $x(t) = exp[M]x(t-1)$
    Calculate the total amount of tumor cells on day t:
    $N(t) = \mathbf{1}_n^T x(t)$
end

Algorithm 3: Sub-optimal scheduling of radiotherapy on the weekdays

input : Matrices A and R_w^k, for $w = 1, ..., r^k$ and $k = 1, ..., p$, final time T_F^*, initial condition $x(0)$, optimal radiation fractionation schemes u^k, for $k = 1, ..., p$, and the corresponding doses $[\rho]_w$, for for $w = 1, ..., r^k$.

output: A treatment plan and its outcome when radiation is scheduled on the weekdays until the maximum dose is achieved, for each compartment.

Define the radiation days per fractionated dose for compartment k as rad_d^k, with $rad_d^k = round(7(round(u^{k^*} T_F^*)/5))$, and the set $\kappa^k = r^k$.
Define the length of $x(0)$ as n.
for $t = 1 : T_F^*$ **do**
    Set $M = A$.
    if $t \mod 7 = 0$ *or* $t \mod 7 = 6$ **then**
        If the day is a weekend day, do not radiate:
        $M = M$
    else
        If the day is a weekday, do radiate:
        for $k = 1 : p$ **do**
            if $rad_d^k(\kappa^k) > 0$ **then**
                Subtract one day of the days left for that fractionated dose:
                $rad_d^k(\kappa^k) = rad_d^k(\kappa^k) - 1$
                Subtract the effect of radiation in compartment k:
                $M = M - R_{\zeta^k}^k$
            end
            Check if there are still radiation days left for that fractionated dose:
            if $rad_d^k(\kappa^k) \leq 0$ **then**
                $\kappa^k = \kappa^k - 1$
            end
        end
    end
    Calculate the states on day t:
    $x(t) = exp[M]x(t-1)$
    Calculate the total amount of tumor cells on day t:
    $N(t) = \mathbf{1}_n^T x(t)$
end

Chapter 7

Chemo-radiation model simulations

Some simulations of the combined chemo-radiation model are shown in this chapter, for CRC (colorectal cancer). Unfortunately, no clinical data to compare the outcomes is available, so these model outcomes cannot be validated. The model parameter estimation for radiotherapy is in Section 7.1, and the initial conditions used for the simulations are given in Section 7.2. Section 7.3 shows model simulations of the combined chemo-radiation treatments for the given initial conditions, and Section 7.4 shows outcomes for the combined treatment scheduling. Last, the chapter is summarized in Section 7.5.

7.1 Model parameter estimations for radiotherapy

7.1.1 Radiation effects

The model parameters describing the effect of radiation are different from those describing the chemo drug effects. The advantage of radiotherapy is that many models already exist, which also can be used for the model parameter estimation. The LQ model, described by Equation (2.3), can be used to obtain the radiation effect on the tumor cells. The fraction of cells surviving a dose d_f is described by $S(\alpha_T, \beta_T, d_f)$ hence the fraction of cell death is described by $1 - S(\alpha_T, \beta_T, d_f)$. The parameters α_T and β_T are tissue-dependent. In [72], the cell survival parameters for the LQ (linear-quadratic) model are obtained with an in vitro study for three different human CRC cell lines. There is distinguished between external beam radiation (EBRT), high dose rate (HDR), and low dose rate (LDR). For this thesis, EBRT is considered, for which the parameters can be found in Table 7.1. Since the parameters for radiotherapy are only known for the 3 CRC cell lines HT29, HCT116, SW48, we will consider these cell lines. So the drug effects for chemotherapy will also be considered for this case.

Table 7.1: The tissue dependent survival parameters α_T and β_T for the LQ model described by Equation (2.3) for EBRT for three different CRC cell lines; the parameters are obtained from [72].

CRC cell line	$\alpha_T(Gy^{-1})$	$\beta_T(Gy^{-2})$	$[\alpha/\beta]_T(Gy)$
HT29	0.0842	0.0239	3.52
HCT116	0.198	0.0439	4.51
SW48	0.151	0.0376	4.02

The effect of the parameters in Table 7.1 on the cell survival probability can be seen in Figure 7.1. Cell line HT29 is the least sensitive to radiation, since it has the highest survival probability, and HCT116 is the most sensitive to radiation. This effect can also be deduced from the parameters since a higher $[\alpha/\beta]_T$ ratio corresponds to higher radiation sensitivity. Typically a ratio of 10 Gy is chosen [9], [21], [79], so these $[\alpha/\beta]_T$ ratios are low, and therefore less sensitive, in comparison to the 10 Gy ratio.

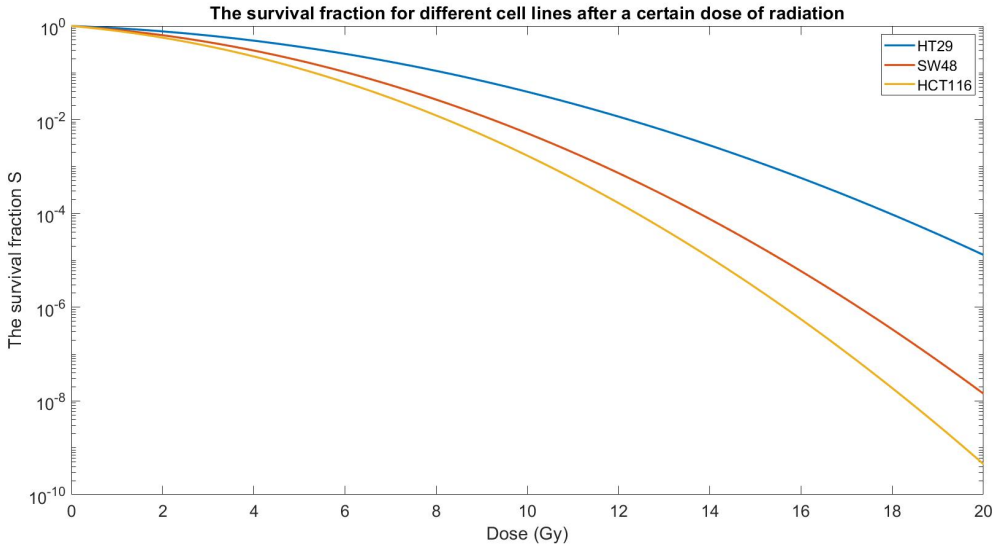

Figure 7.1: A comparison of the cell survival probability for three different CRC cell lines after a dose of radiation; the parameters are chosen as in Table 7.1.

Parameters α_T and β_T are used to express the effect of radiation on the tumor. The effect of radiation per fractionated dose is described by the diagonal matrix R_w^k, where $[\rho]_w$ corresponds to the fractionated dose. The matrix R_w^k has size nxn, corresponding to the number of different cell lines and compartments. The diagonal elements of R_w^k describe the effect of a radiation dose $[\rho]_w$ on cell lines $i = 1, ..., m$ in compartment k:

$$[R_w^k]_{jj} = \begin{cases} 0, & j \leq (k-1)m \\ r_i - (-\alpha_{T,i}[\rho]_w - \beta_{T,i}[\rho]_w^2), & (k-1)m < j \leq km, \quad i = j \mod m \\ 0, & j > km \end{cases} \tag{7.1}$$

So the entries of R_w^k that do not represent compartment k are zero, and the entries of R_w^k that do represent compartment k represent the effect of dose $[\rho]_w$. The effect of radiation

is defined as the growth rate of cell line i, r_i, minus the fraction of cells killed by dose $[\rho]_w$, $(-\alpha_{T,i}[\rho]_w - \beta_{T,i}[\rho]_w^2)$. In the special case $[\rho]_w = 0$, R_w^k is a matrix with all zero entries.

7.1.2 Side effects caused by radiotherapy

The parameters that quantify the side effects caused by radiation also need to be determined. The side effects are represented by the NTCP model, which determines the maximum fractionated dose allowed for a certain total dose. In Equation (6.7) and Equation (6.8) are the parameters that need to be determined: the tissue-dependent D_{50}, γ_{50} and $[\alpha/\beta]_N$ and organ sparing factor s. One of the side effects of radiating CRC is the possibility of late rectal bleeding. From a study where different NTCP models were fitted to patient data of late rectal bleeding, the obtained logit model parameters were $D_{50} = 83.5$ and $\gamma_{50} = 1.53$ [75].

When the target region is near the bladder, the radiation can cause additional undesired consequences. For example, consider a CRC with metastases in the lymph nodes that are near the bladder, the side effects that can arise by radiating the metastases are urinary incontinence and urinary urgency. The NTCP logit model parameters for urinary incontinence are $D_{50} = 96.7$ and $\gamma_{50} = 1.14$, and for urinary urgency $D_{50} = 67.6$ and $\gamma_{50} = 0.760$ [76]. The parameters are summarized in Table 7.2.

Table 7.2: The tissue dependent parameters for the NTCP logit model described by Equation (6.8) and Equation (6.7) for three different side effects.

Side effect	D_{50}	γ_{50}	Ref.
Late rectal bleeding	82.5	1.53	[75]
Urinary incontinence	96.7	1.14	[76]
Urinary urgency	77.7	1.16	[76]

The normal tissue sensitivity ratio is taken as $[\alpha/\beta]_N = 3$ for all compartments, which is a common estimate [9], [21]. The probability curves for these three side effects can be seen in Figure 7.2, where the probabilities increase with the typical sigmoidal shape of the NTCP models. For a total dose of 50 Gy, the probability of having urinary urgency is most likely, and the probability of having urinary incontinence least likely. However, for a fractionated dose of 11 Gy, the probability of late rectal bleeding becomes more likely than urinary urgency.

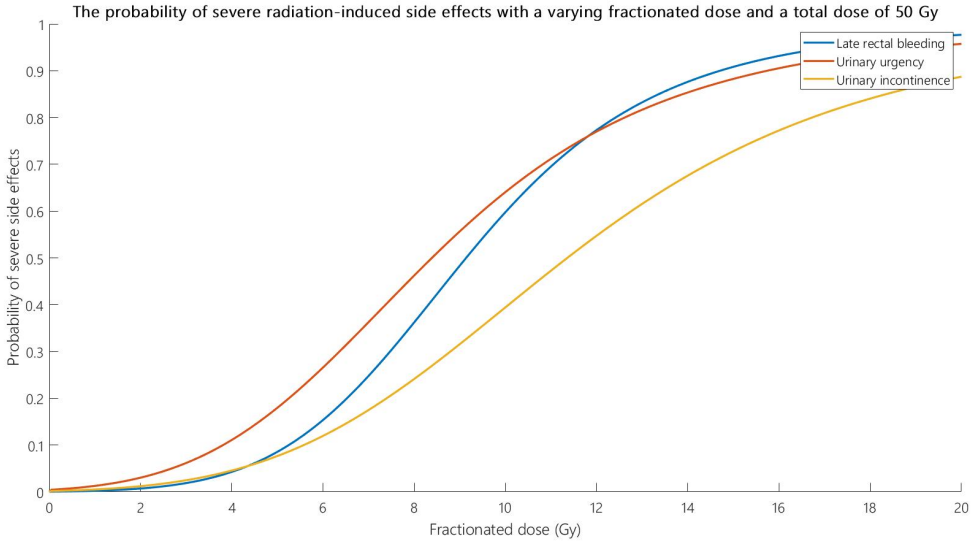

Figure 7.2: The probability of having severe radiation-induced side effects with a varying fractionated dose and a 50 Gy total dose. The tissue dependent parameters are given in Table 7.2 and the normal tissue ratio is taken as $[\alpha/\beta]_N = 3$ and the organ sparing factor as $s = 0.8$.

7.1.3 Parametric investigation for radiotherapy

To get a feeling of how the parameters for radiotherapy influence the treatment plan and the final tumor size, a parametric investigation is done. For a patient with an initial tumor diameter of 60 mm, no metastases, and all cell lines equally represented, the parameters are varied to see what their effect is. The final treatment time is chosen as 60 days, and the maximum total dose as 70 Gy. The optimization performed is described by Equation (6.22) up to Equation (6.16) since one compartment is considered and fixed final treatment time and total dose is used. This formulation is altered by removing $\sum_{s=1}^{d} D_s[\tilde{l}]_s$ from the cost function so that the influence of chemotherapy is not considered, and the separate radiotherapy optimization is performed. By varying some parameters, the effect on the optimal fractionation scheme and the final tumor size can be seen. The optimal fractionated doses give the fractionation scheme for a corresponding total dose of 70 Gy. The final tumor size, given by the total final number of tumor cells, $N(T_F) = \mathbf{1}_n^T x(T_F)$, and final tumor diameter, $\varnothing(T_F)$, can be found in Table 7.3. The initial amount of tumor cells and the initial tumor diameter is also given for comparison.

The first example, with $s = 0.9$, $[\alpha/\beta]_N = 3$, and $h_{max} = 0.1$, gives as outcome to radiate 41 days with 1.6 Gy and 19 days with 0.2 Gy. Since a treatment duration of 60 days is chosen, is it optimal to radiate on each day, however small the dose. Not radiating causes the tumor to grow again, and radiating with a small dose might not be enough to shrink the tumor, but at least it inhibits the growth.

Table 7.3: An investigation of the influence of the parameters on the radiotherapy fractionation scheme and final tumor size. The initial tumor diameter is 60 mm with an equal distribution over the three different CRC cell lines, the final time is 60 days and the maximum allowed dose 70 Gy.

Parameters	**Initial tumor size**		**Model outcomes for radiotherapy**		
s, $[\alpha/\beta]_N$, h_{max}	$N(0)$	$\varnothing(0)$	**Frac. scheme**	$N(T_F)$	$\varnothing(T_F)$
0.9, 3, 0.1	$1.63 \cdot 10^{11}$	60	41 times 1.6 Gy/frac 19 times 0.2 Gy/frac	$1.17{\cdot}10^{7}$	2.50
0.9, 2, 0.1	$1.63 \cdot 10^{11}$	60	36 times 1.8 Gy/frac 24 times 0.2 Gy/frac	$8.82{\cdot}10^{6}$	2.27
0.8, 3, 0.1	$1.63 \cdot 10^{11}$	60	24 times 2.6 Gy/frac 36 times 0.2 Gy/frac	$2.91{\cdot}10^{6}$	1.57
0.9, 3, 0.05	$1.63 \cdot 10^{11}$	60	60 times 1.0 Gy/frac	$8.32{\cdot}10^{7}$	4.80
0.8, 3, 0.05	$1.63 \cdot 10^{11}$	60	36 times 1.8 Gy/frac 24 times 0.2 Gy/frac	$8.82{\cdot}10^{6}$	2.27

When the $[\alpha/\beta]_N$ ratio in the healthy tissues is lowered from 3 to 2, the allowed fractionated dose changes since this modification influences the probability of having severe side effects. Making the ratio smaller means that the healthy tissues are less sensitive to radiation, and a higher fractionated dose can, therefore, be used. The effect is a slightly smaller final tumor.

Changing $s = 0.9$ to $s = 0.8$ means that the dose the OAR (organ at risk) receives is only 80% of the dose the target region receives, compared to the 90% that it first received. Hence to obtain a 0.1 probability of severe side effects, a higher fractionated dose can be given, resulting in 2.6 Gy per fraction, and a smaller final tumor is obtained. On the contrary, when the maximum probability of severe side effects is decreased to 0.05, and $s = 0.9$ is used again, only 1.0 Gy per fraction can be used, and a larger final tumor is the consequence. When changing the organ sparing factor s to 0.8 again, an equal treatment plan and final tumor size is obtained as with $s = 0.9$ and $h_{max} = 0.1$.

7.2 Initial conditions

The primary tumor is again taken as CRC, with three CRC cell lines (HT29, HCT116, SW48) as an option for the initial condition. When multiple compartments are used, they are chosen as lymph node metastases near the bladder, the migration rate for this is calculated in Section 4.3.2. The diameter of metastasis in the lymph node of CRC is approximated between 5 and 10 mm since the average short axis of the largest regional lymph node with metastasis is 5.6 mm [77]. The wider range between 5 and 10 mm is taken since the sizes of the lymph nodes can vary. It is also known that 90% of the nodal metastases of CRC occur in lymph nodes that have a diameter of less than 1 cm, and nodes that have a diameter that is larger than 5 mm are considered morbid for rectal cancer [78]. The volume of the lymph nodes is

approximated as a sphere, and the diameter of a CRC cell is again estimated as $11 \cdot 10^{-3}$ mm. With this information, the total number of tumor cells in a lymph node can be calculated.

A total of ten initial conditions will be determined, for which the combined chemo-radiation treatments are calculated. Most initial conditions are taken with cancer cells present in only one compartment so that the different effect in optimal treatments can be compared. The initial conditions with metastases are taken as three compartments maximum since the model practically works the same in each compartment. The model can, of course, be used for extremely complicated cases with many metastases. The limitation is the practical implementation, hence the number of metastases the LINAC (linear accelerator), the machine that emits highly energized particles, can radiate.

Table 7.4 and Table 7.5 report the initial conditions for the primary site and metastases respectively. Each entry of $x(0)_k$ consists of the number of tumor cells of cell line HT29, HCT116, SW48, respectively, for compartment k. The initial condition for the model is composed of the initial conditions of the separate tumors, hence:

$$x(0)_{tot}^T = \begin{bmatrix} x(0)_{CRC}^T & x(0)_{lymph1}^T & x(0)_{lymph2}^T \end{bmatrix} \tag{7.2}$$

If more compartments need to be used, they can be added as well. Potential compartments can be added too, namely compartments where no tumor cells are found but that are in proximity of the tumor and are therefore in danger of becoming cancerous. The diameter of the primary site and each metastasis is given in mm, represented by $\varnothing_{CRC}$ and $\varnothing_{lymph}$. The initial conditions are given numbers that are used throughout this chapter.

Table 7.4: A set of initial conditions for CRC with metastases in the lymph nodes. The initial tumor diameter (in mm) and initial number of tumor cells per CRC cell line are given for the primary tumor site.

$\boldsymbol{x(0)_{tot}}$	$\boldsymbol{x(0)_{CRC}}$	$\boldsymbol{\varnothing_{CRC}}$
1	$\begin{bmatrix} 1.63 \cdot 10^{11} & 0 & 0 \end{bmatrix}^T$	60
2	$\begin{bmatrix} 0 & 1.63 \cdot 10^{11} & 0 \end{bmatrix}^T$	60
3	$\begin{bmatrix} 0 & 0 & 1.63 \cdot 10^{11} \end{bmatrix}^T$	60
4	$\begin{bmatrix} 5.41 \cdot 10^{10} & 5.41 \cdot 10^{10} & 5.41 \cdot 10^{10} \end{bmatrix}^T$	60
5	$\begin{bmatrix} 4.33 \cdot 10^{11} & 4.33 \cdot 10^{11} & 4.33 \cdot 10^{11} \end{bmatrix}^T$	120
6	$\begin{bmatrix} 6.49 \cdot 10^{11} & 6.49 \cdot 10^{11} & 0 \end{bmatrix}^T$	120
7	$\begin{bmatrix} 0 & 6.49 \cdot 10^{11} & 6.49 \cdot 10^{11} \end{bmatrix}^T$	120
8	$\begin{bmatrix} 6.49 \cdot 10^{11} & 0 & 6.49 \cdot 10^{11} \end{bmatrix}^T$	120
9	$\begin{bmatrix} 2.00 \cdot 10^{12} & 2.00 \cdot 10^{12} & 2.00 \cdot 10^{12} \end{bmatrix}^T$	200
10	$\begin{bmatrix} 3.01 \cdot 10^{12} & 3.01 \cdot 10^{12} & 0 \end{bmatrix}^T$	200

Table 7.5: A set of initial conditions for CRC with metastases in the lymph nodes. The initial tumor diameter (in mm) and the initial number of tumor cells per CRC cell line is given for the metastases tumor sites.

$\boldsymbol{x(0)_{tot}}$	$\boldsymbol{x(0)_{lymph1}}$ $\boldsymbol{x(0)_{lymph2}}$	$\boldsymbol{\varnothing_{lymph1}}$ $\boldsymbol{\varnothing_{lymph2}}$
9	$\begin{bmatrix}3.13\cdot10^7 & 3.13\cdot10^7 & 3.13\cdot10^7\end{bmatrix}^T$	5
	$\begin{bmatrix}2.50\cdot10^8 & 2.50\cdot10^8 & 2.50\cdot10^8\end{bmatrix}^T$	10
10	$\begin{bmatrix}4.70\cdot10^7 & 0 & 4.70\cdot10^7\end{bmatrix}^T$	5
	$\begin{bmatrix}0 & 3.76\cdot10^8 & 3.76\cdot10^8\end{bmatrix}^T$	10

The first eight initial conditions are taken without any metastases, with different distributions over the cell lines to see the effect in treatment. The last two initial conditions are taken with lymph node metastases near the bladder. The possible side effect for the primary site is late rectal bleeding, for lymph node 1 urinary urgency, and lymph node 2 urinary incontinence. Even though it is likely that the side effects of both lymph nodes are equal, they are taken differently to observe the different effects in the fractionation scheme.

7.3 Model simulations for combined chemo-radiation treatments

In this section, the combined chemo-radiation optimization is solved for the initial conditions given in Section 7.2. First, the simulations are obtained for the chemotherapy-alone treatment, so the combined treatments can be compared to them. Then, the optimal combined chemo-radiation treatments are calculated with fixed total treatment duration and total radiation dose, in Section 7.3.1. Last, the model simulations are also performed with varying total treatment durations and total radiation doses, in Section 7.3.2.

The optimization for the chemotherapy-alone treatment is described by Equation (3.23) up to Equation (3.26) with $g_{max} = 0.20$. The initial conditions are taken as in Table 7.4 and Table 7.5 with a total treatment duration of 100 days. The optimal drug durations and the final tumor sizes can be found in Table 7.6. The optimal number of days to give each drug are described by τ_1, τ_2, τ_3 for capecitabine, irinotecan and 5-FU respectively, with $\tau_s = T_F l_s^*$. The total number of cells at the end of treatment is represented by $N_{tot}(T_F)$. For initial conditions 9 and 10 multiple compartments are considered, so the total number of tumor cells and total tumor diameter are given. Since these tumor cells are distributed over multiple compartments, it is calculated as the sum over all compartments:

$$N_{tot}(T_F) = \sum_{k=1}^{p} N_k(T_F) \tag{7.3}$$

Using the total tumor volume, $N_{tot}(T_F)$, it can be estimated as sphere again, and the tumor diameter of that is given as $\varnothing_{tot}(T_F)$. The initial tumor sizes are also given for comparison and are calculated on the same way. For initial conditions 9 and 10, the initial tumor diameters are therefore not 215 mm but 200 mm (the metastases only have an effect on the diameter in the decimals).

Table 7.6: Optimal drug durations and final tumor sizes for chemotherapy-alone treatments, the optimization is described by Equation (3.23) to Equation (3.26). Initial conditions are described in Table 7.4 and Table 7.5. Parameters chosen as $T_F = 100$ and $g_{max} = 0.20$.

	Initial tumor size		**Optimal drug durations**	**Final tumor size**	
$\boldsymbol{x(0)}$	$\boldsymbol{N_{tot}(0)}$	$\boldsymbol{\varnothing_{tot}(0)}$	$\boldsymbol{\tau_1,\ \tau_2,\ \tau_3}$	$\boldsymbol{N_{tot}(T_F)}$	$\boldsymbol{\varnothing_{tot}(T_F)}$
1	$1.63 \cdot 10^{11}$	60	100, 0, 0	$4.68{\cdot}10^{11}$	85.4
2	$1.63 \cdot 10^{11}$	60	0, 100, 0	$3.90{\cdot}10^{12}$	173
3	$1.63 \cdot 10^{11}$	60	0, 100, 0	$1.33{\cdot}10^{12}$	121
4	$1.63 \cdot 10^{11}$	60	13, 87, 0	$2.24{\cdot}10^{13}$	310
5	$1.30 \cdot 10^{12}$	120	13, 87, 0	$1.80{\cdot}10^{14}$	620
6	$1.30 \cdot 10^{12}$	120	35, 65, 0	$1.34{\cdot}10^{14}$	563
7	$1.30 \cdot 10^{12}$	120	0, 100, 0	$2.09{\cdot}10^{13}$	303
8	$1.30 \cdot 10^{12}$	120	14, 86, 0	$2.41{\cdot}10^{14}$	684
9	$6.02 \cdot 10^{12}$	200	13, 87, 0	$8.31{\cdot}10^{14}$	1034
10	$6.02 \cdot 10^{12}$	200	34, 66, 0	$6.21{\cdot}10^{14}$	938

For the chemotherapy-alone treatments, drug 3 is never used. This is logical when looking at the drug effect parameters in Table 4.3 for the cell lines HT29, HCT116, and SW48. Drug 1 and 2 have better effects on these three CRC cell lines and are therefore always preferred over drug 3. When the initial condition is chosen such that only one cell line is present, logically, only one drug is used for the whole treatment duration. When multiple cell lines are present, the optimization determines the optimal amount of days to use each drug. In this case, the final tumor size is significantly larger than for tumors that only have one cell line present. This can be seen for initial conditions 1, 2, 3, where only one cell line is present, in comparison to initial condition 4, where the cell lines are all equally present. This consequence is explained by the diverse effect the drugs have on the cell lines. For example, when drug 2 is given, cell line 3 (SW48) continues to grow at the unrestrained rate, since this cell line is resistant to drug 2.

The side effects always stay below the maximum tolerated level; hence the drugs are used for the whole treatment horizon. The final tumor sizes are more significant than the initial tumor sizes for all initial conditions. When looking at the parameters in Table 4.3, the drugs only have an inhibiting effect on the tumor cells but are not strong enough to make them decrease.

7.3.1 Fixed treatment duration and total radiation dose

In this subsection, the combined chemo-radiation treatment plans are calculated for fixed treatment duration and total radiation dose. The optimization described by Equation (6.22) to Equation (6.28) will be used on the initial conditions described in Section 7.2. The final treatment time is fixed (100 days), as well as the total radiation dose (70 Gy for compartment 1, CRC, and 50 Gy for compartment 2, lymph 1, and compartment 3, lymph 2). The side effects that can arise are late rectal bleeding for compartment 1, urinary urgency for compartment 2, and urinary incontinence for compartment 3, for which the parameters are described in Table 7.2. The maximum NTCP for radiotherapy is taken the same in all compartments, as $h^1_{max} = h^2_{max} = h^3_{max} = 0.05$. The organ sparing factor s is chosen as 0.8 for each OAR.

The maximum probability for chemotherapy-induced side effects is $g_{max} = 0.20$. The optimal amount of days each drug has to be used is described by τ_1, τ_2, τ_3. The radiotherapy treatment fractionation scheme is calculated for each compartment, described by the fractionated dose, since a fixed total dose is considered. The total final number of tumor cells over all compartments will be described by $N_{tot}(T_F) = \sum_{k=1}^{p} N_k(T_F)$. The total final tumor diameter, $\varnothing_{tot}(T_F)$, is the diameter of a sphere with N_{tot} cells, given in mm. The optimal treatment plans and final tumor sizes can be found in Table 7.7, where CT refers to chemotherapy and RT to radiotherapy.

First, it should be noted that the values in Table 7.7 are not realistic; for example, $0 < N(T_F) < 1$ is in practice not possible. The number of cells should always be a round number since partial cells are impossible. However, the values are kept like this so they can be compared.

For all initial conditions, the optimal radiation plan for the primary site is to radiate 31 days with 1.8 Gy per fraction, and 69 days with 0.2 Gy per fraction. Since the treatment duration is 100 days, the optimal treatment plan is to administer a dose every day, and else the tumor would grow again.

Interestingly, the radiation treatment plan for each compartment does not change when the initial condition is varied. The treatment plan of radiation does not depend on the distribution over the different cell lines since the effect of radiation is set. Of course, the higher the dose, the better the effect. The treatment plan of radiation depends on the parameters s, h_{max}, P_{max}, $[\alpha/\beta]_N$, D_{50}, and γ_{50} and TF. When changing either of these parameters, the treatment plan of radiation changes, which can be seen when multiple compartments are used. For initial conditions 9 and 10, a different radiation treatment plan is obtained for the metastases compartments than for the primary site.

The chemotherapy treatment plan, however, depends on the initial condition. The optimal duration of each drug changes when the initial condition is alternated since there is the freedom to switch between drugs depending on which is the best for the initial tumor. The most effective drug for HT29 is capecitabine and for both HCT116 and SW48, irinotecan. The effectiveness of the anti-cancer drugs can be deduced from the drug effect parameters in Table 4.3 and from the optimal treatment schedule in Table 7.7 for initial conditions 1 up to 3.

When comparing Table 7.7 to Table 7.6, it can be seen that the chemotherapy treatment plan changes for initial conditions 4, 5, 6, 8, 9 and 10. This can be explained by looking at the parameters in Table 4.3 and Table 7.1. When only chemotherapy is considered for initial condition 4, the optimal combination of drugs is to use drug 1 for 13 days and drug 2 for 87 days, which is logical since drug 2 is the most effective against HCT116 and SW48. However, when radiotherapy is also added, the optimal treatment plan for chemotherapy changes into using drug 1 for 85 days and drug 2 for 15 days. Radiotherapy is the least effective on HT29, so drug 1 needs to be used longer to obtain the optimal outcome.

When comparing the final tumor sizes between Table 7.7 and Table 7.6 the difference is immense. While the final tumor sizes with chemotherapy are all bigger than their initial tumor size, the final tumor sizes when also using radiotherapy are practically negligible (all less than 1 mm). The influence of adding radiotherapy is great, even without considering a radio-sensitizing effect, which is not incorporated in the model.

Table 7.7: Model outcomes for the optimization described by Equation (6.22) to Equation (6.28) for initial conditions described in Table 7.4 and Table 7.5. Parameters chosen as $T_F = 100$, $P^1_{max} = 70$, $P^2_{max} = 50$, $P^3_{max} = 50$, $h^k_{max} = 0.05 \; \forall \; k$, $s = 0.8$, $g_{max} = 0.20$.

	Initial tumor size		**CT**	**RT**	**Final tumor size**	
$\boldsymbol{x(0)}$	$\boldsymbol{N_{tot}(0)}$	$\boldsymbol{\varnothing_{tot}(0)}$	$\boldsymbol{\tau_1, \tau_2, \tau_3}$	**Fract. scheme**	$\boldsymbol{N_{tot}(T_F)}$	$\boldsymbol{\varnothing_{tot}(T_F)}$
1	$1.63 \cdot 10^{11}$	60	100, 0, 0	$\begin{pmatrix} 31 \cdot 1.8Gy/frac \\ 69 \cdot 0.2Gy/frac \end{pmatrix}_{CRC}$	6206	0.202
2	$1.63 \cdot 10^{11}$	60	0, 100, 0	$\begin{pmatrix} 31 \cdot 1.8Gy/frac \\ 69 \cdot 0.2Gy/frac \end{pmatrix}_{CRC}$	0.0646	0.00441
3	$1.63 \cdot 10^{11}$	60	0, 100, 0	$\begin{pmatrix} 31 \cdot 1.8Gy/frac \\ 69 \cdot 0.2Gy/frac \end{pmatrix}_{CRC}$	0.00281	0.00160
4	$1.63 \cdot 10^{11}$	60	83, 17, 0	$\begin{pmatrix} 31 \cdot 1.8Gy/frac \\ 69 \cdot 0.2Gy/frac \end{pmatrix}_{CRC}$	6592	0.206
5	$1.30 \cdot 10^{12}$	120	83, 17, 0	$\begin{pmatrix} 31 \cdot 1.8Gy/frac \\ 69 \cdot 0.2Gy/frac \end{pmatrix}_{CRC}$	52736	0.413
6	$1.30 \cdot 10^{12}$	120	100, 0, 0	$\begin{pmatrix} 31 \cdot 1.8Gy/frac \\ 69 \cdot 0.2Gy/frac \end{pmatrix}_{CRC}$	24840	0.321
7	$1.30 \cdot 10^{12}$	120	0, 100, 0	$\begin{pmatrix} 31 \cdot 1.8Gy/frac \\ 69 \cdot 0.2Gy/frac \end{pmatrix}_{CRC}$	0.270	0.0071
8	$1.30 \cdot 10^{12}$	120	83, 17, 0	$\begin{pmatrix} 31 \cdot 1.8Gy/frac \\ 69 \cdot 0.2Gy/frac \end{pmatrix}_{CRC}$	79093	0.472
9	$6.02 \cdot 10^{12}$	200	83, 17, 0	$\begin{pmatrix} 31 \cdot 1.8Gy/frac \\ 69 \cdot 0.2Gy/frac \end{pmatrix}_{CRC}$ $\begin{pmatrix} 13 \cdot 2.6Gy/frac \\ 87 \cdot 0.2Gy/frac \end{pmatrix}_{lymph1}$ $\begin{pmatrix} 8 \cdot 4.0Gy/frac \\ 92 \cdot 0.2Gy/frac \end{pmatrix}_{lymph2}$	244326	0.688
10	$6.02 \cdot 10^{12}$	200	100, 0, 0	$\begin{pmatrix} 31 \cdot 1.8Gy/frac \\ 69 \cdot 0.2Gy/frac \end{pmatrix}_{CRC}$ $\begin{pmatrix} 13 \cdot 2.6Gy/frac \\ 87 \cdot 0.2Gy/frac \end{pmatrix}_{lymph1}$ $\begin{pmatrix} 8 \cdot 4.0Gy/frac \\ 92 \cdot 0.2Gy/frac \end{pmatrix}_{lymph2}$	117395	0.539

Table 7.7 shows that the treatment plans do not depend on the tumor size, but only on the distribution over the different cell lines, which can be seen for initial conditions 4 and 5. This might not be very intuitive since it is expected that the bigger the tumor, the longer the treatment or higher the radiation. However, the model minimizes the total number of tumor cells and continues doing that as long as the side effects allow for it. If it is desired to stop the minimization process when a specific final tumor size has been reached, so the patient is not over treated, there are two possible options. One is to calculate the optimal treatment plans and stop the treatment earlier: the right time to stop can be calculated based on the model. The other option is to add a termination criterion in the implementation.

Another observation is that, when the initial tumor diameter is doubled, the final tumor diameter is also doubled if the rest is kept the same. This can be seen for initial conditions 4 and 5. With initial condition 5, the initial tumor diameter is twice as with initial condition 4, and this also results in double the final tumor diameter. The number of tumor cells is precisely eight times as much when the tumor diameter is doubled since the volume is estimated as a sphere. When the initial number of tumor cells is doubled, the final number of tumor cells will, of course, also be doubled.

When multiple compartments are cancerous, hence for initial conditions 9 and 10, a different optimal treatment plan for each compartment is obtained. Since different side effects are considered for each compartment, and different maximum doses are used, the optimal fractionated dose is also different. Calculation of the optimal fractionation scheme per compartment that can be radiated is an advantage of this formulation of the optimization problem.

The total final diameter is given in Table 7.7. For initial conditions 9 and 10 multiple compartments are considered, and the total final tumor diameter is distributed over multiple compartments. The specification of the tumor diameters per compartment is given in Table 7.8.

Table 7.8: Specification of the tumor diameters per compartment for initial condition 9 and 10, for the model outcomes in Table 7.7.

	$x(0) = 9$	$x(0) = 10$
$\varnothing_{CRC}(T_F)$	0.688	0.535
$\varnothing_{lymph1}(T_F)$	0.0423	0.107
$\varnothing_{lymph2}(T_F)$	0.0547	0.125

7.3.2 Optimizing the treatment duration and total radiation dose

In Section 7.3.1, the treatment time and total radiation dose were fixed. In this subsection, they are taken as a variable. For chemotherapy, this has little effect, except that the drugs can be used longer. The side effects of chemotherapy were not met when using $T_F = 100$ days, so this means that the drugs could be used longer when considering their side effect. For radiotherapy, this has more effects. When the total dose is fixed, the only variable is the fractionated dose. So for the same parameters, the same fractionated dose is chosen that corresponds to h_{max}, this could also be seen in Table 7.7. When varying the total dose, the radiation fractionation can change, dependent on the initial tumor.

The optimization problem described by Equation (6.29) with constraints Equation (6.23) up to Equation (6.28) will now be performed on the initial conditions with no metastases,

hence in Table 7.4. The optimization is not performed on all initial conditions since the same principle holds for each compartment. The possible total doses are chosen between 30 and 100 Gy, and the final treatment times between 90 and 130 days. The rest of the parameters are chosen the same as in Section 7.3.1. The optimal treatment plans and final tumor sizes can be found in Table 7.9. The T_F corresponds to the longest treatment time of the treatment durations for chemotherapy or radiotherapy. Hence, $T_F = \max(T_{CT}, T_{RT})$, where T_{CT} and T_{RT} correspond to the treatment time of chemotherapy and radiotherapy respectively. The sum over all τ's determines the chemotherapy treatment duration, and for radiotherapy, the overall duration is obtained by dividing the total dose with the fractionated dose. The final amount of tumor cells is represented by $N_{tot}(T_F)$ and the final tumor diameter by $\varnothing_{tot}(T_F)$.

Table 7.9: Outcomes of the optimization described by Equation (6.29) with constraints Equation (6.23) up to Equation (6.28) for initial conditions described in Table 7.4. Parameters chosen as $T_F \in \{80 : 5 : 150\}$, $P^1_{max} \in \{30 : 2 : 100\}$, $h^1_{max} = 0.05$, $s = 0.8$, $g_{max} = 0.20$.

	Initial tumor size		**CT**	**RT**	**Final tumor size**	
$\boldsymbol{x(0)}$	$\boldsymbol{N_{tot}(0)}$	$\boldsymbol{\varnothing_{tot}(0)}$	$\boldsymbol{\tau_1, \tau_2, \tau_3}$	**Frac. scheme**	$\boldsymbol{N_{tot}(T_F)}$	$\boldsymbol{\varnothing_{tot}(T_F)}$
1	$1.63 \cdot 10^{11}$	60	118, 0, 0	$150 \cdot 0.6$ Gy/frac	795	0.102
2	$1.63 \cdot 10^{11}$	60	0, 118, 0	$150 \cdot 0.6$ Gy/frac	0.00178	0.00133
3	$1.63 \cdot 10^{11}$	60	0, 118, 0	$150 \cdot 0.6$ Gy/frac	$4.26{\cdot}10^{-5}$	$3.84{\cdot}10^{-4}$
4	$1.63 \cdot 10^{11}$	60	97, 21, 0	$150 \cdot 0.6$ Gy/frac	1048	0.112
5	$1.30 \cdot 10^{12}$	120	97, 21, 0	$150 \cdot 0.6$ Gy/frac	8380	0.223
6	$1.30 \cdot 10^{12}$	120	118, 0, 0	$150 \cdot 0.6$ Gy/frac	3180	0.162
7	$1.30 \cdot 10^{12}$	120	0, 118, 0	$150 \cdot 0.6$ Gy/frac	0.00730	0.00210
8	$1.30 \cdot 10^{12}$	120	97, 21, 0	$150 \cdot 0.6$ Gy/frac	12573	0.2558

The optimal treatment days for chemotherapy now sum up to 118 days, instead of 100 days. The treatment duration is extended since the probability of severe chemotherapy-induced side effects was less than $g_{max} = 0.20$ for the 100-day horizon. The distribution of treatment days over the different drugs are, as expected, the same as with the 100-day horizon. This can be checked by calculating the fractions τ_s/T_F for the different final treatment times.

For radiotherapy, the optimal fractionation scheme has changed to 150 fractions of 0.6 Gy. The same fractionation scheme is again obtained for each of the initial conditions: considering the same parameters are used for all initial conditions, is this logical. The maximum available treatment duration is also used for all initial conditions. When a more extended treatment duration than 150 days is available, the optimal treatment duration will be extended as well. Even though the final tumor size is smaller, due to the longer treatment duration, the obtained gain is negligible. Since the final tumor sizes are already minuscule, the treatment does not have to be prolonged. When the final tumor size is not small enough, increasing the available treatment durations could be considered.

In the model outcomes reported in Table 7.9, the optimal fractionation scheme for radiotherapy is always to give the same fractionated dose for a certain amount of treatment days. A result from literature states that "when the amount of treatment days is fixed, the optimal fractionation schedule is to deliver either a single dose or an equal dose on each treatment day" [21], [79]. Even though the final treatment time is varied, it is fixed when solving each optimization problem, so the outcomes of the model are aligned with the result in [79].

7.4 Comparing treatment scheduling plans

Up to now, the scheduling of the drugs and radiation was not considered. The scheduling can, however, have an influence on the final tumor size, for example, when rest days are incorporated. In this section, the effect of two different treatment schedules is investigated.

The optimal treatment schedule is calculated, adopting the "7 days a week" treatment schedule for radiotherapy described by Algorithm 2 in combination with the chemotherapy scheduling described by Algorithm 1. The sub-optimal treatment schedule is obtained using the "5 days a week" treatment schedule for radiotherapy described by Algorithm 3, in combination with the chemotherapy scheduling described by Algorithm 1. Both treatments are initiated at the same time. The duration of both treatments can be different, so the final tumor size is calculated at the end of the longest treatment.

The outcomes achieved with the optimal and sub-optimal treatment schedules are calculated for the chemotherapy drug durations and radiation fractionation schemes given in Table 7.9. For each of these schedules are the total final number of tumor cells N and the final tumor diameter $\varnothing$ (in mm) given. The difference between the final and initial total number of tumor cells and final tumor diameter is also given by Δ_N and $\Delta_\varnothing$, respectively. The final tumor sizes after both scheduling plans can be found in Table 7.10.

Table 7.10: The final tumor sizes after the optimal treatment schedule, described in Algorithm 2, and after the sub-optimal treatment schedule, described in Algorithm 3. Both schedules are in combination with the chemotherapy schedule in Algorithm 1. The outcome of the scheduling plans are obtained for the treatments in Table 7.9.

	Optimal scheduling		**Sub-optimal scheduling**		**Loss in final size**	
$\boldsymbol{x(0)}$	$\boldsymbol{N_{opt}}$	$\boldsymbol{\varnothing_{opt}}$	$\boldsymbol{N_{subopt}}$	$\boldsymbol{\varnothing_{subopt}}$	$\boldsymbol{\Delta_N}$	$\boldsymbol{\Delta_\varnothing}$
1	795	0.102	$2.78{\cdot}10^{5}$	0.718	$2.77{\cdot}10^{5}$	0.616
2	0.00178	0.00133	5.21	0.0191	5.21	0.0178
3	$4.26{\cdot}10^{-5}$	$3.84{\cdot}10^{-4}$	4.34	0.0179	4.34	0.0175
4	1048	0.112	$2.57{\cdot}10^{7}$	3.25	$2.57{\cdot}10^{7}$	3.14
5	8380	0.223	$2.06{\cdot}10^{8}$	6.50	$2.06{\cdot}10^{8}$	6.27
6	3180	0.162	$1.11{\cdot}10^{6}$	1.14	$1.11{\cdot}10^{6}$	0.979
7	0.00730	0.00210	38.2	0.0370	38.2	0.0349
8	12573	0.256	$3.09{\cdot}10^{8}$	7.44	$3.09{\cdot}10^{8}$	7.18

Table 7.10 shows that the outcomes of the optimal scheduling are, as expected, the same as in Table 7.9. The final tumor sizes with the sub-optimal scheduling are for all initial conditions larger than with the optimal schedule. For the initial conditions 1 up to 4, representing an initial tumor diameter of 60 mm, the most significant difference in tumor diameter is 3.14 mm. For these tumors, the final tumor diameter is, on average, 1.00 mm instead of 0.0539 mm, which is almost twice the final tumor size. For initial conditions 5 up to 8, representing an initial tumor diameter of 120 mm, the most significant difference in tumor diameter is 7.18 mm. For these tumors is the final diameter, on average, 3.78 mm instead of 0.161 mm, which is 23 times as big. So the difference might seem small, but when it is compared to the optimal outcome, it is quite significant. The loss in the final tumor size also becomes more significant when larger initial tumor sizes are used.

The loss in effect is, however, still limited, since the effect of the drugs and radiation is proportional to the size of the tumor. So, even though the tumor grows on the weekends, this can be partly compensated with the fact that the drugs and radiation have become more effective.

An example of tumor diameter and states over time for the different scheduling plans with initial condition 5 can be seen in Figure 7.3. The chemotherapy treatment plan is to give drug 2 for the first 21 days, and drug 1 for the 97 days after. The radiotherapy treatment plan is to give 150 fractions of 0.6 Gy.

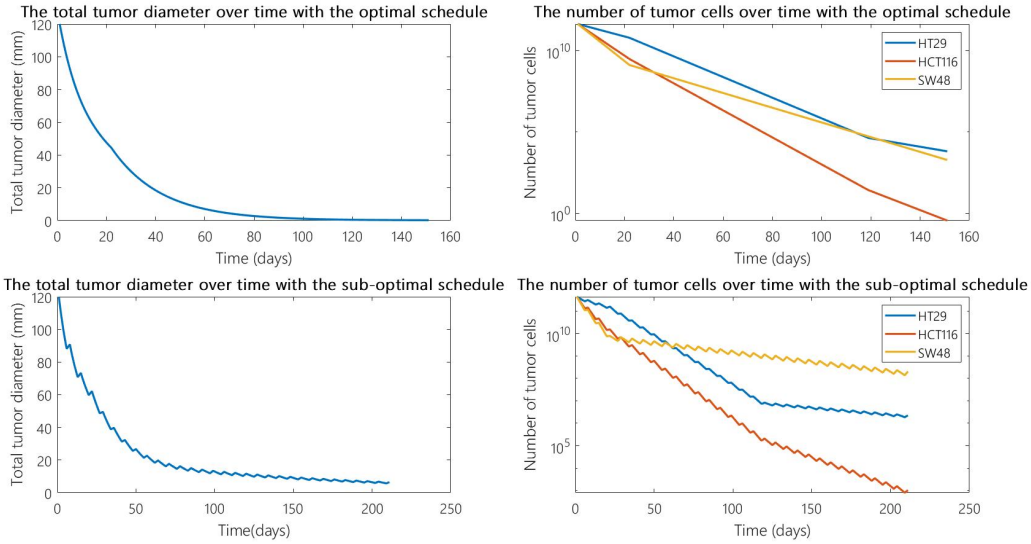

Figure 7.3: A comparison of the optimal and sub-optimal scheduling for initial condition 5. The chemotherapy treatment plan is to give drug 2 the first 21 days, and drug 1 for the 97 days after. The radiotherapy treatment plan is to give 150 fractions of 0.6 Gy.

Figure 7.3 shows that the tumor diameter decreases smoothly over time with the optimal scheduling. With the sub-optimal scheduling, however, the tumor increases on all weekend days, i.e., when it is not radiated. The effect of the different drugs on the different cell lines can also be seen in the number of tumor cells per cell line. When the therapy switches from drug 2 to drug 1, after 21 days, the effect on the variation of SW48 is visible. Since cell line SW48 is resistant to drug 1, the rate also does not change when the chemotherapy treatment is stopped at 118 days.

In Figure 7.3, it can also be seen that the decrease rate of the tumor diameter is almost negligible at the end of the treatment. Especially for the optimal scheduling case, the treatment could be stopped earlier since the gain is small after a specific time.

7.5 Summary

This chapter showed some simulations for the combined chemo-radiation model. First, the model parameters were obtained for radiotherapy. The parameters for the effect of radiation are based on the LQ model. The parameters for the radiation-induced side effects are based on the NTCP model. A small parametric investigation was done for radiotherapy to investigate the effect on the optimal treatment plan. For radiotherapy, the model outcomes show high parametric reliability since many parameters are needed, and the optimal fractionation scheme depends entirely on the parameter values. A total of 10 initial conditions were obtained to simulate the combined chemo-radiation model. The first 8 initial conditions represent a CRC without metastases, with different initial sizes and compositions. Initial conditions 9 and 10 represent a CRC with two metastases in the lymph nodes near the bladder. The possible side effect due to radiating the CRC is late rectal bleeding, for lymph node 1 urinary urgency, and lymph node 2 urinary incontinence.

First, the chemotherapy-alone treatment plans are simulated on this set of 10 initial conditions. The optimal duration to use each drug depends on the initial composition. When simulating the combined chemo-radiation model outcomes with fixed treatment duration and total dose, the chemotherapy drug durations change due to the addition of radiotherapy. The radiotherapy fractionation schemes are equal for all initial conditions per compartment, due to the fact that the parameters are chosen the same for each compartment. The combined chemo-radiation treatment plans are also calculated for varying total treatment duration and total radiation dose. The chemotherapy drug durations could be extended, and a different fractionation scheme was obtained for radiotherapy. The outcome is a smaller final tumor size.

Last, the effect of two different scheduling plans is compared. The final tumor sizes after the optimal "7 days a week" and the sub-optimal "5 days a week" radiation schedule, both in combination with the chemotherapy scheduling, were obtained for a set of treatment plans. The loss in the final tumor size becomes larger when a larger initial tumor is considered. Another observation made is that the treatment can, in some cases, be stopped earlier since the gain is small after a specific time.

Chapter 8

Conclusions and recommendations

8.1 Conclusions

The main goal of this thesis was to propose novel approaches to optimize cancer treatment efficiency when combining chemotherapy and radiotherapy by using control-theoretical methods as well as radiotherapy models. A generally applicable model is obtained and used to optimize the duration of treatment with different chemotherapeutic drugs and optimize fractionation schemes for radiotherapy. The model is especially appropriate for heterogeneous tumors, since it describes the effect of therapies on different tumor cell lines, and includes the possibility of mutations. Metastases are included since the model considers different tumor compartments, and the possibility of migrations between compartments are modeled as well. Undesired consequences due to toxicities are incorporated, and an upper bound can be set to limit the possible damage.

The predictive power of the model was tested on a dataset for the drug irinotecan. The dataset lacked some crucial information, such as the tumor size per compartment and composition of the different cell lines. Some assumptions were made, and optimization for the initial tumor composition was performed, so the model could be used to predict the tumor dynamics of the patients. Even though the patient data had varying responses to the drug, the model could replicate most patients sufficiently well, with a mean difference between the true and predicted tumor diameter of 4.04 mm over all time points and all patients. This corresponds to a mean percentage difference in tumor diameter of 5.17% when the size of the tumor is taken into consideration. The prediction could be improved significantly when flexible drug effects were considered to account for cell lines that are not incorporated in the model. The mean difference in tumor diameter could be reduced to 1.41 mm, and the mean percentage difference to 1.59%. The clinical treatments that were provided to the patients could not be improved much, as irinotecan already had the most significant effect among all considered drugs on most cell lines.

Combined chemo-radiation model outcomes were also tested on CRC (colorectal cancer). Due to the lack of patient data, the results could not be validated. The addition of radiotherapy

showed great significance in the final tumor sizes, as it is a more effective treatment option. The optimal fractionation scheme for radiotherapy depends on the chosen parameters, regardless of the initial tumor composition. As a result, the same optimal fractionation scheme for a compartment was obtained for all simulated initial compositions. Optimal drug usage, on the other hand, depends on the initial tumor composition, as well as the radiotherapy effects. The treatment plans for radiotherapy also showed greater parametric reliability than those for chemotherapy since more parameters are needed, and the optimal fractionation scheme depends entirely on the parameter values.

The scheduling of radiotherapy and chemotherapy are considered as two separate problems, for each treatment alone, since they are also applied as two separate treatments. For chemotherapy, the strongest drug is administered first, where the strongest drug is defined as the drug that has the most effect on the initial composition when given on its own. For radiotherapy, two different scheduling plans were obtained: the optimal "7 days a week" radiation plan and a sub-optimal "5 days a week" radiation plan. The optimal and sub-optimal scheduling were both combined with chemotherapy scheduling and compared to each other. The loss in the obtained final tumor size with the optimal and sub-optimal scheduling becomes larger when a larger initial tumor is considered on the same treatment horizon. For a 150 day horizon a loss of almost 4 mm was obtained when an initial tumor size of 120 mm was considered. The loss was partly compensated due to the proportional effect of drugs and radiation.

The model we proposed for combined chemo-radiation therapy shows promising applications for cancer treatment design. The possibility to model tumor compartments and specify heterogeneous properties is beneficial. The use of positive switched systems for combined chemo-radiation treatments is a novel approach to obtain optimal drug usage and fractionation schemes for each compartment.

To conclude, this thesis successfully used control-theoretic methods to model cancer evolution and design combined chemo-radiation treatments. Positive switched systems can be used to obtain optimal treatment durations for drugs and optimal radiation fractionation schemes for each body compartment, resulting in improved treatment efficiency.

8.2 Future recommendations

Several recommendations can be made to improve the model. First, the model validation must be conducted further. Combined chemo-radiation treatments, as well as radiotherapy-alone treatments, have not been compared to patient data, and results could, therefore, not be validated. Several other additions can also be made that can improve the clinical accuracy of the model.

The clinical dataset showed a delayed response to the anti-cancer drugs for some patients in Section 5.1, which is not incorporated in the model. This delay, however, did not occur for all patients, and it is unclear when the anti-cancer treatment starts being effective. It could be interesting to investigate when this delayed response occurs so that it can be incorporated into the model.

The effect of the human immune system can be incorporated to take care of a small enough number of tumor cells. In Section 6.3, it could be seen that the effect of the therapies is reduced when the tumor size gets very small. It could be possible to stop the treatment

earlier, which would be beneficial for the patient with regard to side effects, and let the immune system take care of the remaining tumor cells.

The chemotherapeutic drug doses were now always taken as the MTD (maximum tolerated dose). However, it could be explored if lower doses can be used to obtain similar treatment responses. One way to incorporate this into the model is by using the optimization formulation in Equation (3.13) up to Equation (3.15) and relaxing the first constraint to $[l^{(i)}]_s \geq 0$. However, relaxing this constraint implies that drug mixing can occur per time interval, so a solution should be obtained for this. Also, the drug effect parameters represent the effect when the drug is given at its MTD. So before different doses can be used, the relation between the drug dose and the treatment response should be studied.

Furthermore, when combining chemotherapeutic agents with radiotherapy, often, increased radiation sensitivity is observed in the clinic [80]. Understanding the mechanisms between the anti-cancer agents and radiation could lead to further improvements in the accuracy of the model predictions.

Appendix A

Model parameter estimation

A.1 An example of the growth rate parameter estimation

The estimation of the growth rate parameters are obtained from existing murine tumor models. This section shows how the parameters are fitted. As mentioned, in Section 4.3.1, an exponential curve is fitted through the line in the xenograft that represents the growth of the tumor without the influence of drugs, typically referred to as vehicle or control. The xenograft on which the parameter estimation for HT29 is based is shown in Figure A.1. The tumor volume over time can be seen for multiple lines, where the control line refers to no drug administration represented by $-\square-$. On day 0 of the graph, $1.3{\cdot}10^6 \pm 5\%$ cells of HT29 were injected in the mice. They were then split up in random groups of 6 mice, and the their tumor volume was measured on set days.

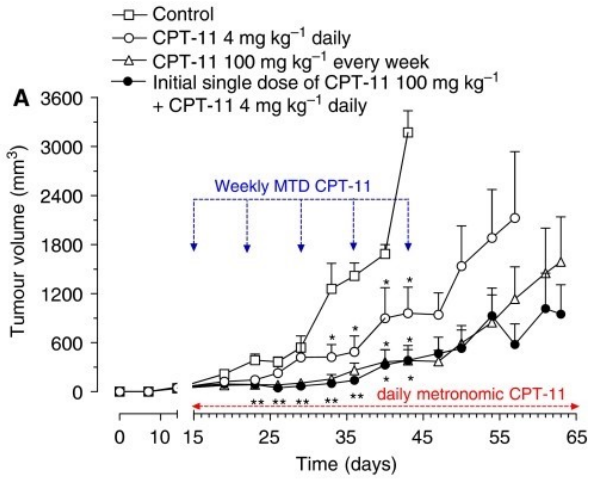

Figure A.1: A xenograft representing the effect of irinotecan (CPT-11) on HT29 cells, obtained from [54].

A graph digitizer was used to obtain the data points shown in Figure A.1 so an exponential curve could be fitted through the points. This is done for the control line, which represents the natural tumor growth without the influence of drugs. The data points that are used to fit the exponential line through are from day 15 to day 43 since the drug administration is also done for that time interval and they can be compared fairly. The data points with the obtained fitted curve are shown in Figure A.2.

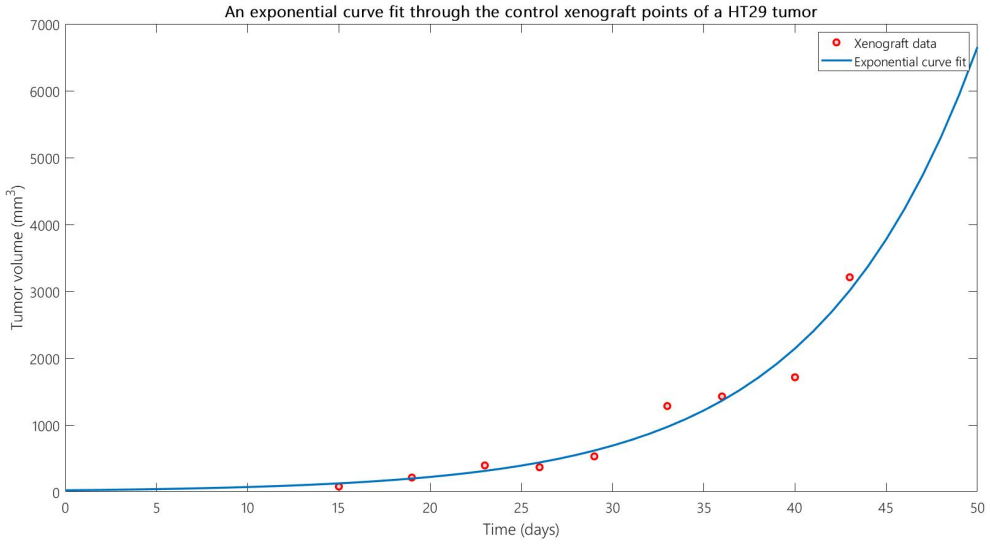

Figure A.2: Fitting of an exponential curve through the data points of the xenograft for HT29 cells obtained from [54].

The function of the exponential curve in Figure A.2 is:

$$y(t) = 23.2e^{0.113t} \tag{A.1}$$

where $y(t)$ represents the tumor volume in mm^3 and t represents the time in days. The growth rate parameter can be obtained from Equation (A.1), and is 0.113. The model represents the growth of the amount of tumor cells, whereas this xenograft describes the tumor volume. Since only the rate is considered, and not the starting point of the exponential curve, the transformation to the amount of cells does not have to be made. The growth rate of 0.0976 in Table 4.2 can be obtained, by following the same procedure for the xenografts obtained from [52] and [53], and taking the average.

A.2 An example of the drug effect parameter estimation

A similar procedure as for the growth rate parameters is followed for the drug effect parameters. An example will be shown for the effect of irinotecan on HT29, the xenograft given in Figure A.1 is used for this. The MTD schedule corresponds to the line where 100 mg/kg of irinotecan is given weekly, represented by $-\triangle-$. The data points are obtained with a graph digitizer, and an exponential curve is fitted through the points of day 15 to day 43, which can be seen in Figure A.3.

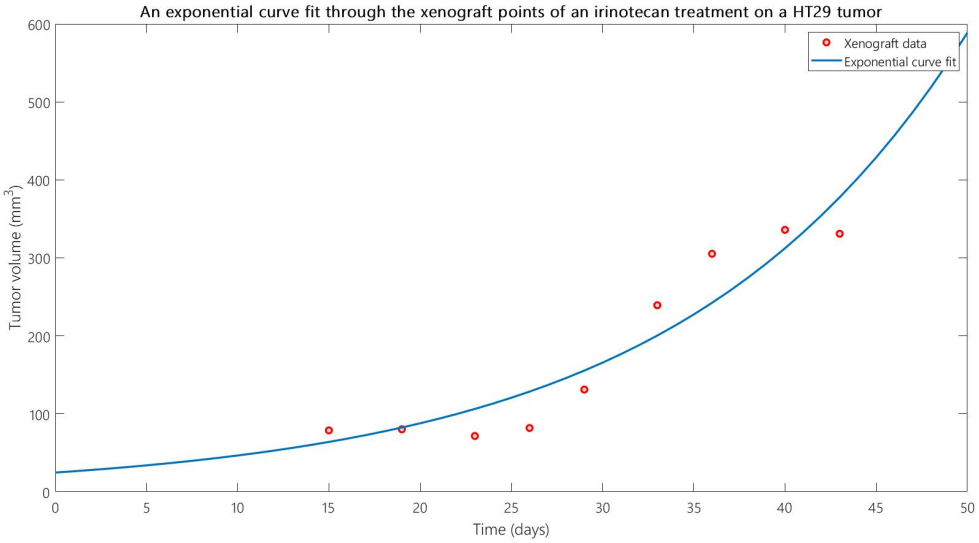

Figure A.3: Fitting of an exponential curve through the data points of the xenograft representing the effect of the MTD schedule for irinotecan on HT29 cells, obtained from [54].

The formula of the function in Figure A.3 is given by:

$$y(t) = 24.7e^{0.0638t} \tag{A.2}$$

where $y(t)$ represents the tumor volume in mm^3 and t the time in days. The tumor growth rate with the effect of irinotecan is 0.0638. The drug effect parameter in Table 4.4 can then be calculated as $0.0976 - 0.0638 = 0.0338$, with 0.0976 the obtained growth parameter for HT29.

Appendix B

Model validation with clinical data

B.1 Comparison at each clinically measured point

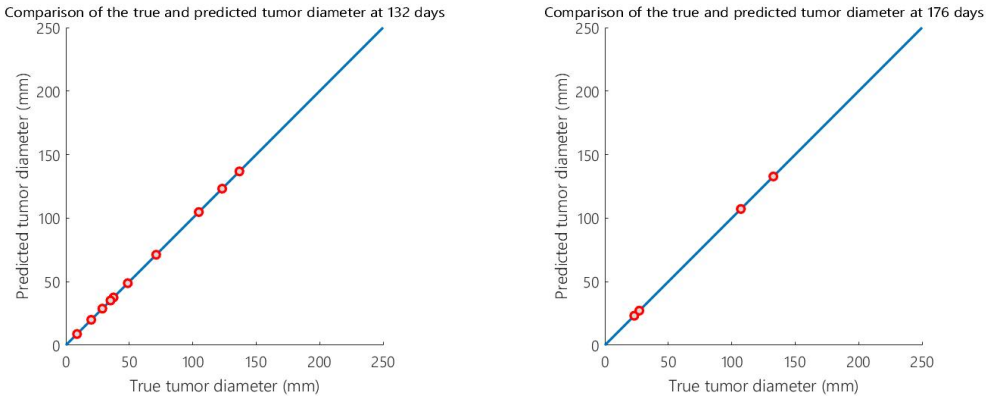

Figure B.1: The true and predicted tumor diameter plotted against each other at 132 days (left) and 176 days (right). Optimization is performed as in Equation (5.8) to Equation (5.10) and parameters are taken as in Section 4.3.

B.2 Comparison over the whole treatment duration

Table B.1: The mean difference, standard deviation and maximum difference in the true and predicted amount of tumor cells and tumor diameter, per patient. The underlined patients have CRC as primary tumor and the red numbers are higher than the average of that column. The optimization performed is Equation (5.11) up to Equation (5.12).

	Difference in tumor cells			Difference in diameter(mm)		
Patient	μ_N	σ_N	$\max_N$	$\mu_\varnothing$	$\sigma_\varnothing$	$\max_\varnothing$
1	$6.65{\cdot}10^{11}$	$3.58{\cdot}10^{11}$	$1.11{\cdot}10^{12}$	19.5	14.4	38.2
2	$3.17{\cdot}10^{9}$	$1.86{\cdot}10^{9}$	$5.14{\cdot}10^{9}$	2.43	1.76	4.37
3	$2.29{\cdot}10^{10}$	$1.53{\cdot}10^{10}$	$4.09{\cdot}10^{10}$	5.58	3.46	10.3
4	$1.57{\cdot}10^{12}$	$3.07{\cdot}10^{11}$	$1.87{\cdot}10^{12}$	29.7	10.5	39.0
5	$3.38{\cdot}10^{11}$	$1.16{\cdot}10^{11}$	$4.59{\cdot}10^{11}$	8.75	4.98	14.2
6	$4.89{\cdot}10^{9}$	$4.12{\cdot}10^{9}$	$1.25{\cdot}10^{10}$	1.74	0.98	2.79
7	$3.43{\cdot}10^{10}$	$1.87{\cdot}10^{10}$	$5.59{\cdot}10^{10}$	3.68	1.42	5.30
8	$3.36{\cdot}10^{8}$	$9.98{\cdot}10^{7}$	$4.45{\cdot}10^{8}$	1.37	0.561	1.96
9	$2.35{\cdot}10^{10}$	$6.13{\cdot}10^{9}$	$3.00{\cdot}10^{10}$	5.77	2.06	7.87
10	0.08	155	332	$1.87{\cdot}10^{-7}$	$1.67{\cdot}10^{-7}$	$3.71{\cdot}10^{-7}$
11	$8.19{\cdot}10^{11}$	$4.45{\cdot}10^{11}$	$1.14{\cdot}10^{12}$	22.4	8.76	28.6
12	$6.46{\cdot}10^{11}$	$3.56{\cdot}10^{11}$	$8.99{\cdot}10^{11}$	12.6	7.56	17.9
13	$3.14{\cdot}10^{10}$	$1.73{\cdot}10^{10}$	$4.37{\cdot}10^{10}$	7.15	3.15	9.41
14	$1.50{\cdot}10^{11}$	$8.27{\cdot}10^{10}$	$2.09{\cdot}10^{11}$	8.11	4.99	11.6
15	$1.03{\cdot}10^{11}$	$5.68{\cdot}10^{10}$	$1.43{\cdot}10^{11}$	5.72	3.84	8.43
16	$1.03{\cdot}10^{11}$	$2.69{\cdot}10^{9}$	$6.80{\cdot}10^{9}$	0.456	0.345	0.700
17	34.3	19.6	48.1	$6.80{\cdot}10^{-9}$	$4.06{\cdot}10^{-9}$	$9.66{\cdot}10^{-9}$
18	$5.48{\cdot}10^{11}$	$3.02{\cdot}10^{11}$	$7.61{\cdot}10^{11}$	10.6	4.85	14.1
19	$7.06{\cdot}10^{10}$	$3.89{\cdot}10^{10}$	$9.81{\cdot}10^{10}$	3.07	2.10	4.56
20	0	0	0	0	0	0
21	$1.19{\cdot}10^{10}$	0	$1.29{\cdot}10^{10}$	1.37	0	1.37
22	0	0	0	0	0	0
23	$6.10{\cdot}10^{-5}$	0	$6.10{\cdot}10^{-5}$	0	0	0
24	0	0	0	0	0	0
25	$2.44{\cdot}10^{-4}$	0	$2.44{\cdot}10^{-4}$	$1.42{\cdot}10^{-14}$	0	$1.42{\cdot}10^{-14}$
26	0	0	0	0	0	0
27	$3.91{\cdot}10^{-3}$	0	$1.71{\cdot}10^{-13}$	$8.53{\cdot}10^{-14}$	0	$8.53{\cdot}10^{-14}$
28	$5.37{\cdot}10^{-3}$	0	$5.37{\cdot}10^{-3}$	$1.14{\cdot}10^{-13}$	0	$1.42{\cdot}10^{-13}$
29	$9.77{\cdot}10^{-4}$	0	$9.77{\cdot}10^{-4}$	0	0	0
30	6.81	0	6.81	$1.08{\cdot}10^{-10}$	0	$1.08{\cdot}10^{-10}$
31	9.76	0	9.76	$5.72{\cdot}10^{-11}$	0	$5.72{\cdot}10^{-11}$
32	0.216	0	0.216	$4.35{\cdot}10^{-12}$	0	$4.35{\cdot}10^{-12}$
33	0.0645	0	0.0645	$9.95{\cdot}10^{-13}$	0	$9.95{\cdot}10^{-13}$
34	0.303	0	0.303	$3.50{\cdot}10^{-12}$	0	$3.50{\cdot}10^{-12}$
35	$8.60{\cdot}10^{-3}$	0	$8.60{\cdot}10^{-3}$	$1.34{\cdot}10^{-12}$	0	$1.34{\cdot}10^{-12}$
36	$1.30{\cdot}10^{9}$	0	$1.30{\cdot}10^{9}$	3.53	0	3.53
37	0.0479	0	0.0479	$2.67{\cdot}10^{-12}$	0	$2.67{\cdot}10^{-12}$
38	0.568	0	0.568	$3.11{\cdot}10^{-11}$	0	$3.11{\cdot}10^{-11}$

B.3 Comparison over the whole treatment duration with variable drug effects

Table B.2: Comparison between the mean difference in tumor diameter with the actual drug effects, the flexible drug effects with a margin of 20 % (constrained) and with fake drug effects (unconstrained). Underlined patients have CRC, and red numbers are bigger than the average of that column.

	Mean difference in diameter (mm)		
Patient	**Real drug effects**	**Constrained**	**Unconstrained**
1	19.5	5.12	5.12
2	2.43	0.441	0.440
3	5.58	1.45	1.45
4	29.7	9.29	2.28
5	8.75	0.0176	0.0161
6	1.73	1.69	1.69
7	3.67	0.0830	0.0830
8	1.397	0.322	$8.00 \cdot 10^{-8}$
9	5.77	1.15	0.249
10	$1.98 \cdot 10^{-7}$	$1.98 \cdot 10^{-7}$	$1.98 \cdot 10^{-7}$
11	22.4	13.0	13.0
12	12.6	3.45	2.13
13	7.18	3.91	3.89
14	8.11	3.39	2.40
15	5.72	2.24	0.97
16	0.46	$2.02 \cdot 10^{-6}$	$7.13 \cdot 10^{-7}$
17	$6.80 \cdot 10^{-9}$	$6.80 \cdot 10^{-9}$	$6.80 \cdot 10^{-9}$
18	10.6	$6.14 \cdot 10^{-7}$	$1.42 \cdot 10^{-7}$
19	3.07	$1.25 \cdot 10^{-6}$	$1.25 \cdot 10^{-6}$
20	0	0	0
21	1.37	$6.88 \cdot 10^{-7}$	$5.12 \cdot 10^{-7}$
22	0	0	0
23	0	0	0
24	0	0	0
25	$1.42 \cdot 10^{-14}$	$1.42 \cdot 10^{-14}$	$1.42 \cdot 10^{-14}$
26	0	0	0
27	$8.53 \cdot 10^{-14}$	$8.53 \cdot 10^{-14}$	$5.18 \cdot 10^{-14}$
28	$1.14 \cdot 10^{-13}$	$1.14 \cdot 10^{-13}$	$1.14 \cdot 10^{-13}$
29	0	0	0
30	$1.08 \cdot 10^{-10}$	$2.84 \cdot 10^{-14}$	$2.84 \cdot 10^{-14}$
31	$5.72 \cdot 10^{-11}$	0	0
32	$4.35 \cdot 10^{-12}$	0	0
33	$9.95 \cdot 10^{-13}$	0	0
34	$3.50 \cdot 10^{-12}$	0	0
35	$1.34 \cdot 10^{-12}$	0	0
36	3.53	$1.31 \cdot 10^{-7}$	$2.79 \cdot 10^{-9}$
37	$2.67 \cdot 10^{-12}$	$1.42 \cdot 10^{-14}$	$1.42 \cdot 10^{-14}$
38	$3.11 \cdot 10^{-11}$	$1.42 \cdot 10^{-14}$	$1.42 \cdot 10^{-14}$

B.4 Comparison between the predicted tumor diameter with the original drug effects and variable drug effects

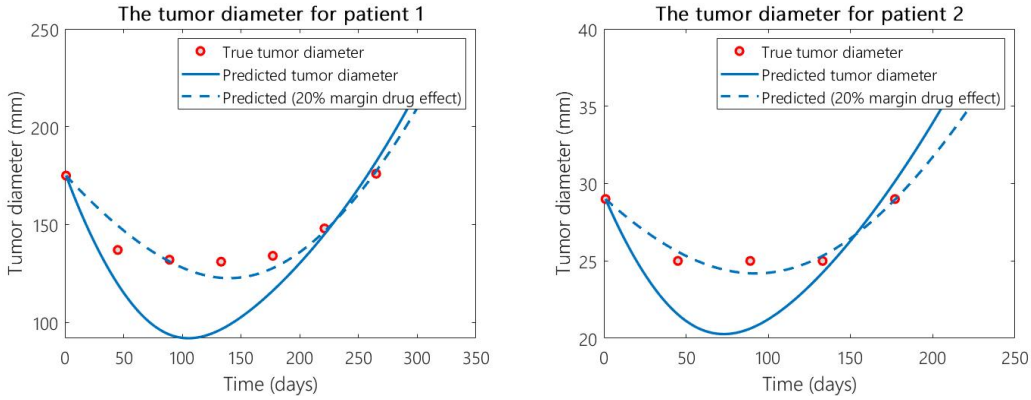

Figure B.2: The true tumor diameter and the predicted tumor diameter, with the original drug effects and with varying drug effects (20% margin), for patient 1 (left), and for patient 2 (right).

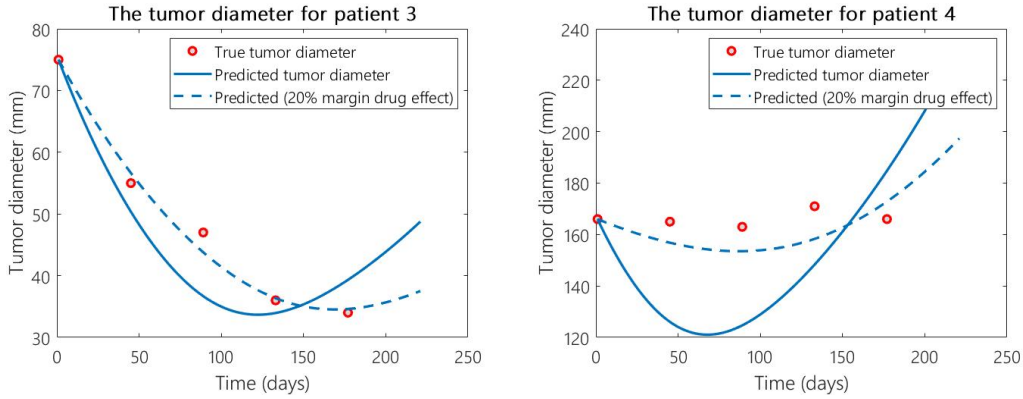

Figure B.3: The true tumor diameter and the predicted tumor diameter, with the original drug effects and with varying drug effects (20% margin), for patient 3 (left), and for patient 4 (right).

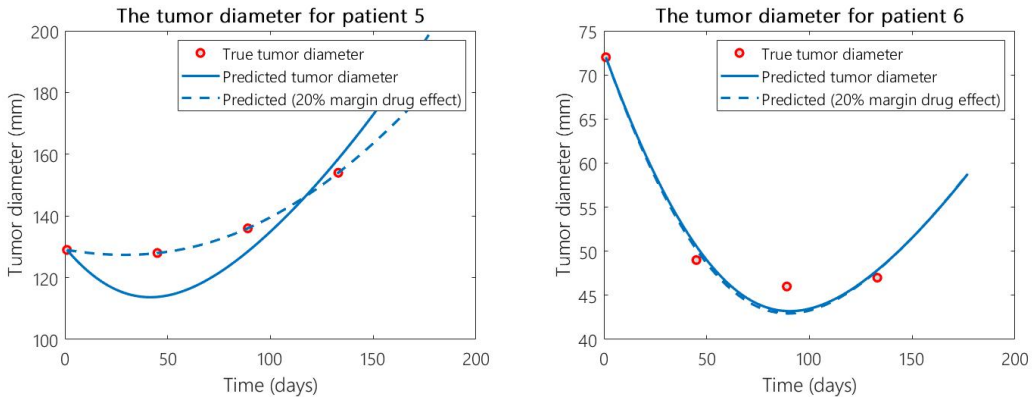

Figure B.4: The true tumor diameter and the predicted tumor diameter, with the original drug effects and with varying drug effects (20% margin), for patient 5 (left), and for patient 6 (right).

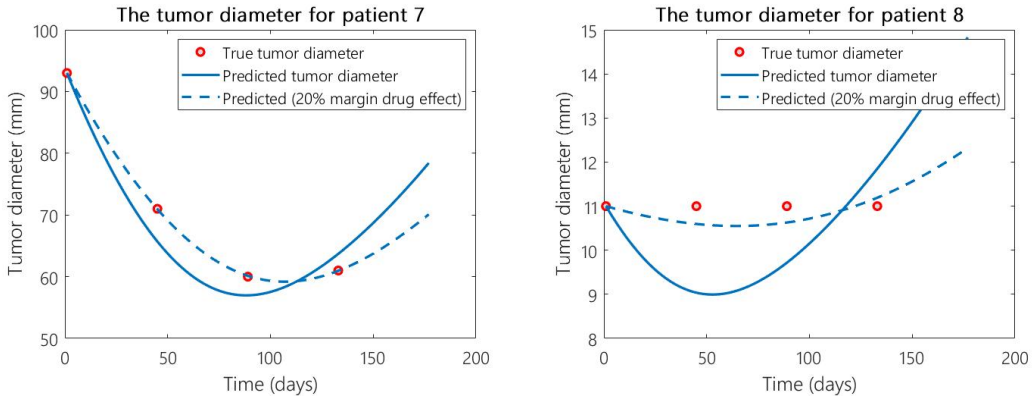

Figure B.5: The true tumor diameter and the predicted tumor diameter, with the original drug effects and with varying drug effects (20% margin), for patient 7 (left), and for patient 8 (right).

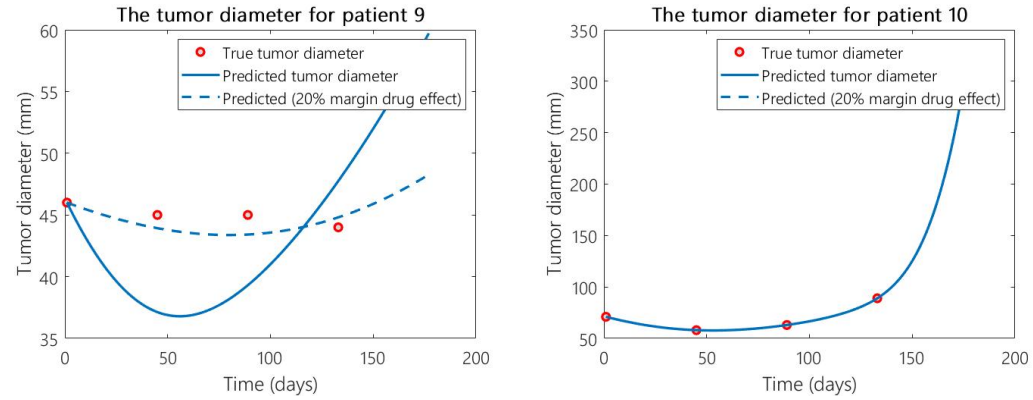

Figure B.6: The true tumor diameter and the predicted tumor diameter, with the original drug effects and with varying drug effects (20% margin), for patient 9 (left), and for patient 10 (right).

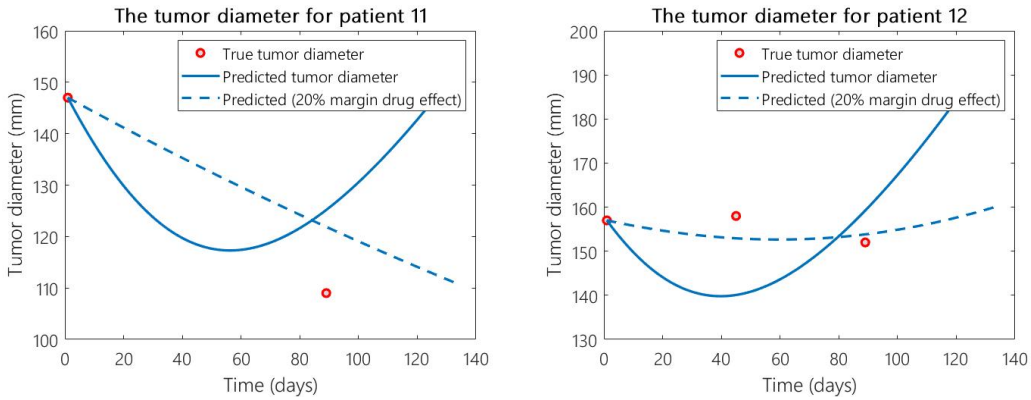

Figure B.7: The true tumor diameter and the predicted tumor diameter, with the original drug effects and with varying drug effects (20% margin), for patient 11 (left), and for patient 12 (right).

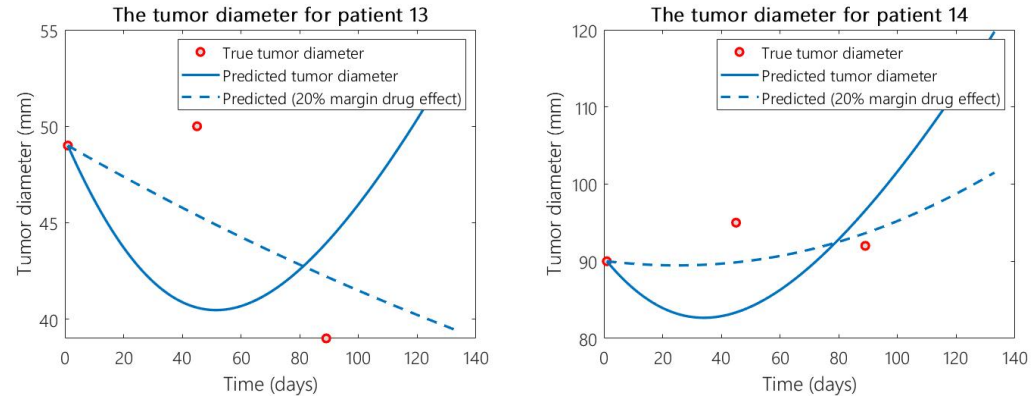

Figure B.8: The true tumor diameter and the predicted tumor diameter, with the original drug effects and with varying drug effects (20% margin), for patient 13 (left), and for patient 14 (right).

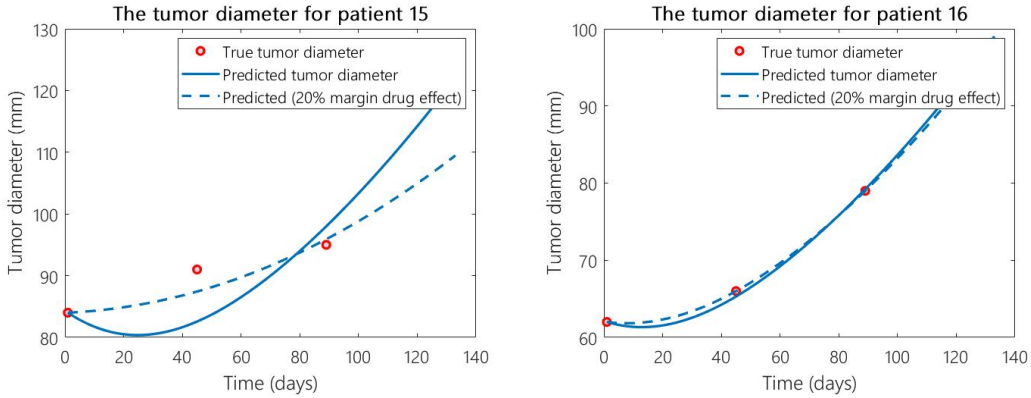

Figure B.9: The true tumor diameter and the predicted tumor diameter, with the original drug effects and with varying drug effects (20% margin), for patient 15 (left), and for patient 16 (right).

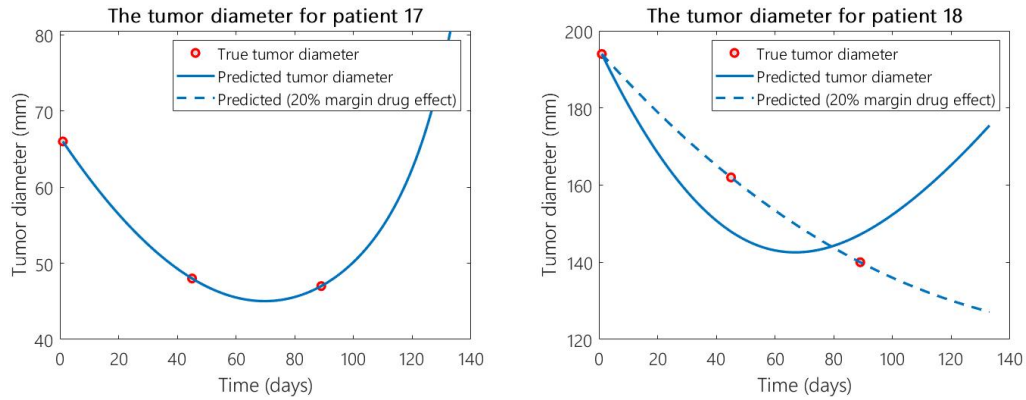

Figure B.10: The true tumor diameter and the predicted tumor diameter, with the original drug effects and with varying drug effects (20% margin), for patient 17 (left), and for patient 18 (right).

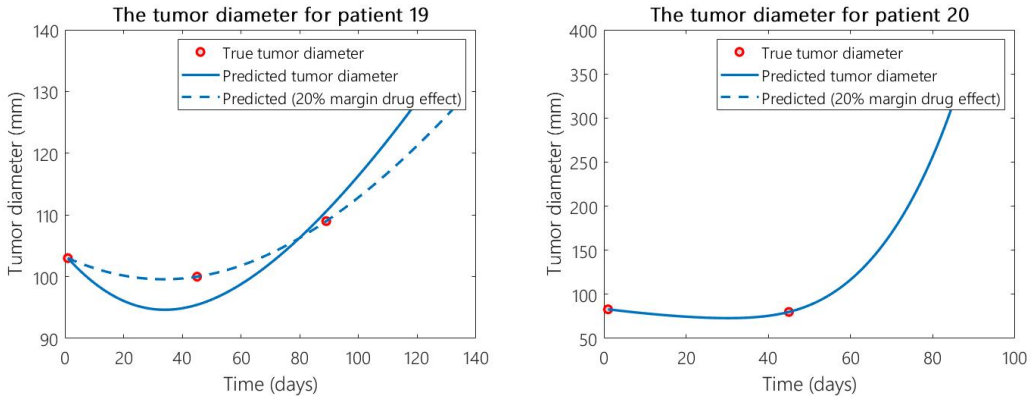

Figure B.11: The true tumor diameter and the predicted tumor diameter, with the original drug effects and with varying drug effects (20% margin), for patient 19 (left), and for patient 20 (right).

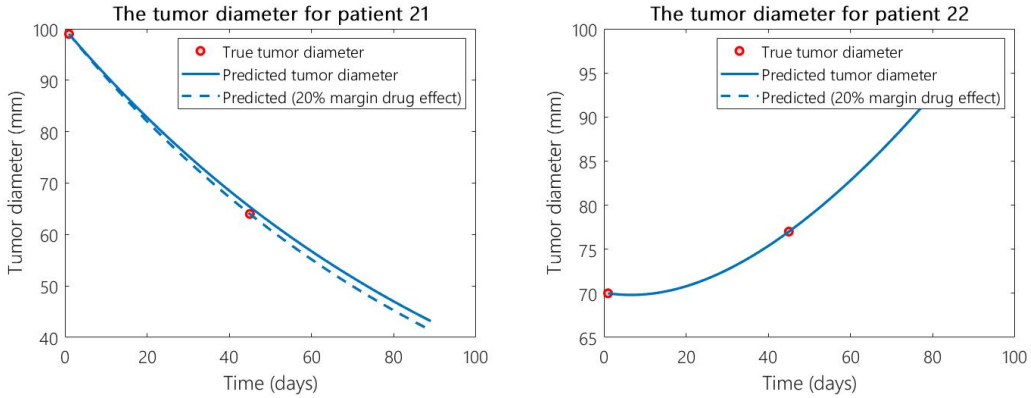

Figure B.12: The true tumor diameter and the predicted tumor diameter, with the original drug effects and with varying drug effects (20% margin), for patient 21 (left), and for patient 22 (right).

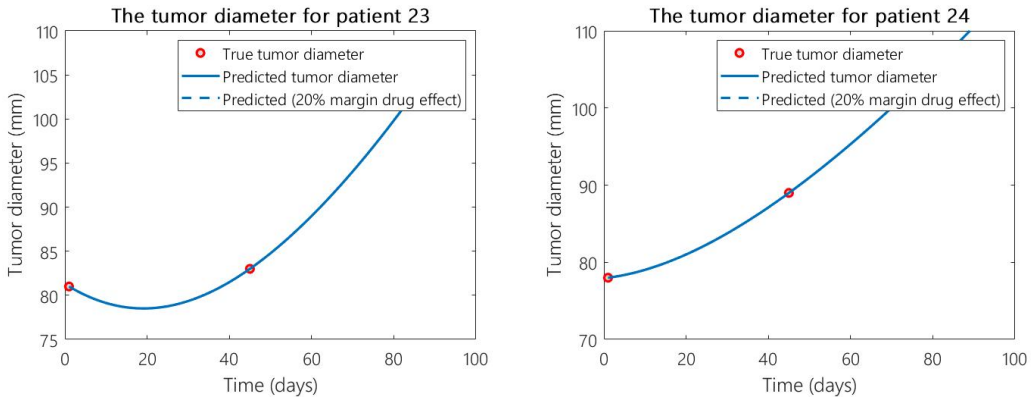

Figure B.13: The true tumor diameter and the predicted tumor diameter, with the original drug effects and with varying drug effects (20% margin), for patient 23 (left), and for patient 24 (right).

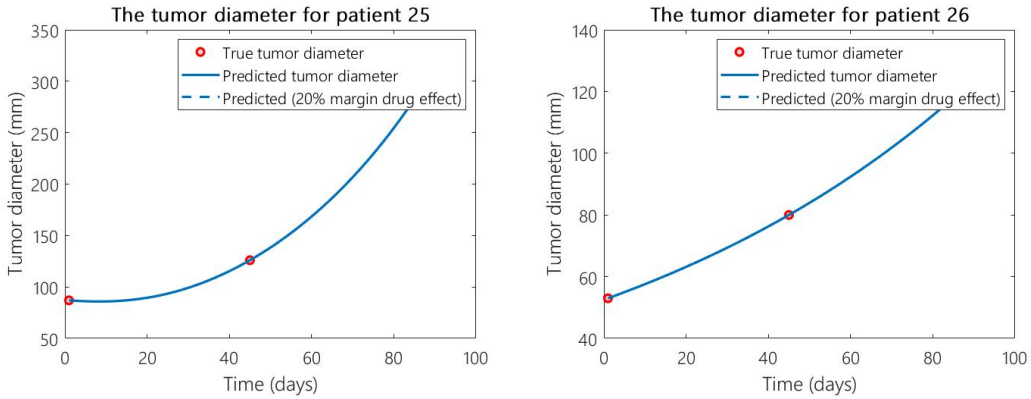

Figure B.14: The true tumor diameter and the predicted tumor diameter, with the original drug effects and with varying drug effects (20% margin), for patient 25 (left), and for patient 26 (right).

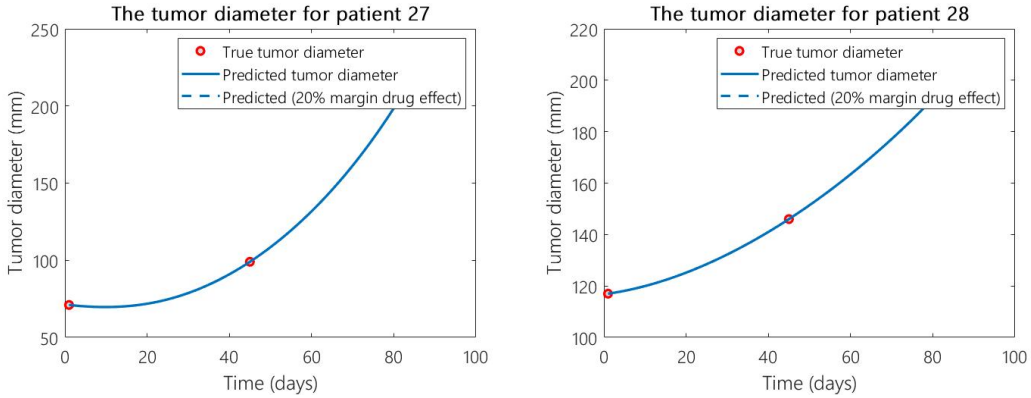

Figure B.15: The true tumor diameter and the predicted tumor diameter, with the original drug effects and with varying drug effects (20% margin), for patient 27 (left), and for patient 28 (right).

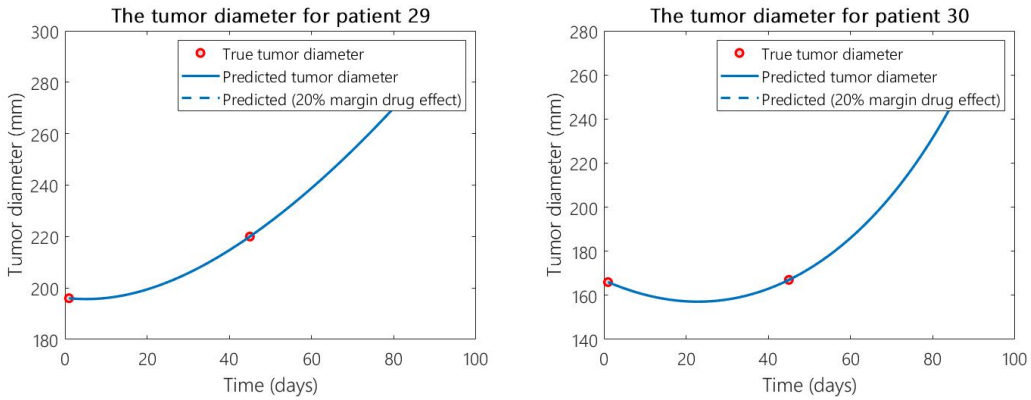

Figure B.16: The true tumor diameter and the predicted tumor diameter, with the original drug effects and with varying drug effects (20% margin), for patient 29 (left), and for patient 30 (right).

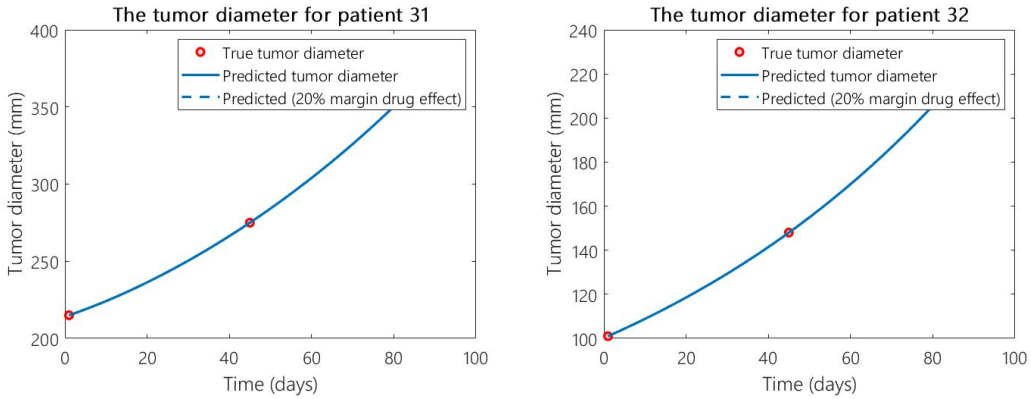

Figure B.17: The true tumor diameter and the predicted tumor diameter, with the original drug effects and with varying drug effects (20% margin), for patient 31 (left), and for patient 32 (right).

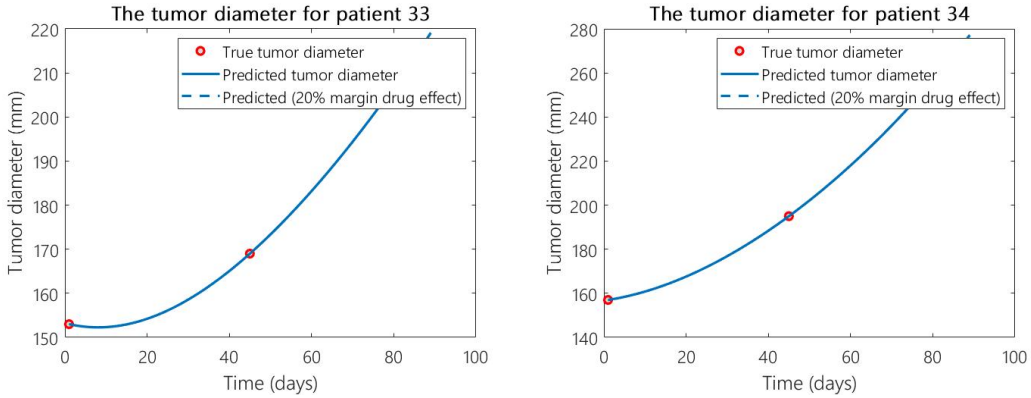

Figure B.18: The true tumor diameter and the predicted tumor diameter, with the original drug effects and with varying drug effects (20% margin), for patient 33 (left), and for patient 34 (right).

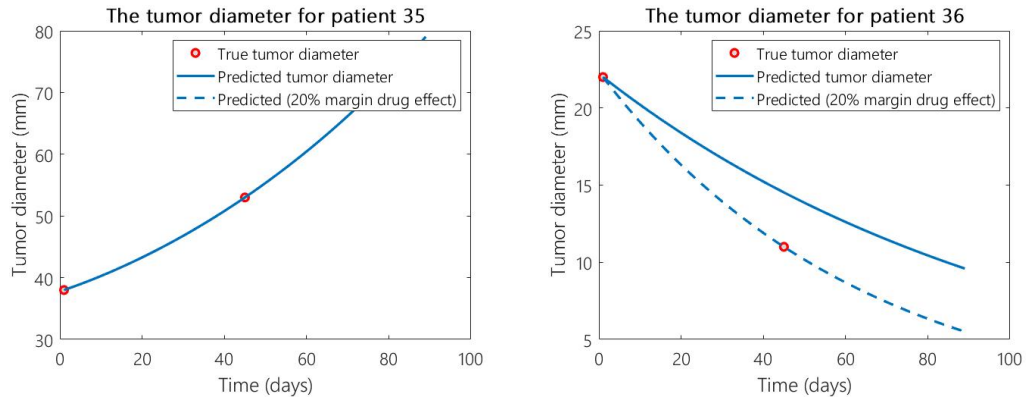

Figure B.19: The true tumor diameter and the predicted tumor diameter, with the original drug effects and with varying drug effects (20% margin), for patient 35 (left), and for patient 36 (right).

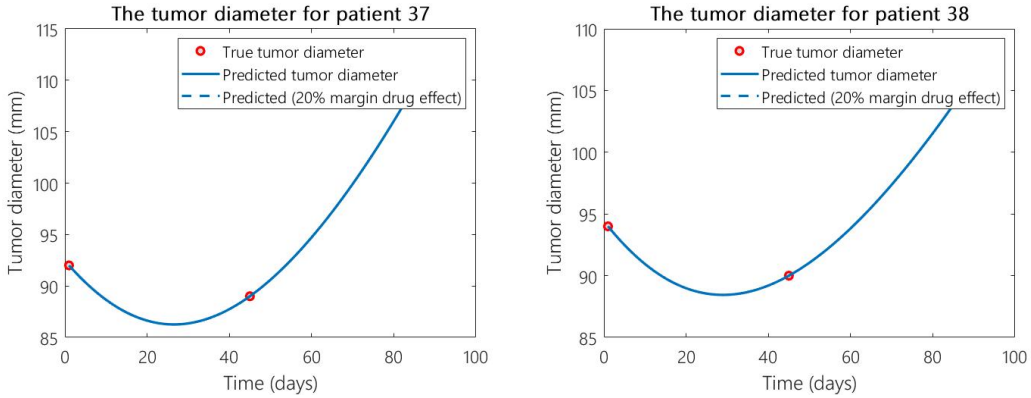

Figure B.20: The true tumor diameter and the predicted tumor diameter, with the original drug effects and with varying drug effects (20% margin), for patient 37 (left), and for patient 38 (right).

B.5 Model optimization on clinical data

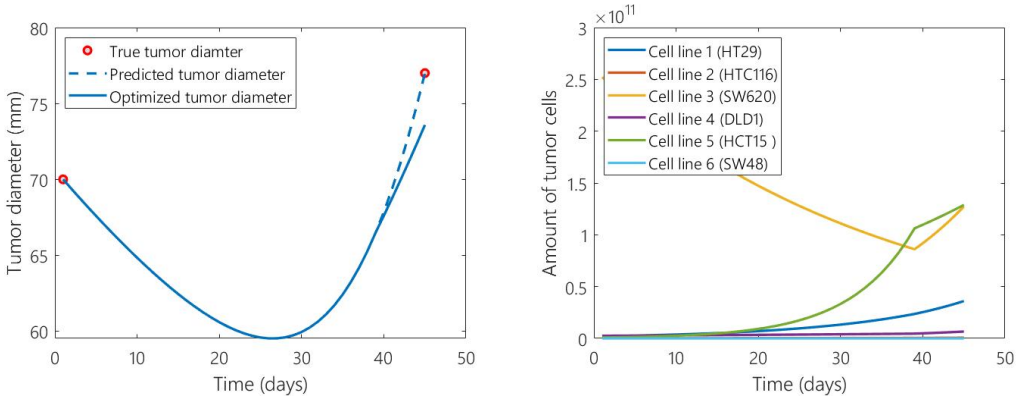

Figure B.21: The true, predicted and optimized tumor diameter (left), and the optimized states (right) for patient 22. Optimization is performed as in Equation (3.17) up to Equation (3.19) and parameters are taken as in Section 4.3.

Bibliography

[1] Bray, F., Ferlay, J., Soerjomataram, I., Siegel, R. L., Torre, L. A., & Jemal, A. (2018). Global cancer statistics 2018: GLOBOCAN estimates of incidence and mortality worldwide for 36 cancers in 185 countries. *CA: a cancer journal for clinicians, 68*(6), 394-424.

[2] Bray, F., Ferlay, J., Soerjomataram, I., Siegel, R. L., Torre, L. A., & Jemal, A. (2018). Global cancer statistics 2018: GLOBOCAN estimates of incidence and mortality worldwide for 36 cancers in 185 countries. *CA: a cancer journal for clinicians, 68*(6), 394-424.

[3] Baskar, R., Lee, K. A., Yeo, R., & Yeoh, K.-W. (2012). Cancer and radiation therapy: current advances and future directions. *International journal of medical sciences, 9*(3), 193.

[4] Enderling, H., Anderson, A. R., Chaplain, M. A., Munro, A. J., & Vaidya, J. S. (2006). Mathematical modelling of radiotherapy strategies for early breast cancer.*Journal of Theoretical Biology, 241*(1), 158-171.

[5] Grassberger, C., & Paganetti, H. (2016). Methodologies in the modeling of combined chemoradiation treatments. *Physics in Medicine & Biology, 61*(21), R344.

[6] Rockne, R., Alvord, E., Rockhill, J., & Swanson, K. (2009). A mathematical model for brain tumor response to radiation therapy. *Journal of mathematical biology, 58*(4-5), 561.

[7] McAneney, H., & O'Rourke, S. (2007). Investigation of various growth mechanisms of solid tumour growth within the linear-quadratic model for radiotherapy. *Physics in Medicine & Biology, 52*(4), 1039.

[8] Shi, J., Alagoz, O., Erenay, F. S., & Su, Q. (2014). A survey of optimization models on cancer chemotherapy treatment planning. *Annals of Operations Research, 221*(1), 331-356.

[9] Salari, E., Unkelbach, J., & Bortfeld, T. (2015). A mathematical programming approach to the fractionation problem in chemoradiotherapy. *IIE Transactions on Healthcare Systems Engineering 5*(2), 55-73.

[10] Durante, M., Tommasino, F., & Yamada, S. (2015). Modeling combined chemotherapy and particle therapy for locally advanced pancreatic cancer. *Frontiers in oncology, 5*, 145.

[11] Colombino, M., Dhingra, N. K., Jovanovic, M. R., & Smith, R. S. (2016). *Convex reformulation of a robust optimal control problem for a class of positive systems.* Paper presented at the Decision and Control (CDC), 2016 IEEE 55th Conference on Decision and Control.

[12] Hernandez-Vargas, E. A., Colaneri, P., & Middleton, R. H. (2012). *Sub-optimal switching with dwell time constraints for control of viral mutation.* Paper presented at the Decision and Control (CDC), 2012 IEEE 51st Annual Conference on Decision and Control.

[13] Hernandez-Vargas, E. A., Colaneri, P., & Middleton, R. H. (2014). Switching strategies to mitigate HIV mutation. *IEEE Transactions on Control Systems Technology, 22*(4), 1623-1628.

[14] Hernandez-Vargas, E. A., Colaneri, P., & Middleton, R. H. (2013). Optimal therapy scheduling for a simplified HIV infection model. *Automatica, 49*(9), 2874-2880.

[15] Hernandez-Vargas, E., Colaneri, P., Middleton, R., & Blanchini, F. (2011). Discrete-time control for switched positive systems with application to mitigating viral escape. *International journal of robust nonlinear control, 21*(10), 1093-1111.

[16] Giordano, G., Rantzer, A., & Jonsson, V. D. (2016). *A convex optimization approach to cancer treatment to address tumor heterogeneity and imperfect drug penetration in physiological compartments.* In Proceedings of the IEEE Conference on Decision and Control.

[17] Devia, C. A., Giordano, G., *Optimal duration and planning of switching treatments taking drug toxicity into account: a convex optimisation approach*, submitted, 2019.

[18] Blanchini, F., Colaneri, P., & Middleton, R. H. (2014). A convexity result for the optimal control of a class of positive nonlinear systems. *IFAC Proceedings Volumes, 47*(3), 1507-1512.

[19] Colaneri, P., Middleton, R. H., Chen, Z., Caporale, D., & Blanchini, F. (2014). Convexity of the cost functional in an optimal control problem for a class of positive switched systems. *Automatica 50*(4), 1227-1234.

[20] Bianconi, E., Piovesan, A., Facchin, F., Beraudi, A., Casadei, R., Frabetti, F., ... & Perez-Amodio, S. (2013). An estimation of the number of cells in the human body. *Annals of human biology, 40*(6), 463-471.

[21] Bortfeld, T., Ramakrishnan, J., Tsitsiklis, J. N., & Unkelbach, J. (2015). Optimization of radiation therapy fractionation schedules in the presence of tumor repopulation. *INFORMS Journal on Computing, 27*(4), 788-803.

[22] Rantzer, A., & Bernhardsson, B. (2014). *Control of convex-monotone systems.* Paper presented at the Decision and Control (CDC), 2014 IEEE 53rd Annual Conference on Decision and Control.

[23] How cancer starts, grows and spreads - Canadian Cancer Society. (n.d.). Retrieved from https://www.cancer.ca/en/cancer-information/cancer-101/what-is-cancer/how-cancer-starts-grows-and-spreads/?region=on.

[24] Jamal-Hanjani, M., Quezada, S. A., Larkin, J., & Swanton, C. (2015). Translational implications of tumor heterogeneity. *Clinical cancer research, 21*(6), 1258-1266.

[25] Curvo-Semedo, L. (2020). Rectal Cancer: Staging. *Magnetic Resonance Imaging Clinics, 28*(1), 105-115.

[26] Piñeros, M., Parkin, D. M., Ward, K., Chokunonga, E., Ervik, M., Farrugia, H., ... & Znaor, A. (2019). Essential TNM: a registry tool to reduce gaps in cancer staging information. *The Lancet Oncology, 20*(2), e103-e111.

[27] Dickens, E., & Ahmed, S. (2018). Principles of cancer treatment by chemotherapy. *Surgery 36*(3), 134-138.

[28] Symonds, R. P., & Foweraker, K. (2006). Principles of chemotherapy and radiotherapy. C*urrent Obstetrics & Gynaecology, 16*(2), 100-106.

[29] Powathil, G., Kohandel, M., Sivaloganathan, S., Oza, A., & Milosevic, M. (2007). Mathematical modeling of brain tumors: effects of radiotherapy and chemotherapy. *Physics in Medicine & Biology, 52*(11), 3291.

[30] Geng, C., Paganetti, H., & Grassberger, C. (2017). Prediction of Treatment Response for Combined Chemo- and Radiation Therapy for Non-Small Cell Lung Cancer Patients Using a Bio-Mathematical Model. *Scientific Reports, 7*(1), 13542.

[31] Simon, R., & Norton, L. (2006). The Norton-Simon hypothesis: designing more effective and less toxic chemotherapeutic regimens. *Nature Clinical Practice Oncology, 3*(8), 406-407.

[32] Smith, S., & Prewett, S. (2017). Principles of chemotherapy and radiotherapy. *Obstetrics, Gynaecology and Reproductive Medicine, 27*(7), 206-212.

[33] Mackie, T. R., Holmes, T. W., Reckwerdt, P. J., & Yang, J. (1995). Tomotherapy: optimized planning and delivery of radiation therapy. *International Journal of Imaging Systems and Technology 6*(1), 43-55.

[34] Shepard, D. M., Ferris, M. C., Olivera, G. H., & Mackie, T. R. (1999). Optimizing the delivery of radiation therapy to cancer patients. *Siam Review, 41*(4), 721-744.

[35] Matuszak, M. M., Kashani, R., Green, M., Owen, D., Jolly, S., & Mierzwa, M. (2019). Functional Adaptation in Radiation Therapy. *Seminars in Radiation Oncology, 29*(3), 236-244.

[36] Rancati, T., & Fiorino, C. (2019). *Modelling radiotherapy side effects: practical applications for planning optimisation.* CRC Press.

[37] Moiseenko, V., Song, W. Y., Mell, L. K., & Bhandare, N. (2011). A comparison of dose-response characteristics of four NTCP models using outcomes of radiation-induced optic neuropathy and retinopathy. *Radiation Oncology, 6*(1), 61.

[38] Bakhshandeh, M., Hashemi, B., Mahdavi, S. R. M., Nikoofar, A., Vasheghani, M., & Kazemnejad, A. (2013). Normal tissue complication probability modeling of radiation-induced hypothyroidism after head-and-neck radiation therapy. *International Journal of Radiation Oncology, Biology, Physics, 85*(2), 514-521.

[39] Zorzan, I. (2014). An introduction to positive switched systems and their application to HIV treatment modeling.

[40] Hernandez Vargas, E. A. (2011).*A control theoretic approach to mitigate viral escape in HIV.*(Doctoral dissertation, National University of Ireland Maynooth).

[41] Favoriti, P., Carbone, G., Greco, M., Pirozzi, F., Pirozzi, R. E. M., & Corcione, F. (2016). Worldwide burden of colorectal cancer: a review. *Updates in surgery, 68*(1), 7-11.

[42] Siegel, R. L., Miller, K. D., & Jemal, A. (2019). Cancer statistics, 2019. *CA: a cancer journal for clinicians, 69*(1), 7-34.

[43] Qureshi, A., Verma, A., Ross, P., & Landau, D. (2010). Colorectal cancer treatment. *BMJ clinical evidence*, 2010.

[44] Drugs Approved for Colon and Rectal Cancer. (2019, May 20). Retrieved from https://www.cancer.gov/about-cancer/treatment/drugs/colorectal

[45] Molinari, C., Marisi, G., Passardi, A., Matteucci, L., De Maio, G., & Ulivi, P. (2018). Heterogeneity in Colorectal Cancer: A Challenge for Personalized Medicine?. *International journal of molecular sciences, 19*(12), 3733.

[46] Sagaert, X., Vanstapel, A., & Verbeek, S. (2018). Tumor Heterogeneity in Colorectal Cancer: What Do We Know So Far?. *Pathobiology, 85*(1-2), 72-84.

[47] Authenticated Colorectal Cancer Cell Lines for Cancer Research. (n.d.). Retrieved from https://www.sigmaaldrich.com/technical-documents/articles/biology/colorectal-cancer-cell-lines.html.

[48] Berg, K. C., Eide, P. W., Eilertsen, I. A., Johannessen, B., Bruun, J., Danielsen, S. A., ... & Myklebost, O. (2017). Multi-omics of 34 colorectal cancer cell lines-a resource for biomedical studies. *Molecular cancer, 16*(1), 116.

[49] Hao, S. J., Wan, Y., Xia, Y. Q., Zou, X., & Zheng, S. Y. (2018). Size-based separation methods of circulating tumor cells. *Advanced drug delivery reviews, 125*, 3-20.

[50] Eisenhauer, E. A., Therasse, P., Bogaerts, J., Schwartz, L. H., Sargent, D., Ford, R., ... & Rubinstein, L. (2009). New response evaluation criteria in solid tumours: revised RECIST guideline (version 1.1). *European journal of cancer, 45*(2), 228-247.

[51] National Cancer Institute. *Radiation/Chemotherapy Databases.* Retreived from https://seer.cancer.gov/data/treatment.html

[52] Carson, R., Celtikci, B., Fenning, C., Javadi, A., Crawford, N., Perez-Carbonell, L., ... & Van Schaeybroeck, S. (2015). HDAC inhibition overcomes acute resistance to MEK inhibition in BRAF-mutant colorectal cancer by downregulation of c-FLIPL. *Clinical cancer research, 21*(14), 3230-3240.

[53] Prewett, M., Deevi, D. S., Bassi, R., Fan, F., Ellis, L. M., Hicklin, D. J., & Tonra, J. R. (2007). Tumors established with cell lines selected for oxaliplatin resistance respond to oxaliplatin if combined with cetuximab. *Clinical Cancer Research, 13*(24), 7432-7440.

[54] Bocci, G., Falcone, A., Fioravanti, A., Orlandi, P., Di Paolo, A., Fanelli, G., ... & Del Tacca, M. (2008). Antiangiogenic and anticolorectal cancer effects of metronomic irinotecan chemotherapy alone and in combination with semaxinib. *British journal of cancer, 98*(10), 1619.

[55] Na, Y. S., Kim, S. M., Jung, K. A., Yang, S. J., Hong, Y. S., Ryu, M. H., ... & Lee, J. S. (2010). Effects of the HDAC inhibitor CG2 in combination with irinotecan, 5-fluorouracil, or oxaliplatin on HCT116 colon cancer cells and xenografts. *Oncology reports, 24*(6), 1509-1514.

[56] Ozawa, Y., Kusano, K., Owa, T., Yokoi, A., Asada, M., & Yoshimatsu, K. (2012). Therapeutic potential and molecular mechanism of a novel sulfonamide anticancer drug, indisulam (E7070) in combination with CPT-11 for cancer treatment. *Cancer chemotherapy and pharmacology, 69*(5), 1353-1362.

[57] Lee, J., Lee, I., Han, B., Park, J. O., Jang, J., Park, C., & Kang, W. K. (2011). Effect of simvastatin on cetuximab resistance in human colorectal cancer with KRAS mutations. *JNCI: Journal of the National Cancer Institute, 103*(8), 674-688.

[58] Napolitano, S., Martini, G., Rinaldi, B., Martinelli, E., Donniacuo, M., Berrino, L., ... & Merolla, F. (2015). Primary and acquired resistance of colorectal cancer to anti-EGFR monoclonal antibody can be overcome by combined treatment of regorafenib with cetuximab. *Clinical Cancer Research, 21*(13), 2975-2983.

[59] Ishiguro, M., Iida, S., Uetake, H., Morita, S., Makino, H., Kato, K., ... & Sugihara, K. (2007). Effect of combined therapy with low-dose 5-aza-2-deoxycytidine and irinotecan on colon cancer cell line HCT-15. *Annals of surgical oncology, 14*(5), 1752-1762.

[60] Seierstad, T., Folkvord, S., Røe, K., Flatmark, K., Skretting, A., & Olsen, D. R. (2007). Early changes in apparent diffusion coefficient predict the quantitative antitumoral activity of capecitabine, oxaliplatin, and irradiation in HT29 xenografts in athymic nude mice. *Neoplasia (New York, NY), 9*(5), 392.

[61] Neijzen, R., Wong, M. Q., Gill, N., Wang, H., Karim, T., Anantha, M., ... & Ng, S. S. (2015). Irinophore C™, a lipid nanoparticulate formulation of irinotecan, improves vascular function, increases the delivery of sequentially administered 5-FU in HT-29 tumors, and controls tumor growth in patient derived xenografts of colon cancer. *Journal of controlled release, 199*, 72-83.

[62] Wei, L., Wang, Z., Xia, Y., & Liu, B. (2019). The mechanism and tumor inhibitory study of Lagopsis supine ethanol extract on colorectal cancer in nude mice. *BMC complementary and alternative medicine, 19*(1), 173.

[63] Liu, T., Wang, X., Hu, W., Fang, Z., Jin, Y., Fang, X., & Miao, Q. R. (2019). Epigenetically Down-Regulated Acetyltransferase PCAF Increases the Resistance of Colorectal Cancer to 5-Fluorouracil. *Neoplasia, 21*(6), 557-570.

[64] Di Gennaro, E., Piro, G., Chianese, M. I., Franco, R., Di Cintio, A., Moccia, T., ... & Arra, C. (2010). Vorinostat synergises with capecitabine through upregulation of thymidine phosphorylase. *British journal of cancer, 103*(11), 1680.

[65] de la Cueva, A., de Molina, A. R., Álvarez-Ayerza, N., Ramos, M. A., Cebrián, A., del Pulgar, T. G., & Lacal, J. C. (2013). Combined 5-FU and ChoKα inhibitors as a new alternative therapy of colorectal cancer: evidence in human tumor-derived cell lines and mouse xenografts. *PloS one, 8*(6), e64961.

[66] Prewett, M. C., Hooper, A. T., Bassi, R., Ellis, L. M., Waksal, H. W., & Hicklin, D. J. (2002). Enhanced antitumor activity of anti-epidermal growth factor receptor monoclonal antibody IMC-C225 in combination with irinotecan (CPT-11) against human colorectal tumor xenografts. *Clinical Cancer Research, 8*(5), 994-1003.

[67] Mueller, L. P., Luetzkendorf, J., Widder, M., Nerger, K., Caysa, H., & Mueller, T. (2011). TRAIL-transduced multipotent mesenchymal stromal cells (TRAIL-MSC) overcome TRAIL resistance in selected CRC cell lines in vitro and in vivo. *Cancer gene therapy, 18*(4), 229.

[68] Rick, F. G., Seitz, S., Schally, A. V., Szalontay, L., Krishan, A., Datz, C., ... & Hohla, F. (2012). GHRH antagonist when combined with cytotoxic agents induces S-phase arrest and additive growth inhibition of human colon cancer. *Cell Cycle, 11*(22), 4203-4210.

[69] Li, X. X., Zheng, H. T., Peng, J. J., Huang, L. Y., Shi, D. B., Liang, L., & Cai, S. J. (2014). RNA-seq reveals determinants for irinotecan sensitivity/resistance in colorectal cancer cell lines. *International journal of clinical and experimental pathology, 7*(5), 2729.

[70] Tomasetti, C., & Levy, D. (2010). Role of symmetric and asymmetric division of stem cells in developing drug resistance. *Proceedings of the National Academy of Sciences, 107*(39), 16766-16771

[71] Ahmed, D., Eide, P. W., Eilertsen, I. A., Danielsen, S. A., Eknaes, M., Hektoen, M., ... & Lothe, R. A. (2013). Epigenetic and genetic features of 24 colon cancer cell lines. *Oncogenesis, 2*(9), e71.

[72] Gholami, Y. H., Willowson, K. P., Forwood, N. J., Harvie, R., Hardcastle, N., Bromley, R., ... & Bailey, D. L. (2018). Comparison of radiobiological parameters for 90 Y radionuclide therapy (RNT) and external beam radiotherapy (EBRT) in vitro. *EJNMMI physics, 5*(1), 18.

[73] Weiswald, L. B., Bellet, D., & Dangles-Marie, V. (2015). Spherical cancer models in tumor biology. *Neoplasia, 17*(1), 1-15.

[74] Tirumani, S. H., Shinagare, A. B., O'Neill, A. C., Nishino, M., Rosenthal, M. H., & Ramaiya, N. H. (2016). Accuracy and feasibility of estimated tumour volumetry in primary gastric gastrointestinal stromal tumours: validation using semiautomated technique in 127 patients. *European radiology, 26*(1), 286-295.

[75] Rancati, T., Fiorino, C., Gagliardi, G., Cattaneo, G. M., Sanguineti, G., Borca, V. C., ... & Menegotti, L. (2004). Fitting late rectal bleeding data using different NTCP models: results from an Italian multi-centric study (AIROPROS0101). *Radiotherapy and oncology, 73*(1), 21-32.

[76] Mavroidis, P., Pearlstein, K. A., Dooley, J., Sun, J., Saripalli, S., Das, S. K., ... & Chen, R. C. (2018). Fitting NTCP models to bladder doses and acute urinary symptoms during post-prostatectomy radiotherapy. *Radiation Oncology, 13*(1), 17.

[77] Choi, J., Oh, S. N., Yeo, D. M., Kang, W. K., Jung, C. K., Kim, S. W., & Park, M. Y. (2015). Computed tomography and magnetic resonance imaging evaluation of lymph node metastasis in early colorectal cancer. *World journal of gastroenterology: WJG, 21*(2), 556.

[78] Ganeshalingam, S., & Koh, D. M. (2009). Nodal staging. *Cancer Imaging, 9*(1), 104.

[79] Mizuta, M., Takao, S., Date, H., Kishimoto, N., Sutherland, K. L., Onimaru, R., & Shirato, H. (2012). A mathematical study to select fractionation regimen based on physical dose distribution and the linear–quadratic model. *International Journal of Radiation Oncology, Biology, Physics, 84*(3), 829-833.

[80] Lawrence, T. S., Blackstock, A. W., & McGinn, C. (2003, January). The mechanism of action of radiosensitization of conventional chemotherapeutic agents. In *Seminars in radiation oncology* (Vol. 13, No. 1, pp. 13-21). WB Saunders.

Glossary

List of Acronyms

In the following list the acronyms are given that are used throughout this literature review.

3mE	Mechanical, Maritime and Materials Engineering
5-FU	5-Fluorouracil
ACUP	Adenocarcinoma of unknown primary
AE	Adverse events
AMS	American Mathematical Society
BED	Biologically effective dose
BSA	Body surface area
CPT-11	Irinotecan
CRC	Colorectal cancer
CT	Chemotherapy
CT scan	Computed tomography scan
DCSC	Delft Center for Systems and Control
DSB	Double-strand breaks
EBRT	External beam radiation therapy
EQDX	X Gray equivalent dose
Gy	Gray
HDR	High dose rate
IC50	The half maximal inhibitory concentration

J	Joule
Kg	Kilogram
LDR	Low dose rate
LINAC	Linear accelerator
LQ	Linear-quadratic
MTD	Maximum Tolerated Dose
NTCP	Normal tissue complication probability
OAR	Organ at risk
PD	Progressive disease
RT	Radiotherapy
SSB	Single-strand break
TU	Delft University of Technology
UV	Ultraviolet
WHO	World Health Organization

List of Symbols

In the following lists the mathematical notations and symbols are described that are used throughout this report.

Number Sets

$\mathbb{N}$	The set of natural numbers
$\mathbb{R}$	The set of real numbers
$\mathbb{R}^n$	The set of n-dimensional real vectors, with $n \in \mathbb{N}$
$\mathbb{R}^n_+$	The set of n-dimensional real vectors with non-negative entries, with $n \in \mathbb{N}$
$\mathbb{R}^{mxn}$	The set of mxn real matrices, with $m, n \in \mathbb{N}$
$\mathbb{R}^{mxn}_+$	The set of mxn real matrices with non-negative entries, with $m, n \in \mathbb{N}$
$\mathbb{R}_+$	The set of non-negative real numbers
$\mathbb{U}^n_+$	The set of unit simplex of size n, hence all non-negative vectors that sum up to 1, with $n \in \mathbb{N}$

Vectors

$[x_i]_j$	The j-th entry of the vector x_i
$\mathbf{1}_n$	The n-dimensional vector with all its entries equal to 1
x^T	The transpose of the vector x

Matrices

$[A]_{ij}$	The (i, j)-th entry of matrix A
A^T	The transpose of the matrix A

Mathematical notations

$\varnothing$	The diameter
$\dot{x}$	The derivative of x
$\max_t f(t)$	The maximum of function $f(t)$ with respect to t
$\min_t f(t)$	The minimum of function $f(t)$ with respect to t
μ	The mean
σ	The standard deviation

List of parameters

α	Parameter representing the coefficient of double-strand breaks caused by radiation in Gy^{-1}
β	Parameter representing the coefficient of combination of two single-strand breaks caused by radiation in Gy^{-2}
γ_{50}	The slope of the response curve at the D_{50} point

$\mu_{ck,i}$	The migration rate of cell line i from compartment k to compartment c
ρ	The vector of fractionated doses for radiotherapy
$\tilde{r}_i^s$	Growth rate of cell line i with the influence of drug s
A	A Metzler matrix describing the tumor dynamics without the influence drugs
d	Number of different drugs
D_s	A positive diagonal nxn-matrix describing the effect of the drug s
D_{50}	The radiation dose that gives a NTCP response probability of 50%
m	Number of different mutant species
n	The combinations of mutant species and compartments, $n = mp$
n_f	Number of radiation fractions
p	Number of different compartments
P_{tot}	The total radiation dose
$q_{ij,k}$	Probability of cell line j mutating into cell line i in compartment k
r_i^k	Growth rate of cell line i in compartment k
R_w	The positive diagonal nxn-matrix describing the effect of radiation dose $[\rho]_w$
s	The organ sparing factor
T^*	The optimal treatment horizon
T_F	The finite treatment horizon
T_{max}	The maximum treatment duration regarding the chemotherapy-induced side effects
w	The vector for varying drug effects

List of variables

$[\tilde{l}]_s$	The treatment duration of drug s, given as fraction of the final treatment time
$[l]_s$	The concentration of drug s, normalized to the MTD
d_f	Radiation dose for fraction f
t	Continuous time
u	The vector of radiation durations for each fractionated dose

List of functions

$\psi_i^k(l)$	The overall drug dose response in compartment k for mutant cell line i
$BED(d_f)$	The biologically effective dose of d_f
$l(t)$	The control vector in $\mathbb{U}_+^q$, where $[l(t)]_s$ represents the normalized concentration of drug s at time t
$N(t)$	The number of tumor cells after time t
$S(d_f)$	Surviving fraction of tumor cells after radiotherapy dose d_f
$x(t)$	The states representing the number of cells of each cell line in each compartment